Understanding Immunosenescence in Aging-Related Diseases With Quantitative Proteomics

by

Zhiyun Cao

Bachelor's Degree, Xiamen University, 2009

Submitted to the Graduate Faculty of

the Kenneth P. Dietrich School of Arts and Sciences in partial fulfillment

of the requirements for the degree of

Doctor of Philosophy

University of Pittsburgh

2014

UNIVERSITY OF PITTSBURGH

the Kenneth P. Dietrich School of Arts and Sciences

This dissertation was presented

by

Zhiyun Cao

It was defended on

June 3rd, 2014

and approved by

Dr. Renã A. S. Robinson, Assistant Professor, Department of Chemistry

Dr. Joseph Grabowski, Associate Professor, Department of Chemistry

Dr. W. Seth Horne, Assistant Professor, Department of Chemistry

Dr. John A. Kellum, Professor, Department of Critical Care Medicine

Dissertation Advisor: Dr. Renã A. S. Robinson, Assistant Professor, Department of Chemistry

Understanding Immunosenescence in Aging-Related Diseases

With Quantitative Proteomics

Zhiyun Cao, PhD

University of Pittsburgh, 2014

Immunosenescence refers to the gradual deterioration of the immune system during aging. It is widely accepted that immunosenescence is characterized by diminished immune response, low-grade inflammation, and increased propensity for autoimmunity. These changes in the immune system increase the risk and mortality of diseases among the elderly. Poor response to immunotherapies as a result of immunosenescence can further worsen this situation. Fundamental understanding of immunosenescence is helpful for the prevention and treatment of aging-related diseases. Genomics, transcriptomics, proteomics, and metabolomics can give insight to molecular mechanisms of immunosenescence and its contribution to aging-related diseases. In particular, work presented in this dissertation takes advantage of proteomics methods to understand immunosenescence in two aging-related diseases-sepsis and Alzheimer's disease (AD).

To better study sepsis and AD, novel proteomics platforms are developed in this dissertation. Firstly, a robust platform is developed to improve the coverage of the human plasma proteome and establish statistical criteria for the determination of differentially-expressed proteins. Secondly, a novel data acquisition method using pulsed Q dissociation (PQD) in triple-stage mass spectrometry (MS^3) is developed for isobaric tags-based quantitation. This method increases the number of identified and quantified proteins without compromising quantitative accuracy.

In sepsis studies, proteins involved in inflammation, acute phase response, coagulation, and lipid metabolism are associated with age-related risk of severe sepsis among community-acquired pneumonia patients. In AD studies, a human double transgenic knock-in amyloid precursor protein/presenilin-1 (APP/PS-1) mouse model is employed. The proteome of T-cells and other immune cells (e.g., B-cells and macrophages) from this model is characterized and provides a reference map for future studies. T-cells from APP/PS-1 mice have increased oxidative stress during the progression of AD. Proteomics analysis of T-cells from this mouse model provides molecular basis for this phenomenon. Proteins related to cytoskeleton, energy metabolism, apoptosis, and molecular chaperones are also differentially expressed during AD progression.

Overall, works in this dissertation provide novel platforms for protein identification and quantitation. Application of proteomics platforms to the studies of sepsis and AD provides insight to the molecular mechanisms of immunosenescence. Results from these studies may be helpful for the development of novel diagnosis and treatments.

TABLE OF CONTENTS

LIST OF TABLES

LIST OF FIGURES

ACKNOWLEDGEMENTS

First and foremost, I would like to thank my advisor, Dr. Renã A. S. Robinson, for her support in the past five years. It has been my honor to be her first Ph.D. student. Dr. Robinson has taught me a lot of lab techniques from sample preparation to instrument analysis. More importantly, she has provided insightful discussion and suggestions about my projects. She also trained me how to think and write as a scientist. I will always remember that she encourages me to think about the big picture about my projects. I appreciate all her time and concerns to make my Ph.D. experience productive. Thank you, Dr. Robinson!

Besides my advisor, I want to thank the rest of my dissertation committee: Dr. Joseph Grabowski, Dr. W. Seth Horne, and Dr. John A. Kellum! I am very grateful for their insightful comments and suggestions on my dissertation and Ph.D. defense presentation. I appreciate that Dr. Grabowski recommended me for the postdoctoral position at the University of Chicago. I also would like to acknowledge Dr. Kellum for providing plasma samples from sepsis patients for my first Ph.D. project.

My sincere thanks also goes to the previous and present members from our research group! Adam R. Evans and I joined Dr. Robinson's group the same year. Peer pressure from Adam is one of the sources for my motivation in research. I enjoy the time we discuss scientific problems. I also appreciate Adam's help on the instrument troubleshooting, data analysis on PQD experiments, my proposal defense, *etc*. Wentao Jiang and Liqing Gu have helped me a lot on the data analysis and computer issues. I want to thank Christopher Williams for his help in immune cell protein extraction and slot blot experiments. Christina King is a good friend. She is very keen to help. Other previous and present group members that I have had the pleasure to work

with are Dr. Tasneem Muharib Howard; graduate student Rodolfo Gueerero, Jr; and graduate student Daljeet Singh.

In my attempt to do the immunology experiments, Dr. William F. Hawse from the Department of Immunology has always been patient, kind, and helpful. I would like to acknowledge Dr. Hawse for his generosity for mouse CD4+ T-cells and help in these experiments.

Lastly, I want to express my special love and acknowledgement to my parents Guanghui Cao and Shufang Zhang. They are always supportive throughout my life. Their love provides my inspiration and is my driving force. I wish I could show them just how much I love them.

1.0 INTRODUCTION

1.1 IMMUNOSENESCENCE AND AGING-RELATED DISEASES

1.1.1 Aging and Immunity

Aging is associated with progressive decline in physiological functions such as weakened muscle and bone strength, dysfunctional organs and immune system, and reduced metabolic rate[1,2]. These changes make the elderly, defined as aged 65 years and older, more susceptible to diseases including cancer, infectious diseases, and degenerative disorders. For example, the incidence and mortality of cancer is ~ 25- and 40-fold, respectively, in people older than 65 years compared to younger individuals[3,4]. Alzheimer's disease (AD) occurring in people older than 65 years accounts for ~ 90% of cases, although it can happen in early adulthood[5]. The elderly also have higher risk of comorbidities which further increases their mortality[6]. Management of the elderly has generated heavy economic burden. This situation will worsen as the population ages. It is estimated that between 2000 and 2050, the number of people 65 and 85 years and older will increase by 135% and 350%, respectively, in the United States[7]. Better understanding of aging and aging-related diseases is necessary to attenuate the burden caused by the increasing number of elderly persons.

Age-related impairment of the immune system is an important contributor to the increased incidence and mortality of diseases in the elderly. The immune system can protect individuals from pathogen invasion and maintain homeostasis. However, the functions of the immune system change during aging, which is termed immunosenescence. Indeed, the elderly have reduced ability to fight against infections[8-10]. This is caused by defects in both the innate

and adaptive immune system such as reduced phagocytic capacity of macrophages and restricted T- and B-cell diversity[8-10]. In addition, aging is accompanied with low-grade chronic inflammation, which may cause inadvertent damage to organs[11,12]. For example, increased plasma levels of pro-inflammatory proteins increases the risk of cardiovascular disease while healthy aging is associated with relatively low levels of inflammation[13]. Immunosenesence also results in poor response to treatment[11]. In particular, vaccination is an important intervention for disease control and has been used effectively in children and younger adults[11]. However, the beneficial effects of vaccines are limited in the elderly due to dysfunctional B- and T-cells[11]. This again increases the incidence and mortality of diseases in this population.

Overall, because human aging is unavoidable, it is necessary to understand changes associated with this process in hopes to achieve healthy aging and prevent aging-related diseases. Accomplishment of this goal can be facilitated by the fundamental understanding of immunosenesence as it plays crucial roles in the incidence and mortality of aging-related diseases. Findings about immunosenesence may also provide insight to the prevention and treatment of aging-related diseases. Specifically, in this dissertation, the roles of immunosenesence in sepsis and AD are studied. Results presented in this dissertation have helped to generate a more complete picture about the immunopathology of these two diseases.

1.1.2 Immunosenescence and Sepsis [14]*

(*note that part of the information shown in this section is written based on the published paper, Cao, Z.; Robinson, R. A. S. *Proteomics-Clinical Applications* **2014**, *8*, 35)

Sepsis is the systemic inflammatory response syndrome (SIRS) accompanied by infection[15-17] (Figure 1.1). Infections can be caused by pathogens, including Gram-negative or Gram-positive bacteria, fungi, parasites, and viruses as well as secondary infections that occur as a result of nonpathogenic insults, such as trauma and burns[15-17]. The addition of at least one organ dysfunction denotes severe sepsis and subsequent hypotension despite adequate fluid resuscitation and/or the use of vasopressor denotes septic shock[15,17] (Figure 1.1). From SIRS, sepsis, severe sepsis, to septic shock, there is a hierarchical continuum of inflammatory response to infection and increasing mortality rates[18]. For example, severe sepsis and septic shock have mortality rates of 27.3 and 36.4%, respectively[19]. Comorbidities in sepsis patients can exist. For example, cutaneous adverse drug reaction[20], urinary tract infection[21], and community-acquired pneumonia (CAP)[22] are the most common causes of SIRS, sepsis, and severe sepsis, respectively. The most severe cases of infection lead to multiple organ dysfunction syndrome (MODS) and without positive response to treatment, death[23].

To slow inflammatory response and reduce mortality rates, it is important to develop efficient therapeutic strategies for patients with sepsis. Currently, antimicrobial treatments and early goal-directed therapy play important roles in the management of sepsis[24-26]. However, their applications in clinical practice are limited. For example, the choice of a specific antimicrobial treatment can be influenced by the infection site and molecules released from microorganisms may exacerbate inflammatory response[24,25]. Several therapies- glucocorticoids[27], recombinanat human-activated protein C[28], steroids[29], intravenous Ig[30], continuous renal replacement therapy[31], proinflammatory cytokine inhibitors[24], antioxidant supplementation[32], and others[33-35]-have been targeted at sepsis without much success. Overall, more than 40 clinical trials of therapies targeted

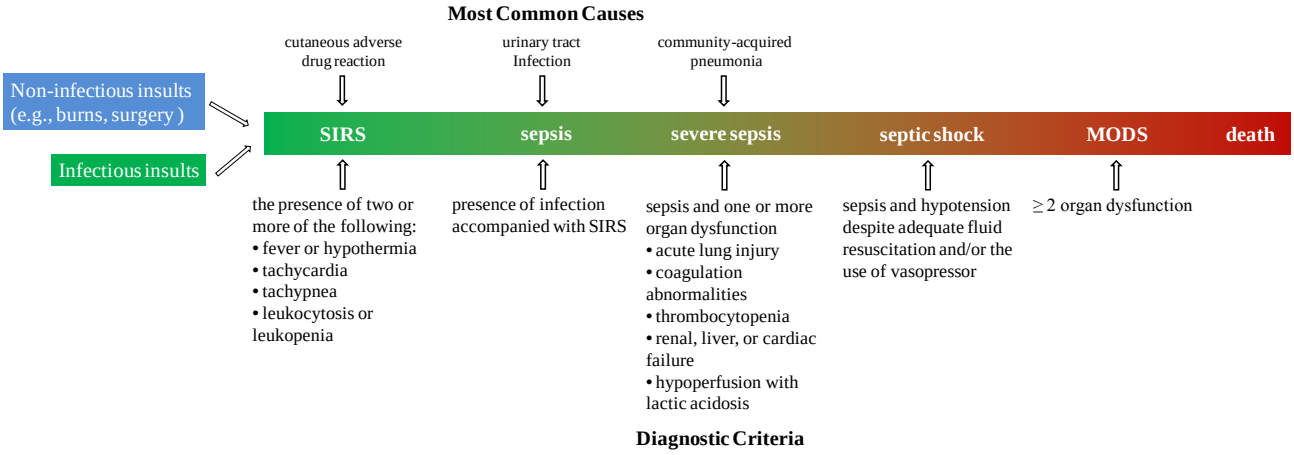

Figure 1.1. Diagram illustrating the progression of septic infection.

at septic patients have failed to lead to a current FDA-approved drug for the universal treatment of sepsis.

The lack of current universal treatment for sepsis can be understood due to the many challenges associated with this condition. Diagnosis of sepsis is complicated by the different faces in which it can present itself among patients (i.e., degree and nature of clinical symptoms can vary tremendously). In addition to patient heterogeneity, there is also temporal heterogeneity within individual patients[36]. The timing of the diagnosis is crucial to initiation of therapy, however, this is difficult because the assays for culture determination can take as long as 48 h[17] and some patients have symptoms for a day prior to hospital admission[37]. In more than half of the cases, clinical symptoms persist without a positive culture[17]. Monitoring of specific biomarkers (e.g., tumor necrosis factor (TNF)-α, interleukin (IL)-1, IL-6, IL-8, and IL-10, procalcitonin, C-reactive protein, and others) yield conflicting results with regards to sensitivity, specificity, and effectiveness in both adults and neonates[17]. Because of the roles of many of these molecules in immune response and inflammation, a single readout of any specific biomarker can be misleading. Biomarker readouts are heavily time-dependent as there is a known acute proinflammatory response that occurs in the first 24 h after infection[37]. Challenges with diagnosis, prognosis, and real-time response to treatment of sepsis-which warrant the development of novel therapeutics and strategies-can be best facilitated by understanding the molecular mechanisms of this condition.

Different tools have been used to investigate molecular mechanisms of sepsis, including genomics, transcriptomics, proteomics, metabolomics, and protein immunoassays[38,39]. In particular, proteomics studies have attracted more attention in the last few decades and unveiled

numerous information underlying this infection[40,41]. One beneficial aspect of proteomics studies is that they can be applied to tissues that arise from sepsis patients or animal models and give insight to host response. Models of sepsis have been developed in rodents (e.g., mice and rats), larger mammals (e.g., pigs and cats), and in humans (e.g., injection of endotoxins or exotoxins)[41,42].

To date, it is widely accepted that sepsis consists of both a proinflammatory response and an anti-inflammatory counter response that happens at the onset of infection and days afterward, respectively[17,34]. At the onset of sepsis, pathogens are recognized by immune cells resulting in the activation of inflammatory response and a cytokine cascade[17]. In addition to the increased levels of cytokines, elevated concentrations of cell surface receptors (e.g., toll like receptors, CD14 antigen) and acute phase proteins (e.g., serum amyloid A proteins, LPS binding proteins, and glycoproteins) are increased in response to sepsis[14]. Persistent proinflammation in sepsis patients may lead to death[43]. For those who survive from the initial inflammation, suppressed immune response may develop[34,43]. This immunosuppression is manifested with increased apoptosis of macrophages, B-cells, and T-cells, enhanced suppressive property of regulatory T-cells, and elevated levels of anti-inflammatory cytokines[34,43]. Immunosuppression in sepsis leads to the inability to clear primary infection and the development of secondary infection[34,43].

Inflammation in sepsis patients results in activation of the pro-coagulation pathway, which causes a proteolytic cascade that increases production of blood clots and contributes to organ failure[23,44]. Sepsis patients and animal models have higher levels of fibrinogen and von Willebrand factor, which enhances the formation of blood clots[14]. In addition, an inhibited anti-coagulant pathway manifested by decreased levels of related proteins (e.g., anti-thrombin and

heparin factor-2) is associated with sepsis[14]. Promoted coagulation in sepsis can in turn exacerbate inflammation. For example, thrombin, which is involved in coagulation, can activate monocytes and endothelial cells and induce the production of pro-inflammatory cytokines. Sepsis also has negative impact on cells and tissues. Reactive oxygen species (ROS) and reactive nitrogen species (RNS), which are produced from neutrophils, macrophages, and other leukocytes, subsequently lead to a buildup of toxic species that can target proteins, lipids, and DNA in host tissues resulting in oxidative damage[45,46].

While sepsis affects people at different ages, the elderly is the most susceptible population to sepsis. Out of ~ 750,000 people diagnosed with sepsis annually, more than 60% of patients are older than 65 years old accounting for ~ 52% of the annual healthcare resources generated by sepsis[47]. An epidemiological study showed that the incidence of sepsis among people > 85 years old is > 100 times higher than that in children[16]. CAP patients ≥ 85 years old have a 3-fold increased risk of severe sepsis compared to those ≤ 50 years old[48]. Aging is also a contributing factor to the increased mortality rates of sepsis in the elderly. For example, among the patients hospitalized with CAP-induced severe sepsis, the mortality rate for patients ≥ 85 years old increased by ~ 8-fold compared to those ≤ 50 years old[48]. Sepsis patients ≥ 65 years old have 3-fold increased mortality compared to those < 65 years old[49].

Although various factors (e.g., impaired performance status, dysregulated nutrition sensing, and reduced social activity) may contribute to age-related incidence and mortality of sepsis, immunosenescence plays essential roles. In particular, involution of thymus in the elderly results in a significantly reduced number of naïve T-cells[8,47,50]. Naïve T-cells from the elderly have restricted T-cell receptor repertoires, reduced production of IL-2, and impaired ability to

differentiate into effector cells[8,47,50]. B-cell activation and production of antibodies is reduced in the elderly as well as antibody affinity to antigens[2,24,25]. These changes compromise the effective immune response to new antigen invasion in the elderly and increase their susceptibility to sepsis. Persistent low-grade inflammation in the elderly also increases the risk of sepsis by inducing the expression of cell surface receptors and promoting the host response to pathogens[51].

The effect of aging on the immune system in sepsis has also been examined. An aged mouse model of sepsis has higher levels of pro-inflammatory cytokines (e.g., IL-6 and TNF-α) and coagulant proteins (e.g., fibrinogen) relative to younger sepsis mice. The elevated levels of these proteins in aged mice correlates with higher mortality[52-54]. However, discrepant results have been obtained in human studies. For example, at day 1 of hospital stay, the levels of IL-6 and IL-10 are similar between CAP patients from age groups of > 85 and < 65 years old[55]. CAP patients from different age groups (i.e., < 50 years, 50-64 years, 65-74 years, 75-84 years, and ≥ 85 years) have similar levels of IL-6, TNF-α, IL-10, D-dimer, and anti-thrombin at day 1 and over the first week of hospitalization, although age-related risk and mortality of severe sepsis occurs in the same cohort of CAP patients[48]. Similarly, patients hospitalized with *Streptococcus pneumonia* infection have no age-related difference in the levels of IL-6 and TNF-α at day 1[56]. However, increased levels of TNF-α are found at day 7 in the elderly which implies that old age is associated with prolonged inflammatory response[56].

Elderly patients with sepsis also have poor long-term outcomes. CAP patients > 85 years have a 1.3- and 2-fold increased risk of 1-year post-discharge mortality than those 75-84 years and 65-74 years, respectively[48]. This may be related to persistent inflammation and coagulation

in the elderly. Higher levels of IL-6 and D-dimer in older patients at hospital discharge are associated with increased mortality[51].

Overall, age-related effects on the immune system are involved in the stages before, during, and after sepsis. Better understanding these effects is beneficial for the development of more efficient methods for disease prevention and treatment. However, current studies only focus on a set of selected proteins involved in inflammation and coagulation. Globally studying changes in proteins between different age groups will generate a more complete picture about age-related risk and mortality of sepsis patients.

1.1.3 Immunosenescence and Alzheimer's Disease

AD is a neurodegenerative disorder characterized with progressive memory defects, cognitive impairment, and changes in behavior and personality[12,57]. AD is an aging-related disease with the incidence increasing almost exponentially after 65 years old[57]. A 2005 epidemiological study shows that ~ 27 billion people are diagnosed with AD worldwide[57]. This number will increase by four-fold by 2050[57]. Early diagnosis of AD is challenging since evident clinical symptoms of AD usually appear at the late stage of this disease. Currently, drugs (e.g., galantamine, donepezil, rivastigmine, tacrine, and memantine) regulating neurotransmitters are used to relieve the symptoms of AD[58,59]. However, these drugs cannot stop or reverse the progression of AD[58,59]. Therefore, better understanding of AD pathology is necessary for the development of novel diagnostic and therapeutic methods.

Much effort has been made to understand changes in AD brain. Two major pathological hallmarks of AD are the accumulation of senile plaques (SP) and neurofibrillary tangles

(NFT)[12,57]. SP are composed of amyloid β (Aβ) peptides which are generated from the proteolysis of amyloid precursor protein (APP) by β- and γ-secretases[12,57]. Hyperphosphorylated tau-proteins are components of NFT[12,57]. The central nervous system (CNS) in AD also has regionalized neuronal death, loss of synaptic connections, increased oxidative stress, mitochondrial dysfunction, and reduced energy metabolism[60-63].

Neuroinflammation is another important hallmark of AD[12,64]. Initial inflammatory response by microglia and astrocytes, two types of immune cells resident in the CNS, is beneficial for the clearance of Aβ plaques[64]. However, in AD, Aβ plaques trigger chronic neuroinflammation manifested by over-activated microglia and astrocytes and elevated levels of pro-inflammatory cytokines, chemokines, and acute phase proteins[12,64]. This chronic inflammation, in turn, enhances the production of Aβ plaques[12,64]. It is unknown whether neuroinflammation is a cause or a consequence of AD, however, it is clear that neuroinflammation and Aβ production are involved in a self-propagating feedback loop with adverse outcomes[12,64].

While changes in the CNS are closely related to AD, cumulative evidence suggests the involvement of the peripheral immune system in the pathogenesis of AD. Low-grade inflammation associated with immunosenescence in the elderly may increase susceptibility to AD[11,12]. Inflammation caused by infectious agents also contribute to the incidence of AD and this effect is enhanced in the elderly due to diminished ability to control infection[65]. Non-steroidal anti-inflammatory drugs (NSAID) have significantly reduced risk of AD which provides additional proof for the involvement of the immune system in AD[12].

However, clinical trials of NSAID on people who are already diagnosed with AD do not give promising results[12]. This may be explained by the further impaired immune system in AD. In AD, a compromised blood-brain barrier (BBB) allows the efflux of Aβ oligomers and pro-inflammatory mediators to the periphery, which induces the peripheral immune response[12,66]. Immune cells (e.g., T-cells and monocytes) from AD patients are activated and secrete increased levels of proinflammatory cytokines[12,66]. These cytokines can cross the BBB and promote neuroinflammation and Aβ production[12,66]. Communication between the CNS and peripheral immune system also alters the distribution of immune cells. Peripheral immune cells in CNS regions that contain Aβ deposits are present in AD[67]. These cells may also exacerbate neuroinflammation. In the periphery, a decreased number of B-cells has been observed in AD[12]. AD patients have a decreased number of naïve T-cells and increased number of memory T-cells[12]. Subpopulations of T-cells also change in AD patients, although conflicting results exist[12]. The function of immune cells is impaired in AD. Macrophages and monocytes have lessened phagocytic ability[68,69]. The cytotoxic function of natural killer cells is impaired although no changes are observed in the number of natural killer (NK) cells[70]. B-cells have reduced anti-Aβ response[12]. T-cells have elevated calcium response, increased apoptosis, and hyper-activity[71-73]. Findings in the peripheral immune system provide more insight into the pathology of AD. Additionally, these can be used as potential peripheral biomarkers for disease diagnosis and prognosis in the periphery. Compared to the biomarkers in the brain, peripheral biomarkers are more easily obtainable.

It is clear that the peripheral immune system is involved in the pathology of AD. However, characterization of the peripheral immune system in AD is far from complete. Animal

models of AD offer an important means to gain more insight into the immunopathogenesis of this disease and in fact dysfunction of the immune system in various mouse models has been reported. The triple transgenic (3xTg) AD mouse model has increased production of senile plaques and neurofibrillary tangles in the brain[74]. In 3xTg mice, reduced weight of immune organs (e.g., thymus, spleen, and adrenal glands) indicates their premature immunosenescence[74]. 3xTg mice have decreased chemotaxis, anti-tumoral NK activity, and IL-2 secretion[74] and show signs of systemic autoimmunity[75]. Regulation of the inflammatory response by blocking IL-1 signaling attenuates cognitive defects in 3xTg mice[76]. In this dissertation, a human double transgenic knock-in amyloid precursor protein/presenilin-1 mouse model (hereafter referred to as APP/PS-1) is employed[77,78]. APP/PS-1 mice show age-dependent progression of AD[77,78]. Specifically, Aβ plaques start to deposit in the brain of APP/PS-1 mice at six months, and they mimic the cognitive deficits associated with early stage AD[77,78]. By 12 months of age, numerous SP are present in the hippocampus and caudal cortex, which corresponds to late stage AD[77,78]. Consistent with findings about human AD, APP/PS-1 mice have increased oxidative stress in brain and neurons[79,80]. They have an impaired immune system indicated by increased activation of microglia[81,82], altered monocyte subpopulations[83], and enhanced cell proliferation of lymphocytes[84]. APP/PS-1 is a useful model in elucidating immunopathogenesis in AD.

Understanding immunosenescence in AD provides insight to the development of novel immunotherapies for this disease. According to the Aβ hypothesis of AD, the clearance of Aβ plaques may aid the recovery of cognitive function. Immunization of APP transgenic mice with Aβ prior to the onset of AD hallmarks significantly reduces levels of Aβ plaques in the brain[85]. Immunization with Aβ also decreases the levels of Aβ plaques in aged APP transgenic mice[86].

More importantly, this reduction in Aβ plaques prevents age-related cognitive defects[86]. These results provide an encouraging means for AD prevention and treatment. Clinical application of Aβ immunization reduces Aβ plaques in AD patients[87]. However, these patients immunized with Aβ have significanly increased risk of developing encephalitis[87]. Although the mechanisms for this observation are still unclear, it has been suggested that over-activation of T-cells in response to Aβ immunization is an important contributor[87]. Therefore, fundamental understanding of the changes in the immune system in AD will be helpful to develop effective therapies.

In conclusion, immunosenescence is an important contributor to sepsis and AD. Currently, systematic biological methods from genomics, transcriptomics, proteomics, to metabolomics are being used in studies about aging and aging-related diseases. In particular, proteomics is the study focusing on the whole set of proteins in a biological system. Proteomics has been employed to understand the molecular mechanisms associated with immunosenescence, sepsis and AD. For example, proteomics studies have revealed that immunosenescence is associated with increased oxidative stress in B- and T-cells[88]. In sepsis, changes in organ proteome (e.g., liver and kidney) give insight into sepsis-induced organ dysfunction[89,90]. Proteomics studies about AD brain and cerebrospinal fluid have been done to investigate pathology of this disease[61,91-95]. In addition, biomarker candidates for sepsis and AD diagnosis and prognosis have been discovered in plasma and urine by proteomics studies[14,96,97]. Biomarker candidates in these tissues are attractive due to their easy accessbility. In this dissertation, proteomics technologies are employed to study alterations in sepsis and AD.

1.2 SHOTGUN PROTEOMICS TECHNOLOGIES

1.2.1 Shotgun Proteomics

Proteomics refers to the study of the whole set of proteins in a biological system (e.g., biofluids, tissues, and cells)[98]. Proteomics studies can provide information about protein abundance, distribution, post-translational modification, function, and interaction[99]. Shotgun or "bottom-up" proteomics technologies, which identify proteins based on their proteolytic peptides, is employed in this dissertation. In a typical shotgun proteomics workflow, proteins extracted from biological tissues are digested with a protease (i.e., trypsin) to generate peptide mixtures, which are separated using liquid chromatography (LC) and electrosprayed into a mass spectrometry (MS) instrument. In the parent MS scan, intact peptide ions are detected and their *m/z* ratios are recorded. Peptide ions are further isolated and subject to collision induced dissociation (CID) to generate tandem mass spectra (MS/MS), in which *b*- and *y*-type fragment ions (Figure 1.2) are detected. Mass difference between adjacent *b*- or *y*-ions can be used to identify amino acid residues in peptide sequences. Database search algorithms (i.e., SEQUEST[100], as described below) are used to identify peptides and their corresponding proteins.

1.2.2 Isobaric Tagging Methods

One important research interest in the field of proteomics is to obtain differences in the relative abundance of proteins between different conditions (e.g., disease *vs.* healthy). Currently, there are many quantitative proteomics methods available[101-103]. Among these methods, isobaric tags offer the advantage to quantify up to ten samples simultaneously[104-106], which significantly reduces instrument acquisition time. More importantly, multiplexing also decreases experimental

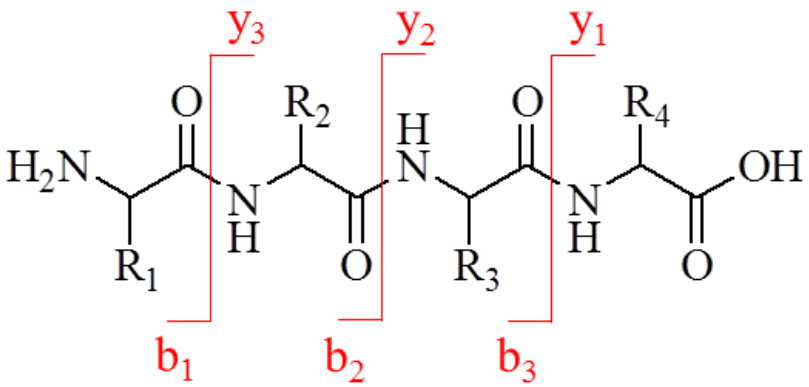

Figure 1.2. The diagram of *b*- and *y*-ions produced by CID fragmentation.

error caused by multiple sample preparation steps and handling. In this dissertation, isobaric tags for relative and absolute quantitation (iTRAQ)[102] (**Chapters 2**, **4**, and **7**) and tandem mass tags (TMT)[107] (**Chapter 3**) are employed for protein quantitation. iTRAQ and TMT are similar and contain three chemical groups in the structure: reporter ion group, balancer group, and amine reactive group (Figure 1.3a). Herein, iTRAQ 4-plex is used as an example to illustrate the principle of isobaric tags (Figure 1.3b). Four different reagents which have the same structure and mass are synthesized. Heavy isotope atoms (e.g., ^{13}C, ^{15}N, and ^{18}O) are incorporated into the reporter and balancer group to keep the overall mass of these two parts identical (e.g. 145 Da). The mass of the reporter group ranges from 114 to 117 Da, and the mass of the corresponding balancer group ranges from 31 to 28 Da. The incorporation of ^{13}C, ^{15}N, and ^{18}O does not change the physical or chemical properties of the labeled peptides, and has no effect on LC separation. N-hydroxysuccinimide is used as a peptide reactive group, and it can react with free primary amino groups (i.e., N-termini and lysine residues, Figure 1.3c). In the iTRAQ-based proteomics experiment (**Chapters 2** and **7**), peptides generated from four biological samples are labeled with different iTRAQ 4-plex reagents. After iTRAQ-labeling, these four peptide mixtures are combined and subject to LC-MS/MS analysis. The same peptides labeled with different iTRAQ reagents elute from the LC column, are ionized and detected in the MS simultaneously. The parent MS scan shows a single unresolved peak for these peptides. This peak is isolated and fragmented to generate reporter ions [i.e., mass-to-charge (*m/z*) 114, 115, 116, and 117), which are detected in the MS/MS spectrum. The existence of isotopic impurities needs to be corrected to generate accurate reporter ion intensity. For example, peak intensity for reporter ion at *m/z* 114

a)

b)

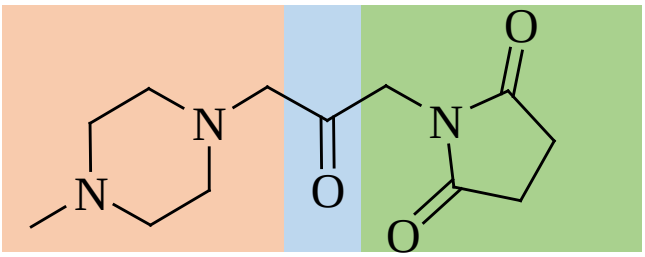

	reporter ion group mass 114-117		balancer group mass 31-28	amine reactive group
reporter ion m/z	114	^{13}C	$^{13}C\ ^{18}O$	
	115	$^{13}C_2$	^{18}O	
	116	$^{13}C_2\ ^{15}N$	^{13}C	
	117	$^{13}C_3\ ^{15}N$		

c)

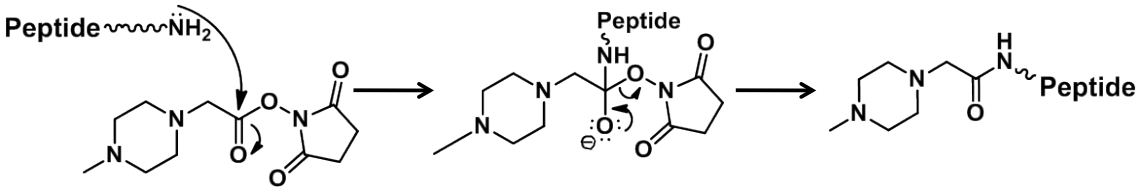

Figure 1.3. a) The general composition of isobaric tags, **b)** structure and isotopic atom composition of iTRAQ 4-plex, and **c)** the reaction between peptides and iTRAQ reagents.

contributed from adjacent reporter ions (e.g., *m/z* 115) should be corrected. The peak intensity for these reporter ions is used to quantify peptides. Protein ratios are obtained using the median ratios of their corresponding peptides.

1.2.3 Separation and Mass Spectrometry

MS represents a powerful tool with high sensitivity, specificity, and through-put and plays a central role in proteomics studies. Coupling of separation technologies, for example, LC, can result in hundreds of proteins identified in one single proteomics experiment. Multi-dimensional protein identification technology (MudPIT) has been developed to increase the number of identified peptides and proteins[108], which allows to more depth into the proteome of biological systems. In this MudPIT experiment, online strong cation exchange (SCX) and reverse phase (RP) LC are employed to sequentially separate peptides based on their charge and hydrophobicity[108]. Offline SCX-RP LC separation, which offers advantages of high flexibility and more comprehensive proteome coverage[109], however, is used in the bulk of work in this dissertation (**Chapters 2, 4, 5, and 7**). One-dimensional RPLC separation is also employed (**Chapter 3**). For other separation techniques used in proteomics studies, we refer the readers to the references as follows[110-113].

SCX separation is carried out on a PolySulfethyl A column. Acidic pH of the mobile phase buffers makes the basic amino acid residues and N-termini positively charged. This helps the retention of peptides on the stationary phase by electrostatic forces. Addition of organic solvent (i.e., acetonitrile) in the mobile phase buffers helps the retention of peptides on the stationary phase by hydrophobic interactions. To elute peptides from the stationary phase, a

gradient with increasing concentration of salt (i.e., KCl) is used. Peptides with more positive charges are eluted later. Eluents from the SCX separation are collected every minute and pooled to generate a user-determined number of fractions. Each SCX fraction is desalted using solid-phase extraction techniques, dried, and reconstituted in an appropriate solution for online RP-LC-MS/MS analysis. RP separation is carried out on a home-made capillary column packed with C_{18} material. In RPLC, peptides are retained on the stationary phase by hydrophobic interaction and eluted by increasing the composition of organic solvent (i.e., acetonitrile) in the mobile phase.

Eluents from RPLC are electrospray ionized (ESI)[114] and introduced into a commercial mass spectrometer, LTQ-Obitrap Velos. LTQ-Orbitrap Velos is a hybrid instrument with two mass analyzers-linear ion trap (LTQ) and Orbitrap[103]. Data-dependent acquisition (DDA) is used to acquire peptide information. Specifically, ions eluted at one retention time are detected in the Orbitrap to generate a parent MS scan with high resolution (i.e., 60,000 at *m/z* 400) and mass accuracy (i.e., < 10 ppm). The most intense peak in the parent MS scan is isolated and fragmented in the LTQ. *B*- and *y*- type fragment ions can be detected in the LTQ or Orbitrap. This is followed by CID fragmentation of the second most intense peak, the third, and so forth. Dynamic exclusion is enabled in this data acquisition process such that peptide ions with the same *m/z* are not detected multiple times within a time window. Dynamic exclusion allows the detection of low-abundance peptides, which increases the number of identified peptides and proteins. Many of the features in DDA are user-defined for a particular experiment.

CID MS/MS in the LTQ provides information for peptide identification. However, this method is not suitable for iTRAQ quantitation. This is due to their low mass cutoff limitation,

preventing the trapping of fragment ions with *m/z* values lower than the 25-30% of the parent ion[115]. The detection of iTRAQ reporter ions with *m/z* 114-117 is not possible in CID fragmentation[115]. To overcome this, higher energy collision induced dissociation (HCD) is employed, whereby peptide ions are fragmented in the HCD collision cell and fragment ions are detected in Orbitrap. HCD provides good fragmentation efficiency for reporter ions, however, b- and y- ion coverage is compromised[115]. Therefore, combination of CID and HCD (CID-HCD)[115] are used for peptide identification and quantitation (**Chapters 2**, **4**, and **7**).

1.2.4 Protein Identification and Quantitation

The raw data collected from shotgun proteomics analysis is processed by database search algorithms (i.e., SEQUEST[100]) to generate a list of proteins and peptides present in the original sample. In this process, SEQUEST[100] digests proteins from a given database *in silico* using the specified enzyme (i.e., trypsin) that is used experimentally. Experimental and theoretical MS/MS spectra are compared and scores (e.g., Xcorr) which evaluate their similarities are returned. Search parameters such as mass tolerance of the parent and fragment ions and static or dynamic modifications (i.e., oxidation on methionine, iTRAQ labeling on N-termini and lysine, etc.) can affect these values. Searching against decoy or reverse databases (i.e., databases with reversed protein sequences) is used to determine the false-discovery rate (FDR) for protein and peptide identification. Typical FDR values used in the assignment of peptides are 0.05 and 0.01, which indicate 95% and 99% confidence in peptide identification, respectively (i.e., 1 in 20 or in 100 assignments are false positives). SEQUEST is built into a software called Proteome Discoverer (PD, Thermo Scientific) for protein and peptide identification. PD has functions to extract

iTRAQ or TMT reporter ion intensities from raw data for peptide quantitation. The median value of peptide ratios is calculated for each protein and for comparisons across different samples. To determine the proteins which are statistically different in relative concentration between samples, student's *t*-test, analysis of variance (ANOVA), and power analysis can be employed. Multiple test correction (e.g., Bonferroni correction) is also necessary to control FDR. Generally, tens to hundreds of proteins which have varied concentrations between different conditions will be identified. Biological function analysis of these proteins using softwares such as Gene Ontology[116] and Ingenuity® System is helpful to gain insight into the molecular mechanisms of diseases.

1.2.5 Immunodepletion of Human Plasma

Human plasma is widely used in disease studies. It offers several advantages. Firstly, it is easy to collect. Secondly, human plasma is informative. Besides the classical proteins (e.g., albumin, IgG), human plasma also contains proteins secreted from different organs and cells[117]. It is believed that alterations in the levels of proteins from organs and cells may reflect the disease state of individuals. However, detection of these proteins is challenging due to their low concentrations and the high dynamic range in human plasma (~ 10^{10}-10^{12}). Various methods have been developed to increase the identification of low-abundance proteins, such as, immunodepletion of high-abundance proteins[117] and equalization of protein concentrations using combinatorial ligand libraries[118] or molecular weight cutoff filters[119]. In this dissertation, an immunodepletion method, multiple affinity removal system (MARS), is employed. MARS is a LC column containing antibodies targeting the six most abundant proteins in plasma (i.e.,

albumin, IgG, IgA, transferrin, haptoglobin, and anti-trypsin). To deplete high-abundance proteins more efficiently, a method, termed as tandem MARS depletion (TMD), has been developed, in which the flow-through fraction containing low-abundance proteins from the first MARS depletion is followed by another MARS depletion (**Chapters 2** and **4**). Flow-through fraction from TMD is used for further proteomics analysis.

1.2.6 Immunoblotting Analysis

Two immunoblotting analysis methods are used in this dissertation: Western blot (**Chapter 4 and 7**) and slot blot (**Chapter 6**). Western blot is used as an independent method to verify protein ratios obtained from quantitative proteomics experiments. In Western blotting analysis, proteins are separated by polyacrylamide gel electrophoresis (PAGE) and transferred to a nitrocellulose membrane. Primary antibodies for targeted proteins are added to incubate with the membrane. This is followed by the addition of secondary antibodies which recognize the primary antibodies. Secondary antibodies are conjugated with alkaline phosphatase, which will develop colorometrically in the presence of 5-bromo-4-chloro-3'-indolyphosphate *p*-toluidine salt and nitrotetrazolium blue.

Slot blot is employed to measure oxidative stress in biological systems. Aging and various diseases are associated with increased oxidative stress[120-123]. Oxidative stress occurs when the levels of ROS and RNS overwhelm the levels of antioxidants. ROS and RNS may damage molecules such as proteins, DNA, and lipids, which leads to the dysfunction of cells and organs. In this dissertation, protein oxidation is used as a read-out of oxidative stress, we refer the readers for oxidative damage to other molecules to the following references[124-126]. Oxidative

damage on proteins causes the formation of carbonyl groups (PCO) on the side chain of amino acid residues (e.g. proline, arginine, lysine, and threonine, Figure 1.4a)[127]. Nitration of tyrosine residues [i.e., 3-nitrotyrosine (3-NT), Figure 1.4a) is an important marker of protein oxidation. To measure the levels of PCO and 3-NT using slot blot, proteins derivatized with 2,4-dinitrophenylhydrazine (DNPH) (Figure 1.4b) or without derivatizaion, respectively, are directly loaded onto a nitrocellulose membrane. Primary antibodies which target at PCO and 3NT are used to assess the oxidative stress, while secondary antibodies provide a detectable readout.

1.3 OVERVIEW OF DISSERTATION

This dissertation employs proteomics techniques to study immunosenescence in sepsis and AD. To better achieve this goal, a novel proteomics workflow for protein quantitation in human plasma is established (**Chapter 2**). New data acquisition methods for isobaric tagging are also developed to increase the number of proteins identified and quantified (**Chapter 3**). Finally, proteomics tools are used to investigate immunosenescence in sepsis (**Chapter 4**) and AD (**Chapters 5-7**). Plasma samples from sepsis patients and immune cells from APP/PS-1 mouse model are employed in sepsis and AD studies, respectively. Although gender affects the risk and mortality of sepsis and AD[128,129], in this dissertation, its effects are not studied. Both male and female patients are enrolled in sepsis studies to obtain general information about immunosenescence in sepsis, whereas due to the easy accessibility of mice with different genders, only male APP/PS-1 mice are used in AD studies to exclude the gender-related effects. Based on the findings in **Chapters 4-7**, further direction for studies about sepsis and AD are

presented in **Chapter 8**. **Chapters 2-7** are written directly as published papers or manuscripts, thus, there is redundant information of defining abbreviated terms.

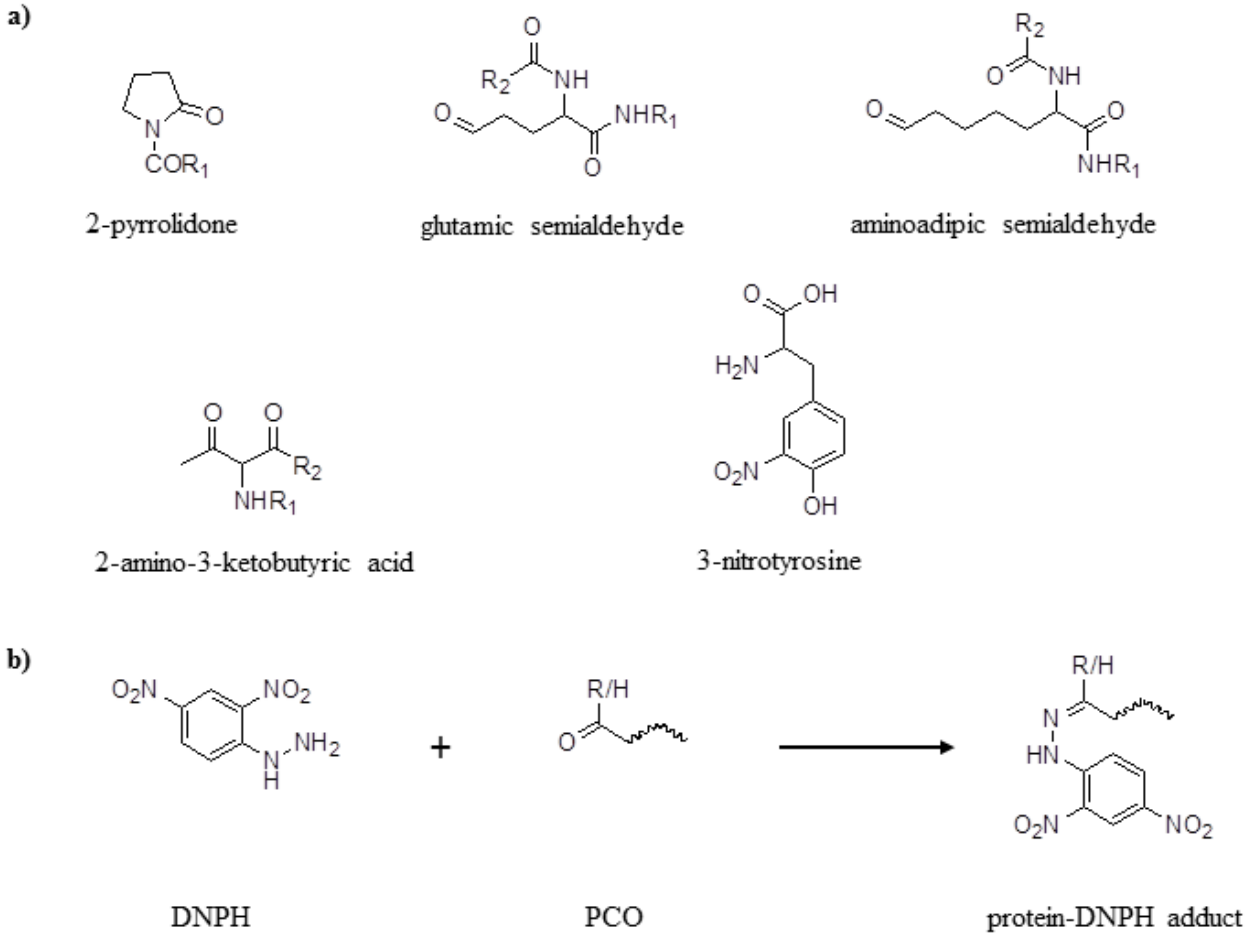

Figure 1.4. a) the structure of carbonylated amino acid residues and 3-nitrotyrosine resulting from protein oxidation: 2-pyrrolidone from proline, glutamic semialdehyde from arginine and proline, α-aminoadipic semialdehyde from lysine, and 2-amino-3-ketobutyric acid from threonine. **b)** the reaction between 2,4-dinitrophenylhydrazine (DNPH) and protein carbonyl groups (PCO).

2.0 ADDITIONS TO THE HUMAN PLASMA PROTEOME VIA A TANDEM MARS DEPLETION iTRAQ-BASED WORKFLOW[130]*

(* note that information in this chapter is written based on a published paper, Cao, Z.; Yende, S.; Kellum, J. A.; Robinson, R. A. S. *International Journal of Proteomics* **2013**, Article ID 654356)

2.1 INTRODUCTION

Discovery studies using plasma proteomics present challenges due to the technical difficulties associated with measuring the large dynamic range (~ 10-12 orders of magnitude) of proteins that exist in the medium[117]. Low-abundance proteins, which are of interest for biomarker applications are often only accessible with involved proteomics workflows that utilize multiple sample fraction steps. While the development of specific clinical immunoassays would resolve this approach, much work needs to be done in this area. Enrichment strategies for low-abundance plasma proteins rely on immunodepletion of high-abundance proteins[131-133], and, more recently, tandem depletion strategies have been employed[134-137]. For example, proteins present in as little as 1-1.6 $\mu g \cdot mL^{-1}$ concentrations are detectable using tandem removal of abundant proteins with human serum albumin and Human 14 (Hu14) multiple affinity removal system (MARS) columns[137]. A two-stage depletion setup that involves serial IgY and Supermix columns has also been effective in increasing the number of detectable low-abundance proteins without affecting quantitative accuracy and precision using isobaric tags for relative and absolute quantification (iTRAQ)[134].

Recently, an updated reference database of human plasma proteins was released from the Human Plasma Proteome Project (HPPP) which includes 1929 nonredundant protein sequences[138]. This list includes proteins that were identified amongst ~ 30 laboratories that

utilized various enrichment and depletion strategies, shotgun proteomics techniques, and liquid chromatography-tandem mass spectrometry (LC-MS/MS) platforms. Herein, we report additions to the released reference database based on results obtained from the analysis of plasma samples in our laboratory by a dual depletion shotgun proteomics technique.

Quantitative proteomics analysis of plasma are useful for identifying clinically relevant biomarkers[139] or in understanding disease mechanisms such as Alzheimer's disease[140]. The inherent biological variability across human patients can require a large number of samples in order to determine differentially-expressed proteins that are statistically relevant. Depending on factors such as instrumental platform and available instrument time, multiplexing strategies are attractive. The commercial iTRAQ reagent allows up to eight samples to be multiplexed and has been effective in identifying biomarkers or differentially-expressed proteins in diseases[141-143]. Limitations to this quantitative approach can include cost of reagent kits and issues with underestimation of ratios[144].

Nonetheless, iTRAQ can provide reliable quantitative information depending on the statistical rigor required for denoting proteins as differentially expressed[7,17-20]. Several reports have stressed the importance of biological and technical replication in iTRAQ-based quantitative studies[142,145-147]. These reports however, do not converge on the same finite set of criteria for determining statistically relevant differentially-expressed proteins. For example, Song et al. suggest that at least 20 or eight biological samples are required in order to use fold-change cutoff values of 1.5 and 2.0, respectively[146]. Chee et al. employ a ± 30% or ± 50% cutoff for technical and biological replicates, respectively[145]. Most recently, a fold-change > two is deemed appropriate when at least six biological sample replicates are employed in order to have

sufficient statistical power[148]. That the criteria should even converge has also been questioned as it has been proposed that fold-change cutoff values are dependent on many factors: replications, number of observed peptides, protein class (e.g., high or low abundance), and so forth; specific values should be defined based on experimental goals and design[149].

Herein, we evaluate a robust tandem depletion quantitative proteomics workflow for its ability to provide additional insight to the human plasma proteome and to provide suitable criteria for the statistically relevant determination of differentially-expressed proteins in human plasma.

2.2 MATERIALS AND METHODS

2.2.1 Plasma Samples

Four plasma samples were obtained from patients enrolled in the Genetic and Inflammatory Markers of Sepsis (GenIMS) study[150]. These patients were initially diagnosed with community-acquired pneumonia upon admittance to the emergency department, and samples were collected; however, further diagnosis revealed improper initial assessment. Thus these samples come from otherwise healthy volunteers. Approval for the participation of human subjects was obtained by the Institutional Review Board of the University of Pittsburgh and other participating sites.

2.2.2 Tandem MARS Immunodepletion (TMD)

The Hu 6 MARS column depletes serum albumin, IgG, α-1-antitrypsin, IgA, transferrin, and haptoglobin proteins. An injection amount of 60 µL of crude plasma was applied to the MARS column (Agilent; Santa Clara, CA, USA), and after the initial depletion, flow-through fractions were concentrated with a 5K molecular weight cutoff concentrator (Agilent; Santa Clara, CA, USA) at 4695 g for 1.5 h. Samples (hereafter referred to as MD) were then stored at -80 ºC or reinjected onto the MARS column for tandem MARS depletion. The second flow-through fractions (hereafter referred to as TMD) were concentrated, and protein concentrations were measured using the BCA protein assay.

2.2.3 Protein Digestion and iTRAQ Labeling

In order to normalize experimental conditions, same amounts of protein (i.e., 100 µg) as determined from a BCA assay were employed. Protein amounts as opposed to sample volumes were used since the concentration of proteins in the flow-through fraction may vary across samples after TMD. A total of 100 µg of protein was denatured with an extraction buffer (0.2 M Tris, 8 M urea, 10 mM $CaCl_2$, pH 8.0), reduced with 1 : 40 molar excess of dithiothreitol for 2 h at 37 ºC, and then alkylated with 1 : 80 molar excess of iodoacetamide for 2 h on ice in the dark. The alkylation reaction was quenched by adding 1 : 40 molar excess of cysteine, and the mixture was incubated at room temperature for 30 min. Molar excesses for each reagent was calculated based on an estimation of the total moles of proteins in each sample (i.e., average molecular weight of 66 kDa). Tris buffer (0.2 M Tris, 10 mM $CaCl_2$, pH 8.0) was added to dilute the urea concentration to 2 M. Each sample was incubated with bovine TPCK-heated trypsin at 50 : 1

substrate : enzyme mass ratio for 24 h at 37 ºC. Digested samples were desalted with an HLB cartridge (Waters; Milford, MA, USA) and dried by centrifugal evaporation. Each sample was labeled with an iTRAQ reagent following the manufacturer's protocol (Applied Biosystems; Foster City, CA, USA) with slight modifications. Briefly, each iTRAQ reagent was solubilized with 70 µL ethanol and transferred to peptide mixtures. After 1.5 h of incubation, the reaction was quenched by adding 50 µL of water. Labeled samples were mixed in 1 : 1 : 1 : 1 ratios for iTRAQ reagents that generate reporter ions m/z 114 : 115 : 116 : 117, respectively.

2.2.4 Offline SCX Fractionation

For strong-cation exchange (SCX) liquid chromatography the separation was carried out on a Polysulfoethyl A 100 mm × 2.1 mm, 5 µm, 200 Å column (The Nest Group Inc,; Southborough, MA, USA) with buffers as follows: mobile phase A, 5 mM monopotassium phosphate (25% v/v acetonitrile, pH 3.0), and mobile phase B, 5 mM monopotassium phosphate and 350 mM potassium chloride (25% v/v acetonitrile, pH 3.0). Dried iTRAQ-labeled samples were resuspended in 300 µL of mobile phase A and injected onto the SCX column. The gradient for SCX was 0-3 min, 0% B; 3-45 min, 0-75% B; 45-50 min, 75-100% B; 50-55 min, 100% B; 55-56 min, 100-0% B; and 56-106 min, 0% B. Thirteen SCX fractions were collected and each fraction was desalted with an HLB cartridge.

2.2.5 LC-MS/MS Analysis

Online desalting and reversed phase chromatography was performed with a Nano 2D-LC system equipped with an autosampler (Eksigent; Dublin, CA, USA). Mobile phase A and B for

these analyses were 3% (v/v) acetonitrile with 0.1% formic acid and 100% (v/v) acetonitrile with 0.1% formic acid, respectively. SCX fractions were solubilized in 50 µL of H_2O with 0.1% formic acid and filtered with a 0.45 µm filter (Thermo Fisher Scientific; Waltham, MA, USA). For each run, 5 µL of sample was loaded onto a trapping column (100 µm i.d. × 2 cm), which was packed in-house with C_{18} 200 Å stationary phase material (Michrom Bioresource Inc.; Auburn, CA, USA) at 3 µL/min in 3% mobile phase B for 3 min. After desalting, the sample was loaded onto the analytical column (75 µm i.d. × 13.2 cm), which was packed in-house with C_{18} 100 Å stationary phase material (Michrom Bioresource Inc.; Auburn, CA, USA). Data-dependent acquisition parameters were as follows: the MS survey scan in the Orbitrap was 60,000 resolution over 300-800 *m/z*; CID was performed in the ion trap with normalized collision energy 35%; HCD was recorded in the Orbitrap with normalized collision energy 45% and 7,500 resolution; the top six most intense ions in the parent MS scan were selected and activated using CID and HCD[115]; dynamic exclusion was enabled with a repeat count of two for a duration of 60 sec; a minimum of 5000 ion counts were necessary for fragmentation events. Each fraction was subject to triplicate LC-MS/MS.

2.2.6 Database Searching

.RAW files were analyzed with Proteome Discoverer 1.2 software (Thermo Scientific; Waltham, MA, USA). Both CID and HCD spectra were used to obtain sequence information against the UniProt human database (04/25/2010, 20295 sequences). Sequest search parameters were as follows: enzyme specificity was trypsin with two maximum miscleavages: precursor mass tolerance was 10 ppm; fragment mass tolerance was 0.8 Da; N-terminus and lysine

modification with iTRAQ (144.102 Da) and cysteine carbamidomethylation (57.021 Da) were set as fixed modifications; tyrosine modification with iTRAQ was set as a dynamic modification. Decoy database searching was employed to generate medium ($p < 0.05$) and high ($p < 0.01$) confidence peptide lists. All peptides with medium and high confidence were pooled into a single data file and used for final protein identification and quantitation. Proteins with at least two spectral counts in a workflow replicate were included for identification. Only proteins with at least two spectral counts in a technical replicate were considered for quantitative and statistical analysis.

2.2.7 Protein Quantification and Statistical Analysis

Peptide ratios (e.g., 115/114, 116/114, and 117/114) were calculated based on peak intensity of each reporter ion. The protein ratios were the median ratio of the corresponding peptide ratios. Coefficient of variance (CV) values were calculated for ratios of proteins quantified in at least two workflow replicates. The mean CV value across workflow replicates was calculated and used as the total biological variation, S_b. The technical variation, S_t, was calculated for proteins quantified in at least two LC-MS/MS analyses within an individual workflow. The relation between the fold-change (F), random variation (S), biological replicates per group (n), and technical replicates (m) has been previously reported[151] and is expressed by the formula

$$n = 2\frac{(Z+T)^2 S^2}{(F-1)^2} \qquad \text{(eq 2.1)}$$

$$S^2 = \frac{S_b^2}{n} + \frac{S_t^2}{nm} \qquad \text{(eq 2.2)}$$

The quantities Z and T depend on the power of the test and the significance level, respectively. The power and significance levels were set as 0.8 and 0.05, respectively, such that the formula approximates to

$$n = \frac{20S^2}{(F-1)^2} \qquad \text{(eq 2.3)}$$

$$F = \frac{4.47S}{n^{1/2}} + 1 \qquad \text{(eq 2.4)}$$

One-way ANOVA analysis ($p < 0.05$) was performed for proteins quantified in at least two workflow replicates utilizing Microsoft Excel.

2.3 RESULTS AND DISCUSSION

A robust quantitative shotgun proteomics workflow (Figure 2.1a) was assessed for its ability to identify new human plasma proteins and to guide future experimental designs. The workflow uses TMD, iTRAQ 4-plex reagents, SCX fractionation, and nanoflow LC-MS/MS on a LTQ-Orbitrap Velos MS. The entire workflow was repeated three times using new aliquots of four plasma samples that were subject to TMD using a Hu 6 MARS column. The time it takes to complete a single workflow replicate is ~ 7 days with a majority of the costs being attributed to the MARS column ($5493 and ~ 200 analyses per column) and the iTRAQ reagents ($1390 and five analyses per kit). Immunodepletion of samples is very reproducible for single-stage MD (Figure 2.1b) and TMD (Figure 2.1c). It is apparent from the chromatograms (Figures 2.1b and c) that high-abundance proteins (i.e., t_r ~ 12.5 min) are substantially depleted after the TMD step. The average % depletion of the six high-abundance proteins is 88% and 92% for MD and TMD,

respectively (Supplemental Table S2.1) and is similar to that obtained using other tandem depletion strategies. It should be noted that albumin was still detectable after TMD; however other abundant proteins (i.e., α-1-antitrypsin, IgG, IgA, transferrin, and haptoglobin) did not have any observed peptide hits. The most abundant protein detected based on spectral counts (SCs) was complement C3 which had an average total SCs of > 4000 across the workflow replicates. The use of a single column to perform dual immunodepletion minimizes the expenses associated with the use of multiple MARS or other depletion columns.

TMD samples were used for further iTRAQ tagging reactions and analyzed with SCX LC-MS/MS (Figure 2.1a). A total of 689 unique proteins were identified from the combined results of the three independent workflow experiments (Supplemental Table S2.2) and are slightly larger than the number of proteins observed in other reports[133,137,146,152]. The proteins identified in this study were compared to the recently release 2011 HPPP plasma protein database to assess the depth of proteome coverage. Based on comparisons of identified proteins to the 1929 nonredundant sequences reported in HPPP, 399 novel proteins with ≥ 2 SC are uniquely observed in these studies (Figure 2.2a). Although the incorporation of a dual depletion step and SCX fractionation increases experimental sample preparation time, our results support the necessity of these (or similar) steps for identification of commonly detected and novel plasma proteins. Due to different experimental designs, LC-MS/MS data acquisition settings, and searching engines, the number of identified proteins may vary a lot across laboratoies. It is also possible that a portion of the identification is a result of profiles specific to the sample employed.

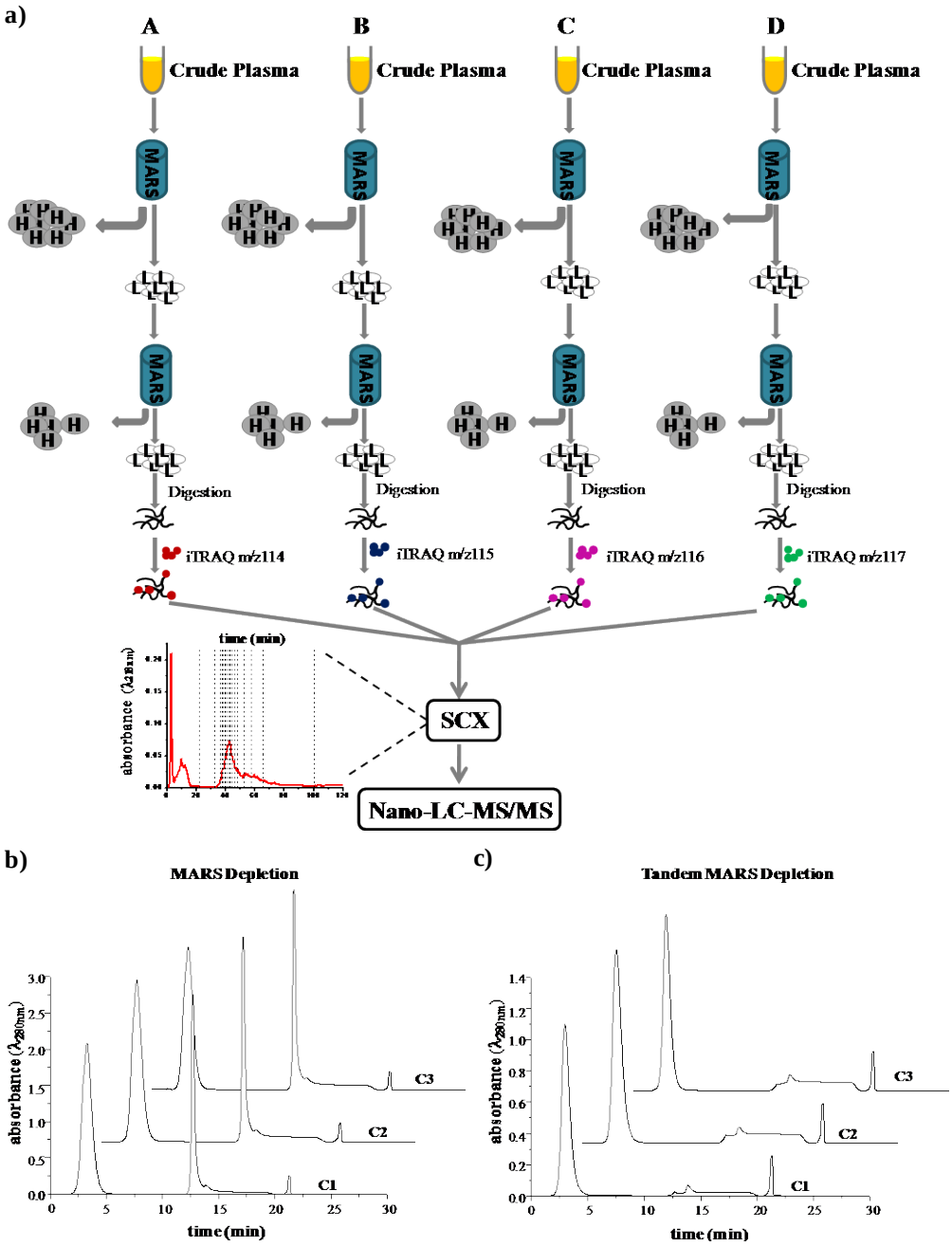

Figure 2.1. Quantitative proteomics workflow for human plasma. **a)** the iTRAQ-based quantitative platform used for plasma proteome analysis in which the flow-through fractions from four crude plasma samples (A-D) are modified with iTRAQ 4-plex reagents, pooled into a single mixture, and separated with offline SCX-LC-MS/MS. Example chromatograms (λ_{280nm}) from three independent injections of plasma sample C upon **b)** MD and **c)** TMD are shown.

Proteins identified are provided in Supplemental Table S2.2. A total of 207 proteins were observed in all three of the workflow experiments, and more than half of the total proteins were observed in a single workflow replicate (Figure 2.2b). With more stringent criteria (i.e., not less than 2 unique peptides for protein identification), 209 proteins were identified across three workflow replicates, and 40 new proteins were identified in these studies in comparison to HPPP database.

The datasets collected from this TMD strategy were used to examine the variation in the entire workflow. iTRAQ reporter ion (i.e., *m/z* 115, 116, 117) ratios were calculated with respect to *m/z* 114 for each protein. Proteins quantified by at least two SCs were used in the assessment of variation. Of the 207 proteins identified in all three workflow replicates, 139 proteins (with at least two SC) were quantified in the Proteome Discoverer analysis. These proteins were used to initially assess the variance in reporter ion ratios across the workflow replicates (of which each includes three technical replicates) by employing well-established statistical approaches[151,153-156]. We refer to a technical replicate as the cumulative results obtained across individual LC-MS/MS analysis of the 13 SCX fractions. Thus within a single workflow experiment three technical replicates were measured. The workflow replicate assesses the variation beginning with the start of the plasma sample preparation.

Figure 2.3a plots the distribution of CV values for proteins as a function of reporter ion ratios (e.g., 115/114, 116/114, and 117/114). The distribution of SD values for proteins as a function of $\log_2$ transformed ratios are provided in Supplemental Figure S2.1. Within a single workflow replicate, the average reporter ion ratio across technical replicates was calculated for

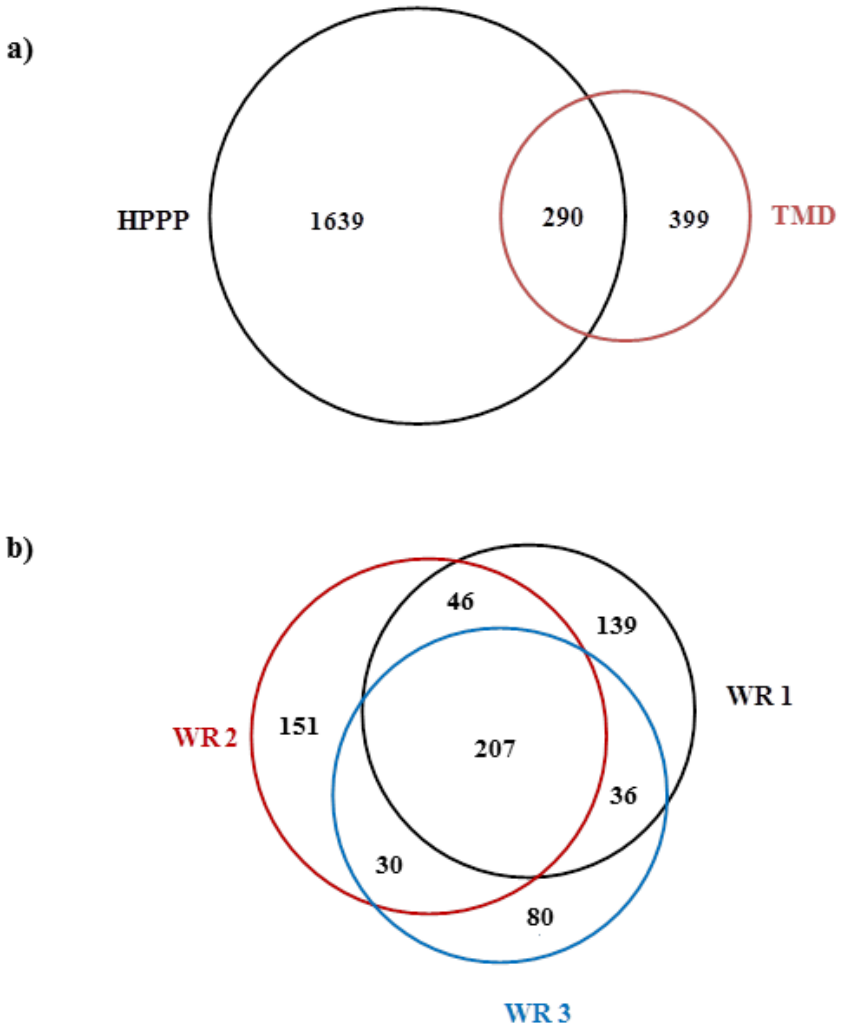

Figure 2.2. Venn diagram for proteins identified using the TMD workflow. **a)** Venn diagram for proteins identified in the human plasma proteome project (HPPP) and the TMD workflow presented herein. **b)** Venn diagram for proteins identified in three workflow replicate (WR) experiments.

individual proteins. The corresponding mean (and median) CV values for ratios 115/114, 116/114, and 117/114 across all proteins quantified in the three workflow replicates was ± 0.16 (0.13), 0.13 (0.11), and 0.11 (0.09), respectively. Seventy-five percent of proteins had a CV < 0.16, and 90% of proteins had a CV < 0.21 when reporter ion 114 was used as the reference channel. Because the reporter ion channel used as the reference can have some effect on quantitation, the mean (and median) CV values were also calculated for different reference channels (Supplemental Table S2.3). When reporter ions *m/z* 115, 116, and 117 were used as the reference channel, 90% of proteins had a CV value < 0.28, 0.21 and 0.24, respectively. This range of CV values that results from selection of different reference channels reflects the variation inherent in the four plasma samples as well as any variation that arises during LC-MS/MS analysis.

Incorporation of multiple workflow or technical replicates does not imply that proteins will be observed in all experiments (Figure 2.2b); therefore CV values were also calculated for the 71 proteins that were only quantified in any two of the three workflow replicates. When reporter ion *m/z* 114 was used as the reference channel, the mean (and median) CV was ± 0.30 (0.23), 0.20 (0.15), and 0.18 (0.15) for ratios 115/114, 116/114, and 117/114, respectively (Supplemental Table S2.3). The higher CV observed for this set of proteins agrees with the notion that less replication (workflow and technical) could lead to higher variation in reporter ion ratios[147,153] as well as biases that arise in low-abundance proteins due to lower numbers of detected SCs and higher variability due to lower intensity signals[149]. Higher variability in reporter ion ratios correlated with proteins that were identified with lower numbers of SCs (Figure 2.3b).

In order to estimate the overall variance of this workflow, CV values were obtained for proteins quantified in at least two of the workflow replicates (N = 210). The mean CV was 0.21, 0.15, and 0.13 for ratios 115/114, 116/114, and 117/114, respectively, and similar values were obtained for other reference channels (Supplemental Table S2.3). Taking the CV values of reference channels 114 into consideration, the overall variation in the entire plasma workflow is ~ 0.16. Herein, the technical variation was assessed by considering proteins observed in multiple LC-MS/MS analyses for individual workflow replicates. The technical variation is ~ 0.10 for proteins quantified in at least two replicates (Supplemental Table S2.4). In order to determine proteins that were quantified similarly across workflow replicates, one-way ANOVA analysis ($p < 0.05$) was carried out. Based on these results, ~ 70 of the 210 quantified proteins have similar ratios across workflow replicates.

Power analysis was also performed in order to assess the fold-change criterion that should be applied based on a given number of biological replicates (Figure 2.3c). We note that our experimental approach (i.e., repeating the workflow using new aliquots of the same plasma samples) does not represent a true biological replicate. However, this analysis still provides statistical insight to the power of biological replication in future experimental designs. The total biological variance (S_b), technical variance (S_t), power, and significance level applied were 0.16, 0.10, 80%, and 0.05, respectively. As indicated in Figure 2.3c, if ten biological replicates per group are used then a fold-change cutoff of 1.3 can be applied, and only two replicates are required to use the commonly applied 2.0 fold-change cutoff. Technical replicates do not appear to have a significant effect on the fold-change criterion when multiple biological replicates will be used (Figure 2.3c). These data provide additional evidence to support the notion that

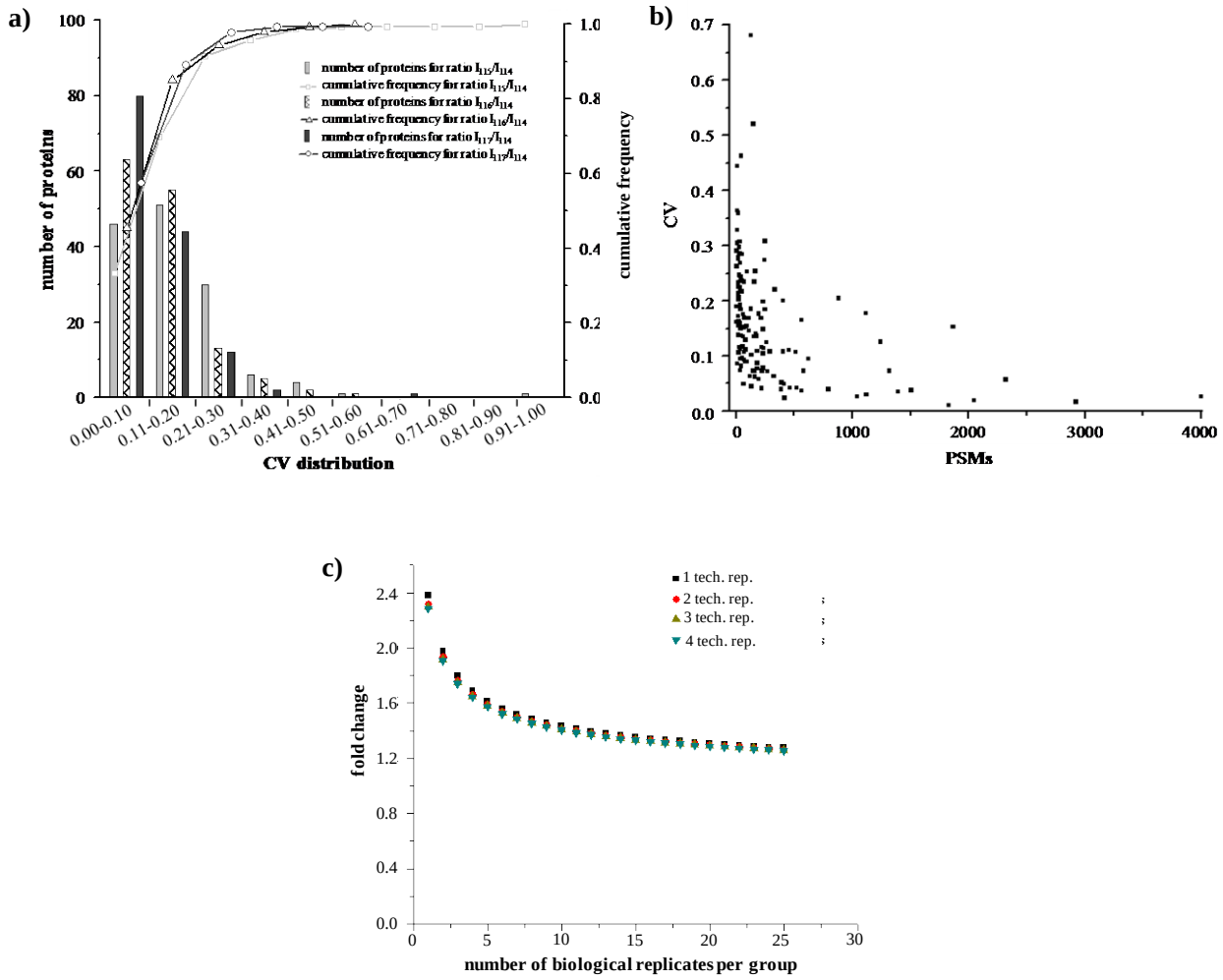

Figure 2.3. The variation of proteomics workflow for human plasma. **a)** The distribution of CV values for I_{115}/I_{114} (grey rectangular), I_{116}/I_{114} (shaded rectangular), and I_{117}/I_{114} (black rectangular) for proteins quantified in each of the three independent experiments (N = 139 proteins). The cumulative frequency of proteins with specific CV values for I_{115}/I_{114} (dashed square), I_{116}/I_{114} (dashed triangle), and I_{117}/I_{114} (dashed circle) are shown. **b)** Plot of the mean CV values for reporter ion ratios relative to reference channel 114 as a function of the number of spectral counts identified for each protein. Only proteins identified in all three workflow replicates are represented in this plot. **c)** Power analysis for iTRAQ-based quantitative platform whereby fold-change values are plotted for a given number of biological replicates as a function of the number of technical replicates (i.e., m = 1 to 4). The power and significant level values were set to 80% and 0.05, respectively.

biological replication (i.e., in these studies workflow replication) is one of the most important factors that should be considered in the experimental design[145,148,151].

2.4 CONCLUSIONS

This chapter has presented a robust quantitative plasma proteomics workflow that involves tandem MARS depletion, iTRAQ tagging, and SCX-LC/MS/MS analysis. The use of TMD and SCX fractionation resulted in the identification of 689 proteins with ≥ two SCs. Compared to the HUPO database, ~ 400 of these proteins were previously unreported. The use of TMD and SCX fractionation significantly increases the number of proteins detected. The overall variation in the presented workflow range from ± 11 to 30%, and power analysis indicates that increasing biological replication would allow a lower fold-change cutoff to be applied to determine statistically relevant differentially-expressed proteins. **Chapter 4** in this dissertation involves the application of this workflow to sepsis whereby biological replicates are also being incorporated into the experimental design.

3.0 MS^3-BASED QUANTITATIVE PROTEOMICS USING PULSED-Q DISSOCIATION

3.1 INTRODUCTION

Quantitative proteomics using mass spectrometry (MS) offers several methods to perform relative quantitation between multiple samples with stable isotopes[101]. Precursor isotopic labeling employs light and heavy chemical tags to generate peptide pairs or triplets in parent MS scans[157,158]. Such methods include stable isotope labeling by amino acids in cell culture (SILAC)[159], acetylation[160], dimethylation[161], isotope-coded affinity tags (ICAT)[162], $^{16}O/^{18}O$ labeling[163], isotope coded protein labeling[164], and neutron encoded labeling[105,106,165]. A second approach uses isobaric tags such as tandem mass tags (TMT)[107], isobaric tags for relative and absolute quantitation (iTRAQ)[102], deuterium isobaric amine-reactive tags (DiART)[166], and dimethyl leucine tags[167]. Proteins can be quantified based on the reporter ion signals generated from tandem mass spectrometry (MS/MS). **Chapter 2** has demonstrated the ability of the iTRAQ-based proteomics method to quantify proteins in complex biological samples. Isobaric tags can offer multiplexing up to ten samples simultaneously through isotopologues resolved with high resolution instruments[104-106]. Combination of precursor isotopic labeling and isobaric tagging results in enhanced multiplexing[168-171].

A major limitation to the isobaric tagging method is ratio distortion of reporter ions. This occurs due to coisolation and cofragmentation of closely spaced peptides within a given isolation window[144]. Gas phase purification[172], analysis of TMT complement reporter ion clusters[173], and triple stage mass spectrometry (MS^3)[174] can help minimize cofragmentation of neighboring peptides and provide accurate reporter ion ratios. MS^3 is possible on any hybrid ion trap/Orbitrap

MS instrument without the need for hardware or software modifications[174]. TMT or iTRAQ-tagged peptide ions are fragmented with collision induced dissociation (CID), from which, the most intense fragment ions are isolated and subject to higher energy collision dissociation (HCD) in order to detect reporter ions[174]. HCD-MS^3 offers high fragmentation efficiency and reproducibility. Additionally, reporter ion detection using the Orbitrap gives high resolution and mass accuracy[104,168,170]. The duty cycle of HCD-MS^3, however, is lower compared to HCD-MS/MS, which reduces the number of identified and quantified proteins[174]. Reporter ion channels have a higher probability of missing signal due to relatively low sensitivity of the MS^3 acquisition and Orbitrap[175]. Particularly, the HCD-MS^3 method, is only applicable to laboratories which have access to high resolution Orbitrap MS instruments.

Pulsed-Q dissociation (PQD) is an alternative fragmentation method for reporter ion detection on linear ion trap (LTQ) platforms[176-178]. PQD-MS/MS on the LTQ offers faster scan rates and improved sensitivity and provides comparable quantitative accuracy compared to the HCD-MS/MS on an Orbitrap[176-178]. PQD for MS^3 data acquisition has not been investigated. Herein, we present a new reporter ion quantitation method using PQD-MS^3 on an LTQ-Orbitrap MS. Recently, our laboratory has shown that selection of y_1 ions (e.g., lysine-TMT tagged ion) for MS^3 data acquisition offers an alternative method to the selection of the most intense fragment ion in CID MS/MS spectra[168]. Therefore, we assessed the performance of top ion and y_1 ion selection of TMT-labeled peptides using PQD-MS^3. Higher numbers of identified and quantified proteins and spectral counts are obtained using PQD-MS^3 compared to HCD-MS^3. PQD-MS^3 methods provide accurate reporter ion ratios comparable to HCD-MS^3. Finally, we demonstrate accurate reporter ion quantitation with PQD-MS^3 on an LTQ instrument.

3.2 EXPERIMENTAL AND MATERIALS

3.2.1 Mouse Brain Samples

Wild-type (WT) male mice (14 months old, C57BL/6J) were purchased from Jackson Laboratory and housed in the Division of Laboratory Animal Resources at the University of Pittsburgh. Mice were fed standard Purina rodent laboratory chow *ad libitum* on a 12 h light/dark cycle. All animal protocols were approved by the Institutional Animal Care and Use Committee at the University of Pittsburgh. Brain tissue was harvested from one such mouse.

3.2.2 Brain Protein Extraction and Digestion

Brains were homogenized in PBS buffer with 8 M urea, centrifuged at 13,000 rpm, and the protein concentration of the supernatant was determined by BCA assay. Proteins (200 µg) were reduced with 1 : 40 molar excess of dithiothreitol for 2 h at 37 °C, and then alkylated with 1 : 80 molar excess of iodoacetamide for 2 h on ice in the dark. The alkylation reaction was quenched by adding 1 : 40 molar excess of cysteine, and the mixture was incubated at room temperature for 30 min. Tris buffer (0.2 M Tris, 10 mM $CaCl_2$, pH 8.0) was added to dilute the urea concentration to 2 M. Proteins were digested with trypsin at 1 : 50 protein : enzyme for 24 h at 37 °C. Protein digests were split into four aliquots with the ratio 1 : 1 : 2 : 5 (10µg : 10µg : 20µg : 50µg) and labeled with TMT-128, 129, 130, and 131 reagents, respectively, according to the manufacturer's protocol (Thermo Fisher Scientific; Waltham, MA, USA). After TMT-labeling, four samples were combined, cleaned up with HLB cartridge (Waters; Milford, MA, USA), and dried with SpeedVac.

3.2.3 LC-MS^3 Acquisition

The combined mixture was separated using nanoflow reversed phase liquid chromatography (nRPLC)[168] and eluted peptides were nanosprayed into an LTQ-Orbitrap Velos instrument. Triplicate injections were performed. Data-dependent acquisition parameters were as follows: parent scan range 300-1800 *m/z*, 60,000 resolution, automated gain control (AGC) $1x10^6$. To keep the cycle time between HCD-MS^3 and PQD-MS^3 similar (~ 2.4 s), the top four or top seven ions from parent MS scans were selected for CID [35% normalized collision energy (NCE), 2.0 isolation window, and 10 ms activation time] followed by either HCD-MS^3 (4.0 isolation window, 60% NCE, activation time 0.1 ms, and AGC 3×10^5) or PQD-MS^3 (4.0 isolation window, 33% NCE, activation Q 0.5, activation time 0.1 ms, and AGC 7×10^4), respectively. PQD-MS^3 was also applied on a LTQ-Orbitrap Velos using the dual ion trap only and a stand-alone LTQ as follows: parent scan range 300-1800 *m/z* and AGC $3x10^4$. The top seven ions from parent MS scans were selected for CID (35% NCE, 2.0 isolation window, 10 ms and 30 ms activation time for LTQ Velos and LTQ data acquisition, respectively) followed by PQD-MS^3 (LTQ Velos data acquisition: 4.0 isolation window, 33% NCE, activation Q 0.5, activation time 0.1 ms, AGC 7×10^4; LTQ data acquisition: 4.0 isolation window, 27% NCE, activation Q 0.7, activation time 0.1 ms, AGC 1.5×10^5). The most intense CID fragment ion within the range 300-800 *m/z* (termed as HCD-MS^3-top ion or PQD-MS^3-top ion) or the CID y_1 fragment ion (m/z 376.3; termed as HCD-MS^3-y_1 or PQD-MS^3-y_1) was selected for MS^3. Dynamic exclusion was disabled in order to increase the probability of acquiring MS^3 spectra without missing reporter ion values.

3.2.4 Data Analysis

.RAW files were searched against the International Protein Index (IPI) mouse proteome database (v3.87, 59534 sequences, 08/16/2012) using SEQUEST with the following parameters: trypsin with two miscleavages, 15 ppm and 1 Da parent mass tolerance for LTQ-Orbitrap and LTQ platform analysis, respectively, 1 Da fragment mass tolerance, static modifications of TMT tags (229.163 Da) on the N-termini and lysine residues, carbamidomethyl (57.021 Da) on cysteine, dynamic modification of oxidation (15.995 Da) on methionine. Decoy database searching was enabled using a reverse protein database with false discovery rates set at 0.01 and 0.05 for high and medium confidence peptides, respectively. Search results were processed and reporter ion intensities were extracted (centroid with smallest delta mass, 20 ppm and 0.4 Da integration tolerances for HCD-MS^3 and PQD-MS^3, respectively) using Proteome Discoverer v1.4 (Thermo Scientific; Waltham, MA, USA).

3.3 RESULTS AND DISCUSSION

The workflow for this study is shown in Figure 3.1. Mouse brain proteins were digested with trypsin, split into four aliquots with the ratio 1 : 1 : 2 : 5, labeled with TMT-128, 129, 130, 131 reagents, respectively. After labeling, the four aliquots were pooled as one single mixture and analyzed by different methods (Figure 3.1). Trypsin was selected as the protease because it gives more identified and quantified peptides and proteins for HCD-MS^3 [168,175]. Direct infusion experiments using TMT-labeled angiotensin II were performed to calculate the time required for HCD-MS^3 and PQD-MS^3 top ion methods (*data not shown*). It was determined that MS^3

fragmentation of the top four and seven ions for HCD-MS^3 and PQD-MS^3, respectively, resulted in similar instrument cycle times between each parent scan (~ 2.4 s). Figures 3.2a, b, d, and f demonstrate an example peptide quantified with HCD-MS^3-top ion and PQD-MS^3-top ion. The peak at *m/z* 683.4247 in the parent scan (Figure 3.2a) has been identified as the peptide N(TMT_6)LLSVAYK(TMT_6) from CID MS/MS data (Figure 3.2b). This peptide corresponds to protein 14-3-3β protein. The y_5 ion (m/z 796.65) was isolated and fragmented in HCD- (Figure 3.2d) and PQD-MS^3-top ion (Figure 3.2f), respectively. Reporter ion ratios of 1.0 : 1.1 : 2.5 : 5.6 and 1.0 : 1.0 : 2.3 : 5.4 were obtained from HCD- and PQD-MS^3-top ion, respectively (inserts of Figure 3.2d and f). Box plots of ratios for all TMT-tagged proteins are shown in Figure 3.3a for HCD- and PQD-MS^3-top ion. Calculated protein ratios obtained in HCD-MS^3-top ion and PQD-MS^3-top ion were 1.0 ± 0.1, 2.0 ± 0.3, 5.6 ± 0.8 (N = 113, average ± standard deviation) and 1.2 ± 0.6, 2.3 ± 1.5, 5.4 ± 3.8 (N=156, average ± standard deviation), respectively. The PQD-MS^3-top ion method provides accurate protein ratios similar to HCD-MS^3. However, lower precision of reporter ion ratios was observed using PQD-MS^3-top ion (Figure 3.3). This can be attributed to lower reproducibility and inefficiency of PQD fragmentation compared to HCD[176-178]. For example, the y_5 ion is the base peak in MS^3 spectra from PQD-MS^3-top ion (Figure 3.2f) indicating low fragmentation efficiency.

A complete list of identified proteins (Supplemental Table S3.1) and peptides (Supplemental Table S3.2) is provided. There is an apparent increase in the total number of identified and quantified proteins and peptides when comparing PQD-MS^3-top ion with HCD-MS^3-top ion. The number of identified spectral counts [(SCs), (total proteins)] was 9897 (135) and 16502 (186) for HCD- and PQD-MS^3-top ion, respectively (Table 3.1). We attribute this

increase to the faster scan rates of the LTQ (PQD-MS^3-top ion)[179]. The LTQ performs more CID MS/MS and PQD-MS^3 scans in the same amount of time compared to Orbitrap HCD-MS^3 (i.e., 50360 vs 30374). This resulted in an increased number of quantified SCs (proteins) from 7473 (113) for HCD-MS^3-top ion to 9776 (156) for PQD-MS^3-top ion (Table 3.1).

Recently, we reported a global combined precursor isotopic labeling and isobaric tagging (cPILOT), which incorporates selective HCD-MS^3 acquisition[168]. The selective MS^3 isolates the y_1 CID fragment arising from C-terminal lysine-TMT tagged peptides and increases MS^3 spectra containing a reporter ion[168]. Herein, the performance of HCD-MS^3-y_1 and PQD-MS^3-y_1 was also assessed. Figure 3.2 shows a sample spectra for the peptide N(TMT_6)LLSVAYK(TMT_6). Selection of the y_1 fragment ion for HCD-MS^3 and PQD-MS^3 (Figures 3.2c and e, respectively) results in reporter ion ratios of 1.0 : 1.1 : 2.2 : 5.7 and 1.0 : 1.0 : 2.0 : 5.6.

Measured $\log_2$ protein ratios are 1.0 ± 0.2, 2.0 ± 0.7, 5.3 ± 0.9 (N = 114, average ± standard deviation) and 1.2 ± 1.1, 2.5 ± 1.5, 6.4 ± 3.8 (N = 199, average ± standard deviation) for HCD-MS^3-y_1 and PQD-MS^3-y_1, respectively (Figure 3.3b). The number of identified and quantified proteins increased by 26% (from 180 to 226) and 75% (from 114 to 200), respectively in PQD-MS^3-y_1 compared with those in PQD-MS^3-y_1 (Table 3.1). Similarly, this increase can be due to the faster scan rate of the LTQ.

Consistent with our previous reports[168], HCD- and PQD-MS^3-y_1 increased the number of identified SCs and proteins compared to the corresponding top ion methods (Table 3.1). Quantified SCs and proteins also increased in PQD-MS^3-y_1 in comparison to PQD-MS^3-top ion, whereas quantified spectral counts decreased in HCD-MS^3-y_1 compared to HCD-MS^3-top ion (no significant difference in the number of quantified proteins) (Table 3.1). This may be

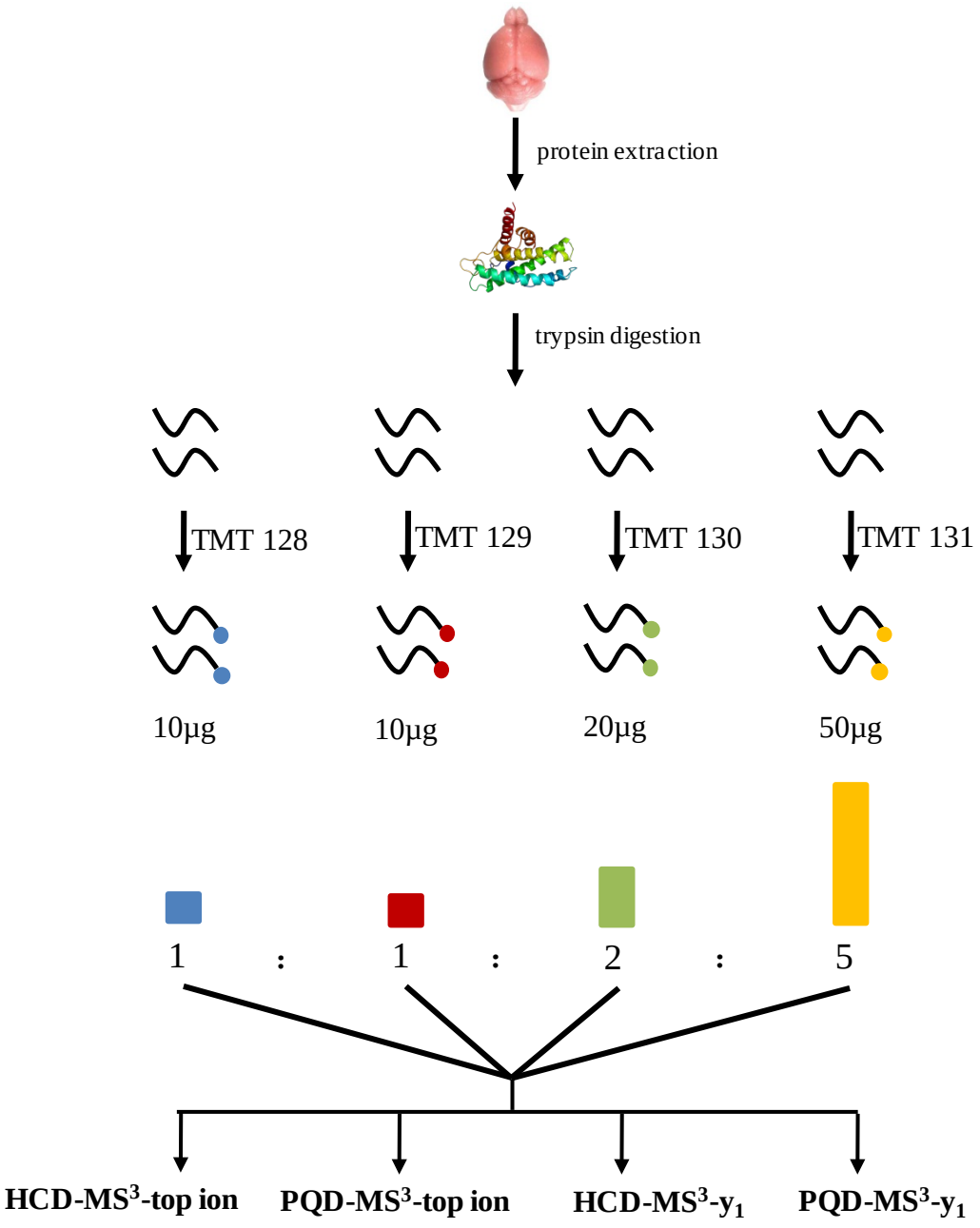

Figure 3.1. Schematic diagram of the proteomics workflow involving mouse brain protein digestion, TMT tags labeling and mass spectrometry analysis with different instrument methods.

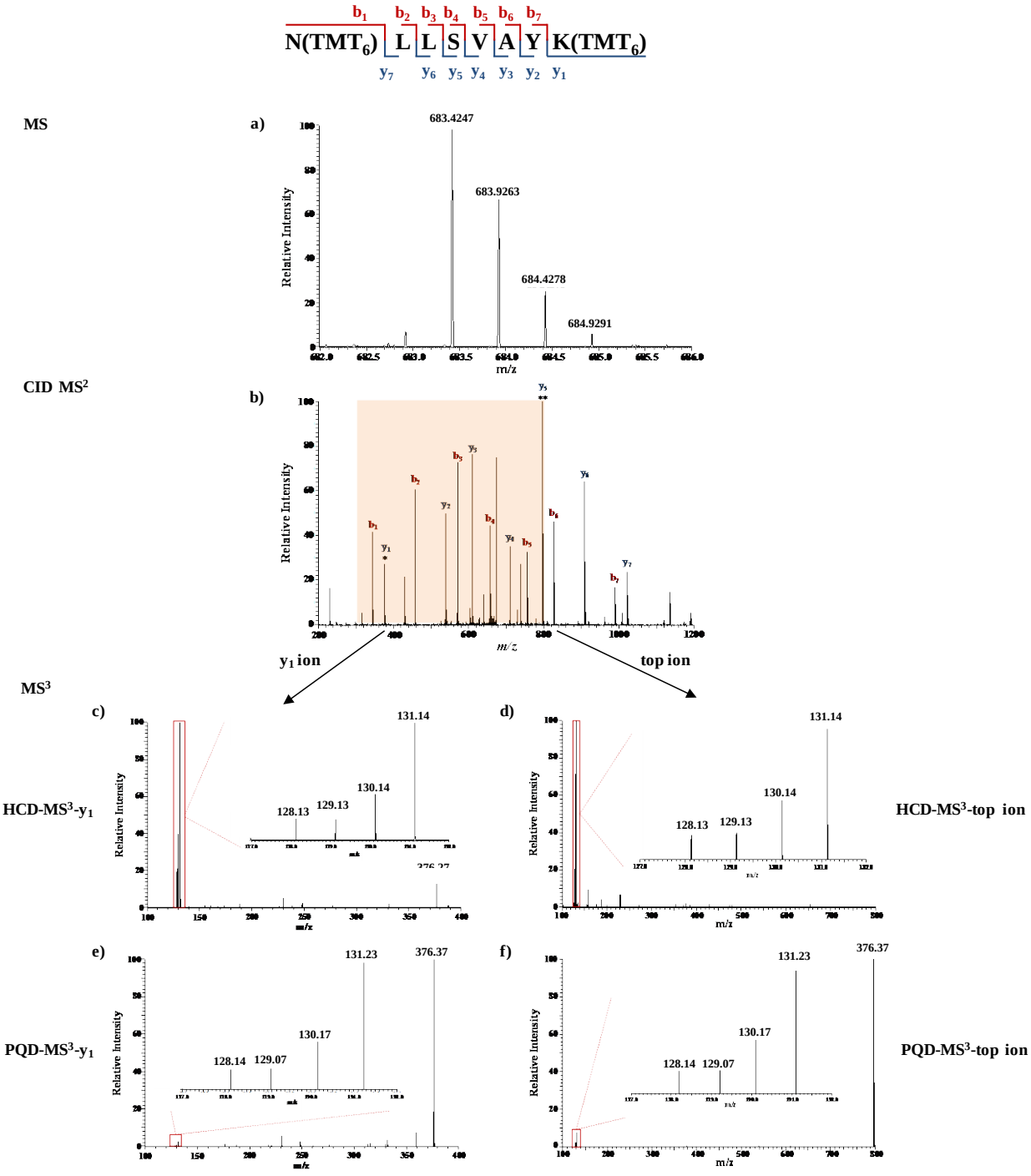

Figure 3.2. Example of HCD- and PQD-MS^3 results. **a)** MS spectrum for the peptide $N(TMT_6)LLSVAYK(TMT_6)$, and **b)** the corresponding CID MS^2 spectrum for the peptide identification. The shaded region corresponds to the m/z range (300-800) for the selection of the most intense ion for

MS^3. The (**) indicates the most intense ion selected for MS^3 in **d)** HCD-MS^3-top ion and **f)** PQD-MS^3-top ion. The (*) indicates the y_1 ion selected for MS^3 in **c)** HCD-MS^3-y_1 ion and **e)** PQD-MS^3-y_1 ion. Inserts in **c-f)** are the corresponding reporter ion intensity.

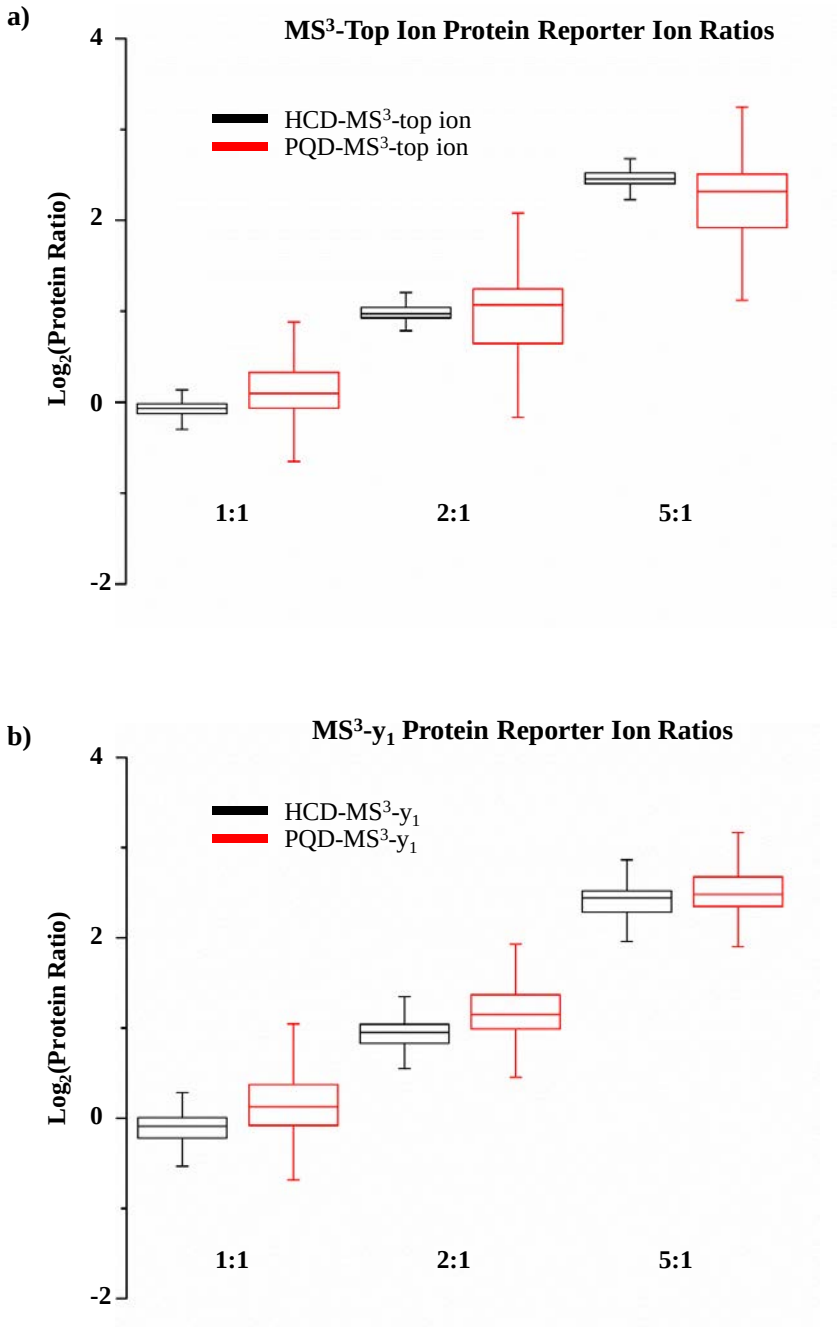

Figure 3.3. Box plots of measured $\log_2$ protein reporter ion ratios using **a)** HCD-MS^3 top ion and PQD-MS^3-top ion and **b)** HCD-MS^3-y_1 and PQD-MS^3-y_1. Theoretical ratios are 1 : 1, 2 : 1, and 5 : 1.

Table 3.1. Number of spectral counts and proteins identified and quantified in each MS^3 method.

	Identification		**Quantitation**	
	Spectral counts	**Protein**	**Spectral counts**	**Protein**
HCD-MS^3-top ion	9897	135	7473	113
PQD-MS^3-top ion	16502	186	9776	156
HCD-MS^3-y_1	13090	180	3530	114
PQD-MS^3-y_1	17392	226	11843	200

explained by the relatively low intensity of y_1 ion and low sensitivity of the Orbitrap. Our data shows that the intensity of y_1 ion is ~ 40% of the base peak in CID MS/MS. Selection of the y_1 ion results in lower signal of reporter ions in MS^3 spectra compared to the top ion method. The low signal can be detectable in the LTQ which has higher sensitivity but not in the Orbitrap. It should be noted that in our previous cPILOT report[168], the tagging chemistry was designed so that *b*-ions did not contain a TMT tag due to the N-termini being capped with a dimethyl group. The presented experiments show that accurate reporter ion quantitation can be obtained using PQD-MS^3-top ion and PQD-MS^3-y_1 methods. Additionally, selective PQD-MS^3-y_1 data collection results in increased protein and peptide identification and quantitation.

Finally, PQD-MS^3 was applied on two other mass spectrometer instruments: LTQ Velos and LTQ. We note that the LTQ Velos experiment was performed on the LTQ-Orbitrap Velos hybrid by performing all scan events using the dual linear ion trap. Using the LTQ Velos, PQD-MS^3-top ion and PQD-MS^3-y_1 resulted in accurate quantitation as 1.3 ± 0.9, 2.2 ± 1.2, 4.2 ± 2.8 (N = 84, average ± standard deviation) and 1.2 ± 0.9, 2.1 ± 1.2, 4.9 ± 2.6 (N = 119, average ± standard deviation), respectively (Figure 3.4). As described above, the number of identified and quantified proteins and peptides increases with the PQD-MS^3-y_1 method (*data not shown*). Similar experiments were performed on the LTQ, however only the PQD-MS^3-top ion resulted in reporter ion signal in MS^3. PQD-MS^3-y_1 using the LTQ did not result in any reporter ion signal in MS^3 spectra, which could be due to low sensitivity in the LTQ compared to the LTQ Velos [180]. When performing PQD-MS^3 experiments on an LTQ, we suggest to only use the top ion selection method. Lower number of identified and quantified proteins and peptides were also obtained using PQD-MS^3 on the stand-alone LTQ, which may be caused by the relatively slower

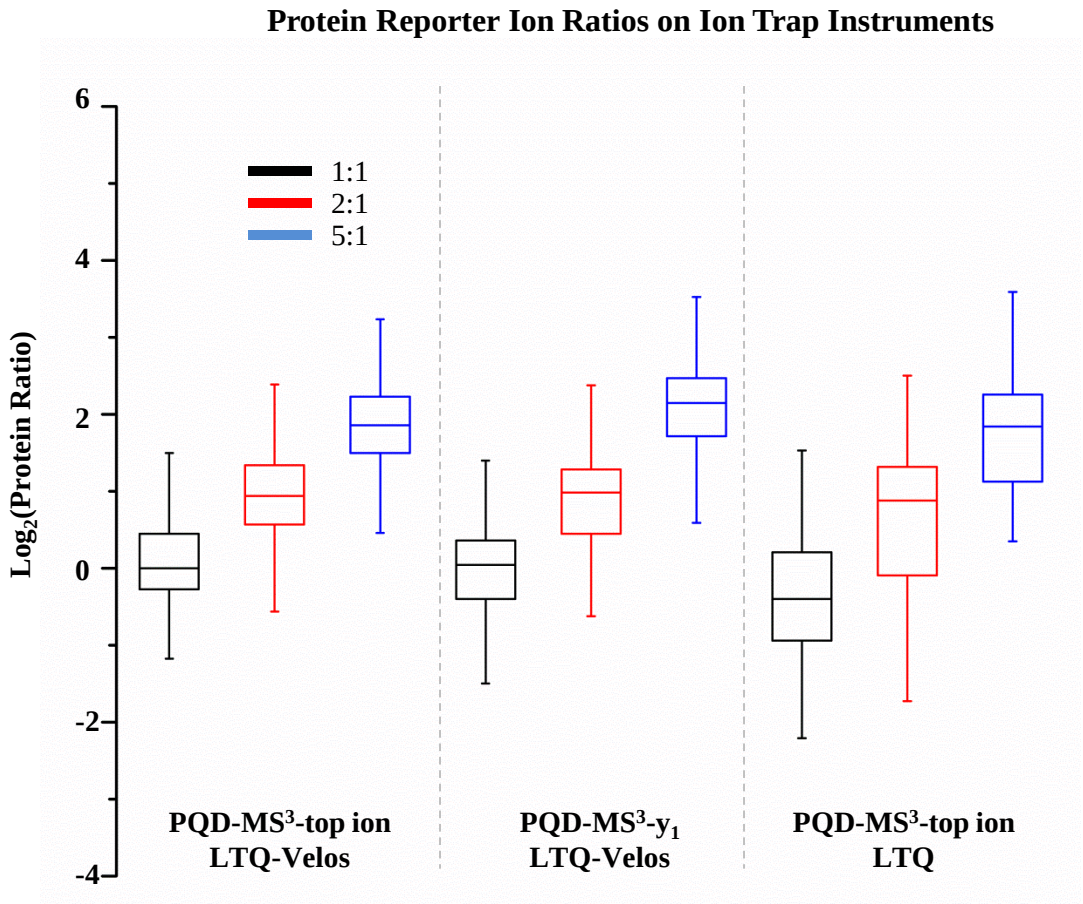

Figure 3.4. Box plots of the measured $\log_2$ protein ratios performing PQD-MS^3-y_1 LTQ Velos (N = 119), PQD-MS^3-top ion-LTQ Velos (N = 84), and PQD-MS^3-top ion-LTQ (N = 28).

scan rate of the LTQ. However, accurate protein reporter ion results, 1.0 ± 0.7, 1. 9± 1.2, 4.2 ±2 .8 (N = 28, average ± standard deviation), were obtained using PQD-MS^3-top ion (Figure 3.4). Overall, these experiments show that accurate proteomics quantitation can be obtained on lower resolution LTQ instruments.

3.4 CONCLUSIONS

This study demonstrates that PQD-MS^3 quantitation of isobaric tags is a feasible proteomics method. PQD-MS^3 takes advantage of the high sensitivity and fast scan rate of linear ion trap which leads to increased numbers of identified and quantified peptides and proteins. Accurate quantitation is achieved using PQD-MS^3 and is comparable to previously described HCD-MS^3 methods. Selective MS^3 fragmentation of the y_1 ion from CID spectra using PQD-MS^3 results in an even higher number of proteins and peptides quantitified. The PQD-MS^3 methods can be useful especially for laboratories which do not have access to an Orbitrap instrument.

4.0 PROTEOMICS REVEALS AGE-RELATED DIFFERENCES IN THE HOST IMMUNE RESPONSE TO SEPSIS[97]*

(*note that information in this Chapter is written based on a published paper, Cao, Z.; Yende, S.; Kellum, J. A.; Angus, D. C.; Robinson, R. A. S. *Journal of Proteome Research* **2013**, *13*, 422)

4.1 INTRODUCTION

Sepsis is a systemic inflammatory state triggered by infection. The additional diagnosis of multiple organ failure and hypoperfusion (e.g., hypotension, decreased urine output) along with sepsis results in severe sepsis[181]. One of the leading causes of sepsis is community-acquired pneumonia (CAP)[22,48,182]. The presence and severity of organ failure is one of the most important determinants of mortality following sepsis[17,183-187]. Severe sepsis affects ~ 750,000 persons annually in the United States[17,23,184-187] and is one of the most common causes of death in intensive care units[17,184-187].

Kellum and coworkers have shown that the incidence of severe sepsis and mortality rate increases sharply after the age of 65[16,188]. For example, CAP patients ≥ 85 years old have a 2.8-fold increased risk of severe sepsis and a 17-fold increased mortality rate compared to patients ≤ 50 years old[48]. The notable age-related differences in severe sepsis risk may be explained in part by immunosenescence underlying chronic disease. Immunosenescence is manifested in the elderly through decreased numbers of T-cells, impaired B-cell function, increased apoptosis of neutrophils, and reduced bactericidal response of macrophages[188-190]. Most studies that examine age-related differences in immune response using animal models and humans have largely focused on either the adaptive immune response or select pathways (inflammatory, coagulation, and fibrinolysis markers) in the innate immune response[189-195]. A comprehensive assessment of

differences in the immune response has not been conducted. Trials testing immunomodulating therapies for sepsis in broad populations have failed to consistently improve outcomes of sepsis patients[25]. An alternative approach is to personalize sepsis therapies based on host characteristics, such as age. To further the development of such a personalized approach, a better understanding of the differences in immune response due to age is necessary.

Herein, we conducted a nested case-control study using patients enrolled in an observational cohort of CAP. A semi-quantitative plasma proteomics workflow previously developed in our laboratory[196], which included tandem immunoaffinity depletion, isobaric tags for relative and absolute quantitation (iTRAQ) labeling, strong cation exchange (SCX) fractionation, and nanoflow liquid chromatography (LC) coupled to high resolution mass spectrometry (MS), was applied to patient samples. We analyzed plasma proteins on presentation to the emergency department (ED) to compare the acute immune response. First, proteins were identified that differed between those who did or did not develop severe sepsis (within 90 days of hospitalization) among younger and older adults separately. We hypothesized that there may be differentially-expressed proteins that are unique to the younger or older adults which would help to explain the increased risk of severe sepsis in older adults. In addition to identifying these sets of proteins, differentially-expressed proteins that are common to the younger and older adult groups were also identified. Interestingly, the direction of fold-change observed for these common proteins varies depending on patient age and thus may explain higher risk of severe sepsis in older adults. These results and the implications of this study are presented herein.

4.2 EXPERIMENTAL AND MATERIALS

4.2.1 Ethics Statement

The Institutional Review Boards at the following hospitals approved the study: Pennsylvania: Allegheny General Hospital, Jefferson Hospital/SHHS, Mercy Hospital, St. Clair Memorial Hospital, St. Francis Medical Center, Sewickley Valley Hospital, University of Pittsburgh Medical Center (UPMC) Braddock, UPMC Horizon, UPMC Lee, UPMC McKeesport, UPMC Passavant, UPMC Presbyterian, UPMC Shadyside, UPMC Southside, UPMC St. Margaret, West Penn Hospital; Connecticut: Bridgeport Hospital, Hartford Hospital, Milford Hospital, New Britain General Hospital, Norwalk Hospital, Yale-New Haven Hospital; Tennessee: Methodist Health Care (single IRB approval for three Methodist University sites); Michigan: Henry Ford Health System, Detroit Receving/Sinai-Grace, Wayne State. Written, informed consent was obtained from all participants or by proxy.

4.2.2 Study Design and Patients

We conducted a nested case-control study using patients enrolled in the GenIMS study[150]. GenIMS is a prospective multicenter observational cohort of patients with CAP enrolled in EDs of 28 academic and community hospitals in four US regions, including southwestern Pennsylvania, Connecticut, southern Michigan and western Tennessee. Details of this study including eligibility criteria have been described previously[48,150].

To compare differences in immune response across different age groups and between patients with and without severe sepsis, we identified a total of 39 patients from four groups. These included: 1) patients 50-65 years old who did not develop severe (hereafter referred to as

young controls [YC]), 2) patients 70-85 years old who did not develop severe sepsis (hereafter referred to as old controls [OC]), 3) patients 50-65 years old who developed severe sepsis within 90 days after presentation to the ED (hereafter referred to as young severe sepsis [YS]), and 4) patients 70-85 years old who developed severe sepsis within 90 days after presentation to the ED (hereafter referred to as old severe sepsis [OS]). To ensure that differences in immune response are attributed to age and not to ethnic differences or underlying chronic diseases, only whites and matched patients according to chronic disease burden were included (Table 4.1).

4.2.3 Plasma Samples and Tandem MARS Depletion

Plasma samples were obtained on day 1 when CAP patients were admitted to the ED and prior to most interventions to ensure that differences in immune response are not affected by therapeutic strategies. Negative results were obtained in the blood culture test used to identify the pathogenic source of the samples obtained from CAP patients. The Hu-6 MARS column (Agilent; Santa Clara, CA, USA) depletes serum albumin, IgG, α1-antitrypsin, IgA, transferrin, and haptoglobin proteins. An injection amount of 60 μL of crude plasma was applied to the MARS column and after the initial depletion flow-through fractions were concentrated with a 5K molecular weight cutoff concentrator (Agilent; Santa Clara, CA, USA) at 4695 g at 4 °C for 1.5 h. Samples were then stored at -80 °C or re-injected onto the MARS column for tandem MARS depletion. The second flow-through fractions (hereafter referred to as TMD) were concentrated and protein concentrations were measured using the BCA protein assay.

Table 4.1. Characteristics of the subjects used in the studies.

	YS [a]	YC [b]	OS [c]	OC [d]
Number of subjects in group	9	10	10	10
Mean age	58.33	57.20	81.50	79.30
Stdev [e] age (+/-)	5.45	4.57	3.21	3.13
Age Range	52-65	52-66	75-85	75-86
# Male patients	4	6	6	1
# Race = white	9	10	10	10
Risk of developing severe sepsis	9	0	10	0
# Patients with SS [f] upon the presence of ED [g]	6	0	8	0
# Patients developing SS in future	3	0	2	0
# Smokers	7	6	8	4
# Patients with respiratory disease	0	0	0	0
# Patients with renal disease	0	0	0	0
# Patients with cardiac disease	0	0	0	0
# Patients with neoplastic disease	0	0	0	0
# Patients with charlson > 0	0	0	0	0

[a] subjects who are at the age of 50-65 and with severe sepsis;
[b] subjects who are at the age of 50-65 and without severe sepsis;
[c] subjects who are at the age of 70-85 and with severe sepsis;
[d] subjects who are at the age of 70-85 and without severe sepsis;
[e] standard deviation
[f] severe sepsis.
[g] emergency department.

4.2.4 Protein Digestion

Protein was denatured with an extraction buffer (0.2 M Tris, 8 M urea, 10 mM $CaCl_2$, pH 8.0), reduced with 1 : 40 molar excess of dithiothreitol (DTT) for 2 h at 37 °C, and then alkylated with 1 : 80 molar excess of iodoacetamide (IAM) for 2 h on ice. The alkylation reaction was quenched by adding 1 : 40 molar excess of Cysteine and the mixture was incubated at room temperature for 30 min. Tris buffer (0.2 M Tris, 10 mM $CaCl_2$, pH 8.0) was added to dilute the urea concentration to 2 M. Each sample was incubated with bovine TPCK-heated trypsin at 1 : 50 substrate : enzyme ratio for 24 h at 37 ºC.

4.2.5 iTRAQ Labeling

Digested samples were desalted with an HLB cartridge (Waters; Milford, MA, USA) and dried by centrifugal evaporation. Each sample was labeled with an iTRAQ reagent following the manufacturer's protocol (Applied Biosystems; Foster City, CA, USA) with slight modifications. Briefly, each iTRAQ reagent was solubilized with 70 μL ethanol and transferred to peptide mixtures. After 1.5 h of incubation, the reaction was quenched with water. Labeled samples were mixed in 1 : 1 : 1 : 1 ratios for iTRAQ reagents that generate reporter ions at *m/z* 114 : 115 : 116 : 117, respectively.

4.2.6 SCX Fractionation

SCX fractionation was carried out on a PolySulfoethyl A 100 mm x 2.1 mm, 5 μm, 200 Å column (The Nest Group, Inc.; Southborough, MA, USA) with buffers as follows: mobile phase A was 5 mM monopotassium phosphate (25% v/v acetonitrile, pH 3.0), and mobile phase B was

5 mM monopotassium phosphate, 350 mM potassium chloride, (25% v/v acetonitrile, pH 3.0). Dried iTRAQ labeled samples were resuspended in 300 µL of mobile phase A and injected onto the SCX column. The gradient for SCX was: 0-3 min, 0% B; 3-45 min, 0-75% B; 45-50 min, 75-100% B; 50-55 min, 100% mobile phase B; 55-56 min, 100-0% B; 56-106 min, 0% B. Thirteen SCX fractions were collected and each fraction was desalted with an HLB cartridge (Waters; Milford, MA, USA).

4.2.7 LC-MS/MS Analysis

Online desalting and reversed phase chromatography was performed with a Nano2D-LC system equipped with an autosampler (Eksigent; Dublin, CA, USA). Mobile phase A and B for these analyses were 3% (v/v) acetonitrile with 0.1% formic acid and 100% (v/v) acetonitrile with 0.1% formic acid, respectively. SCX fractions (5 µL) were loaded onto a trapping column (100 µm i.d. × 2 cm), which was packed in-house with C_{18} 200 Å 3 µm stationary phase material (Michrom Bioresource Inc.; Auburn, CA) at 3 $\mu L \cdot min^{-1}$ in 3% mobile phase B for 3 min. After desalting, the sample was loaded onto an analytical column (75 µm i.d. × 13.2 cm), which was packed in-house with C_{18} 100 Å 3µm stationary phase material (Michrom Bioresource Inc.; Auburn, CA, USA). The gradient was as follows: 0-5 min, 10% mobile phase B; 5-75 min, 10-30% B; 75-95 min, 30-60% B; 95-100 min, 60-90% B; 100-105 min, 90-10% B; 110-120 min, 10% B. The LC eluent was analyzed with positive ion nanoflow electrospray using a LTQ-Orbitrap Velos mass spectrometer (Thermo Scientific, Waltham, MA, USA). Data-dependent acquisition parameters were as follows: the MS survey scan in the Orbitrap was 60,000 resolution over 300-1800 *m/z*; the top six most intense peaks in the MS survey scan were isolated

and fragmented with CID and HCD; CID was performed in the ion trap with normalized collision energy 35%; HCD was recorded in the Orbitrap with normalized collision energy 45% and 7,500 resolution; dynamic exclusion was enabled and a repeat count of two for a duration of 60 s was allowed and selected ions were placed on an exclusion list for 61 s. Each SCX fraction was subject to triplicate LC-MS/MS analysis.

4.2.8 Data Analysis

.RAW files were analyzed with Proteome Discoverer 1.2 software (Thermo Scientific; Waltham, MA, USA). Both CID and HCD spectra were used to obtain sequence information against the Uniprot human database (04/25/2010, 20295 sequences). Sequest search parameters were as follows: two maximum trypsin miscleavages; precursor mass tolerance 10 ppm; fragment mass tolerance 0.8 Da; static modifications were iTRAQ-4plex/+144.102 Da (N-terminus, Lys), and carbamidomethyl modification/+57.021 Da (Cys); dynamic modification of iTRAQ-4plex/+144.102 Da (Tyr). Decoy database searching was employed to generate medium ($p < 0.05$) and high ($p < 0.01$) confidence peptide lists. Peptides with medium and high confidence were used to identify and quantify proteins. The reporter ions (i.e., *m/z* 114-117) were identified with the following parameters: centroid with smallest delta mass, 20 ppm for reporter ion mass tolerance. The isotope correction was employed according to the manufacturer's protocol (AB Sciex; Framingham, MA, USA). Additionally, protein ratios in each experiment were normalized based on the protein median ratio option in the software (i.e., individual protein value is normalized against the median ratio value obtained across all proteins identified in a

given experiment). Only proteins with at least two spectral counts in a technical replicate were considered for further analysis.

4.2.9 Statistics

Coefficient of variation (CV) values were calculated for reporter ion ratios (e.g., 115/114, 116/114, and 117/114) of proteins quantified in at least six iTRAQ experiments. The mean CV value across the iTRAQ experiments was calculated and used as the total biological variation, S_b, which was 0.60 in this study. The technical variation, S_t, was calculated for proteins quantified in at least two LC-MS/MS analyses within an individual iTRAQ experiment, which was 0.11 in this study.

From this power analysis, fold-change cutoff was calculated based on equations (eq 2.1-2.4) shown in **Chapter 2** (Section 2.2.7). Stringent filter criteria were applied to generate a list of statistically significant differentially-expressed proteins as follows: 1) proteins identified and quantified in at least six biological replicates, 2) CV values ≤ 0.60, and 3) fold-change cutoff dependent upon n as such a) ≥ 1.27 or ≤ 0.79 (n=10), b) ≥ 1.28 or ≤ 0.78 (n=9), c) ≥ 1.30 or ≤ 0.77 (n=8), d) ≥ 1.32 or ≤ 0.76 (n=7), e) ≥ 1.35 or ≤ 0.74 (n=6).

4.2.10 Western Blotting Analysis

The changes in the expression of C-reactive protein (CRP), apolipoprotein CIII (ApoCIII), and fibrinogen alpha chain (FAC) were subject to Western blotting analysis. Twenty µg of TMD proteins was denatured in an appropriate sample buffer and electrophoretically separated on a Criterion precast gel (Biorad Laboratories; Hercules, CA, USA) at 140 V.

Proteins from the gel were transferred onto a nitrocellulose membrane paper using a Fast-Transfer Blot System (Biorad; Hercules, CA, USA). Blots were washed three times in Wash blot. BSA blocking solution (3%) was added to the membrane and incubated on a rocker for 2 h. A 1 : 5000 dilution of mouse monoclonal anti-CRP primary antibody (Sigma Aldrich; St. Louis, MO, USA), 1 : 5000 dilution of rabbit polyclonal anti-ApoCIII primary antibody (Abcam; Cambridge, MA, USA), or 1 : 2500 dilution of rabbit monoclonal anti-FAC primary antibody (Abcam; Cambridge, MA, USA) was added and incubated at 4 ºC overnight. The blot was rinsed and incubated with a 1 : 7500 dilution of anti-mouse or anti-rabbit IgG alkaline phosphatase secondary antibody (Sigma Aldrich; St. Louis, MO, USA) for 1 h on a rocker. The blot was rinsed and colorometrically developed using 0.51 mM 5-bromo-4-chloro-3'-indolyphosphate p-toluidine salt (BCIP) and 0.24 mM nitrotetrazolium blue (NBT). The dried blot was scanned using a Canon scanner, saved as a .TIFF file, and densitometry analyses carried out with Scion Image Software. Within each experiment, the intensity for the sample from each group was normalized to the total blot intensity and used to generate mean and standard deviation values.

4.2.11 Ingenuity Pathway Analysis

Differentially-expressed proteins were analyzed using Ingenuity Pathway Analysis (IPA, www.ingenuity.com) to generate a list of pathways that are statistically relevant ($p < 0.05$).

4.3 RESULTS

4.3.1 Data Characterization and Statistical Analysis

An iTRAQ-based semi-quantitative proteomics workflow[196] was employed to identify differentially-expressed proteins in 50-65 and 70-85 year old CAP patients who developed severe sepsis compared to those patients that did not (Table 4.2). The workflow employs TMD on a MARS Hu-6 column to effectively remove high-abundance proteins and allows deeper probing into the plasma proteome[196]. Patient samples from the four groups (i.e., YC, YS, OC and OS) were randomly assigned to iTRAQ reagents in a blind fashion across ten SCX-LC-MS/MS experiments (Table 4.2).

Figure 4.1a shows an example of LC chromatograms for 13 SCX fractions of pooled iTRAQ 4-plex samples. The triplicate LC-MS/MS runs for each fraction are reproducible. Figures 4.1b-g show example spectra for peaks isolated and fragmented. Doubly-charged peptides at *m/z* 748.9046 (Figure 4.1b) and 742.9010 (Figure 4.1c) in SCX fractions seven and six were eluted from the column at t_r 57.20 min and 37.26 min, respectively. The CID MS/MS spectra (Figures 4.1d and e) display a consecutive series of *b*- and *y*-fragment ions used to assign the peptides as $[YYTYLIMNK+2H]^{2+}$ of protein Complement C3 and $[GWVTDGFSSLK+2H]^{2+}$of protein ApoCIII, respectively. A mass increase of 145 Da was observed for b_1 and y_1 ions for each of the two peptides, indicating iTRAQ labeling at the N-terminus and the presence of lysine at the C-terminus. HCD MS/MS spectra (Figures 4.1f and g) also contain series of *b*- and *y*- ions used to confirm the sequence of peptides. The lower *m/z* region of the HCD MS/MS spectra (inserts in Figure 4.1f and g) shows the intensity of the reporter ions which is used to quantify the peptides. The lower *m/z* region of the HCD MS/MS

Table 4.2. Experimental design and iTRAQ quantitation channel assignment.

	Reporter ions			
Experiment	**114**	**115**	**116**	**117**
1	YS[a]	YC[b]	OS[c]	OC[d]
2	YS	YC	OS	OC
3	YS	YC	OS	OC
4	YS	YC	OS	OC
5	YC	OS	OC	YS
6	YC	OS	OC	YS
7	YC	OS	OC	YS
8	OS	OC	YS	YC
9	OS	OC	YS	YC
10	OS	OC	YS	YC

[a] Patients 50-65 years old who developed severe sepsis.

[b] Patients 50-65 years old who did not develop severe sepsis.

[c] Patients 70-85 years old who developed severe sepsis.

[d] Patients 70-85 years old who did not develop severe sepsis.

spectra (inserts in Figure 4.1f and g) shows the intensity of the reporter ions which is used to quantify the peptides. As shown in Figures 4.1f and g, the ratios across the four groups are 1.0 : 0.9 : 1.0 : 1.0 and 1.0 : 1.9 : 2.3 : 1.4 for reporter ions 114 : 115 : 116 : 117 from Complement C3 and ApoCIII, respectively.

Figure 4.2 shows a bar graph of the number of proteins and spectral counts (SCs) identified in each of ten biological replicate experiments. Also, the cumulative number of proteins identified is shown in Figure 4.2. An average of 283 ± 14 proteins and 59645 ± 4129 SCs were identified and similar results were obtained across individual experiments. The total number of proteins identified increases with each pooled sample experiment such that a total of 772 unique proteins were identified from all plasma samples. With more stringent criteria for protein filtering (i.e., at least two unique peptides), a total of 509 proteins were identified. A list of all identified proteins and peptides is provided in Supplemental Table S4.1 and S4.2. Based on SCs, the three most abundant proteins are Complement C3 (49,749 SCs), α-2-macroglobulin (47,273 SCs) and ApoAI (28,261 SCs).

4.3.2 Western Analysis Verification

Western blotting analysis was employed to generate a secondary measurement for several differentially-expressed proteins. Proteins involved in the acute phase response (i.e., CRP), coagulation pathway (i.e., FAC) pathway and lipid metabolism (i.e., ApoCIII) were selected. Figures 4.3a-c display Western blot data for CRP, FAC, ApoCIII, respectively. The histogram plots represent the normalized intensities corresponding to the density of the band spots for each group. The relative abundances (YS : YC : OS : OC) obtained from the Western blotting analysis

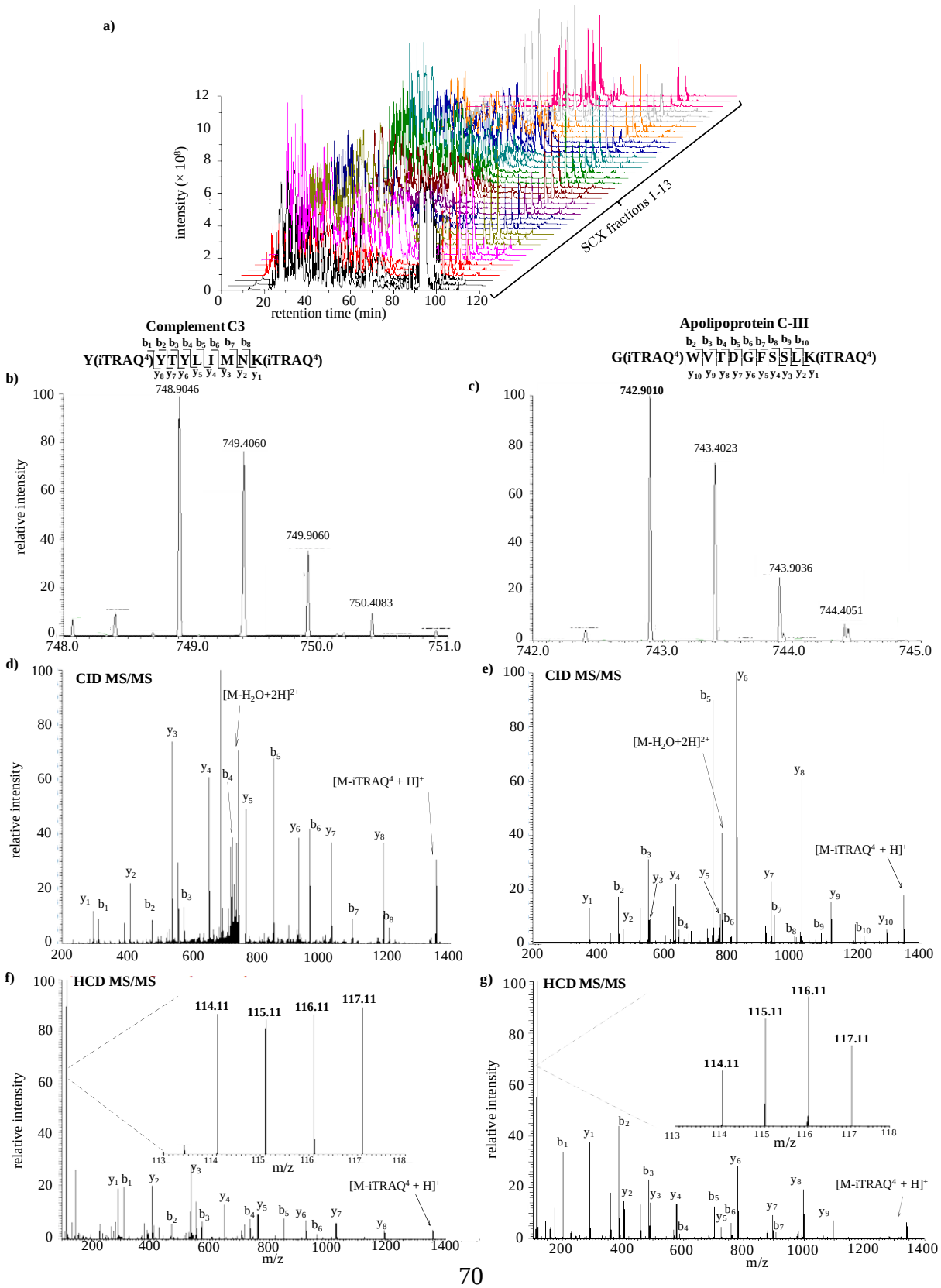
a)
intensity (× 10^8)
retention time (min)
SCX fractions 1-13
b)
Complement C3
Y(iTRAQ⁴)YTYLIMNK(iTRAQ⁴)
748.9046
749.4060
749.9060
750.4083
relative intensity
c)
Apolipoprotein C-III
G(iTRAQ⁴)WVTDGFSSLK(iTRAQ⁴)
742.9010
743.4023
743.9036
744.4051
d)
CID MS/MS
[M-H2O+2H]2+
[M-iTRAQ⁴ + H]+
e)
CID MS/MS
[M-H2O+2H]2+
[M-iTRAQ⁴ + H]+
f)
HCD MS/MS
114.11
115.11
116.11
117.11
[M-iTRAQ⁴ + H]+
m/z
g)
HCD MS/MS
114.11
115.11
116.11
117.11
[M-iTRAQ⁴ + H]+
m/z

Figure 4.1. a) LC chromatogram for individual SCX fractions analyzed in triplicate. Example mass spectra of peptides eluted from **b)** SCX fraction 7 t_r = 57.20 min with *m/z* 748.8046 and **c)** SCX fraction 6 t_r = 37.26 min with m/z 742.9010. CID MS/MS spectra are shown in **d)** and **e)**, respectively. HCD MS/MS are shown in **f)** and **g)**. The inserts are zoomed-in images of the **f)** and **g)** low *m/z* region.

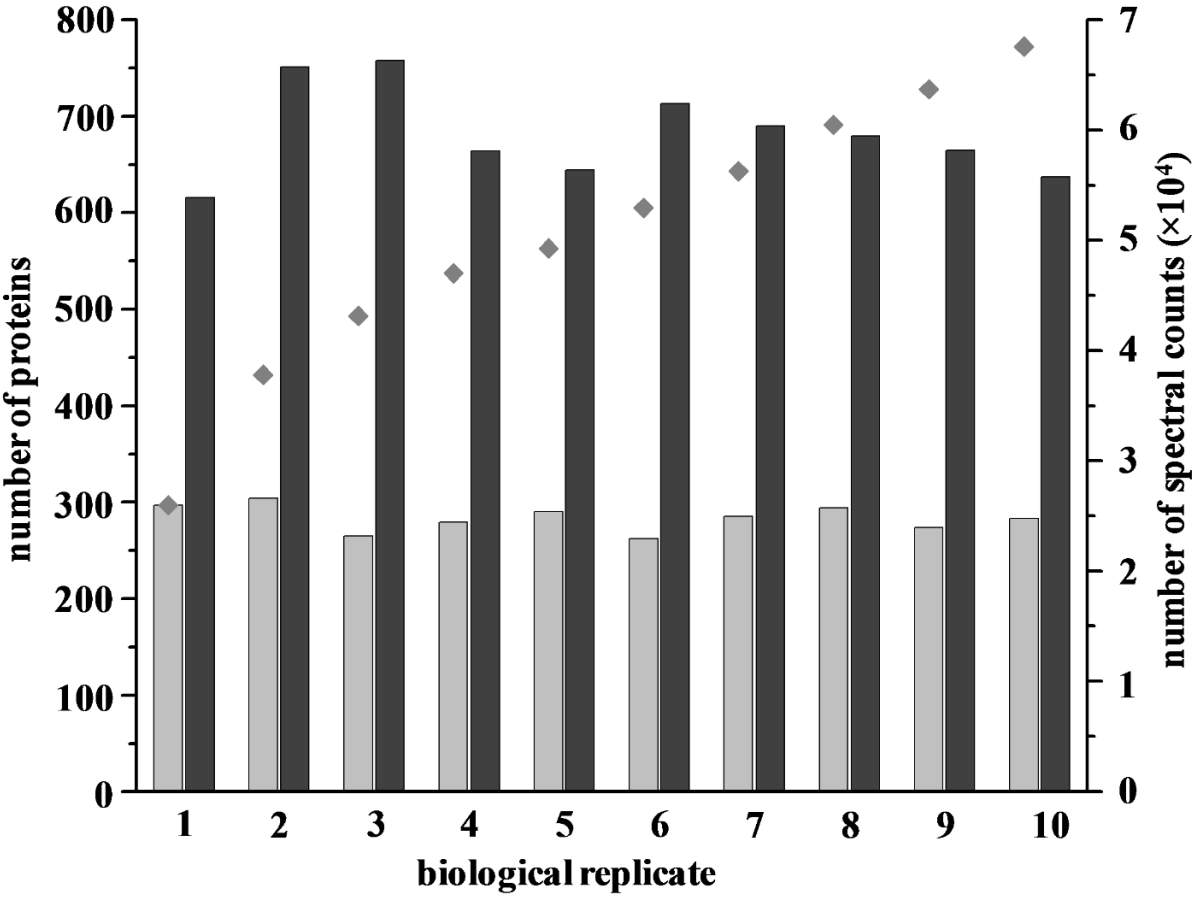

Figure 4.2. Number of proteins (gray bars) and spectral counts (black bars) identified in each experiment. The cumulative number of proteins identified with each subsequent experiment (gray diamond) is also shown.

of CRP, FAC and ApoCIII were 1.0 : 0.4 : 0.4 : 1.8, 1.0 : 0.3 : 0.1 : 0.5, and 1.0 : 1.9 : 2.5 : 1.2, respectively. These observed Western data were similar to the measured iTRAQ results for these proteins (Table 4.3). However, suppression of iTRAQ protein ratios in MS/MS experiments is a noted limitation of this quantitative approach[144]. Proteomics workflows to handle suppression issues at the MS^3 level have been recently reported[168,172-174,197].

4.3.3 Differentially-Expressed Proteins

Protein ratios were obtained from both age groups: YS/YC in 50-65 years old group and OS/OC in 70-85 years old group using YC and OC as reference channels, respectively. Fifty-eight differentially-expressed proteins (Table 4.3) were identified in comparisons from both age groups (i.e., YS/YC and OS/OC). Proteins differentially expressed between younger and older adults within each disease group (i.e., OC/YC and OS/YS) are provided in Supplemental Table S4.3 for interested readers. The measured fold-change values reported in the table include the mean and SD for each protein based on the ratios averaged across all biological replicates. As shown in the Venn diagram (Figure 4.4), 28 proteins are differentially-expressed in 50-65 year olds adults (i.e., YS/YC) in which 14 have higher levels and 14 have lower levels in patients with severe sepsis compared to those with CAP. In the population of 70-85 year olds (i.e., OS/OC), 23 proteins are differentially-expressed, in which 16 and seven have higher and lower levels in patients with severe sepsis, respectively. Of the 58 total differentially-expressed proteins, eight are in common amongst both age groups. Interestingly, however the direction of the fold-change differs in younger and older adults. Specifically, α-1-anti-chymotrypsin (A1ACT), ApoE, FAC,

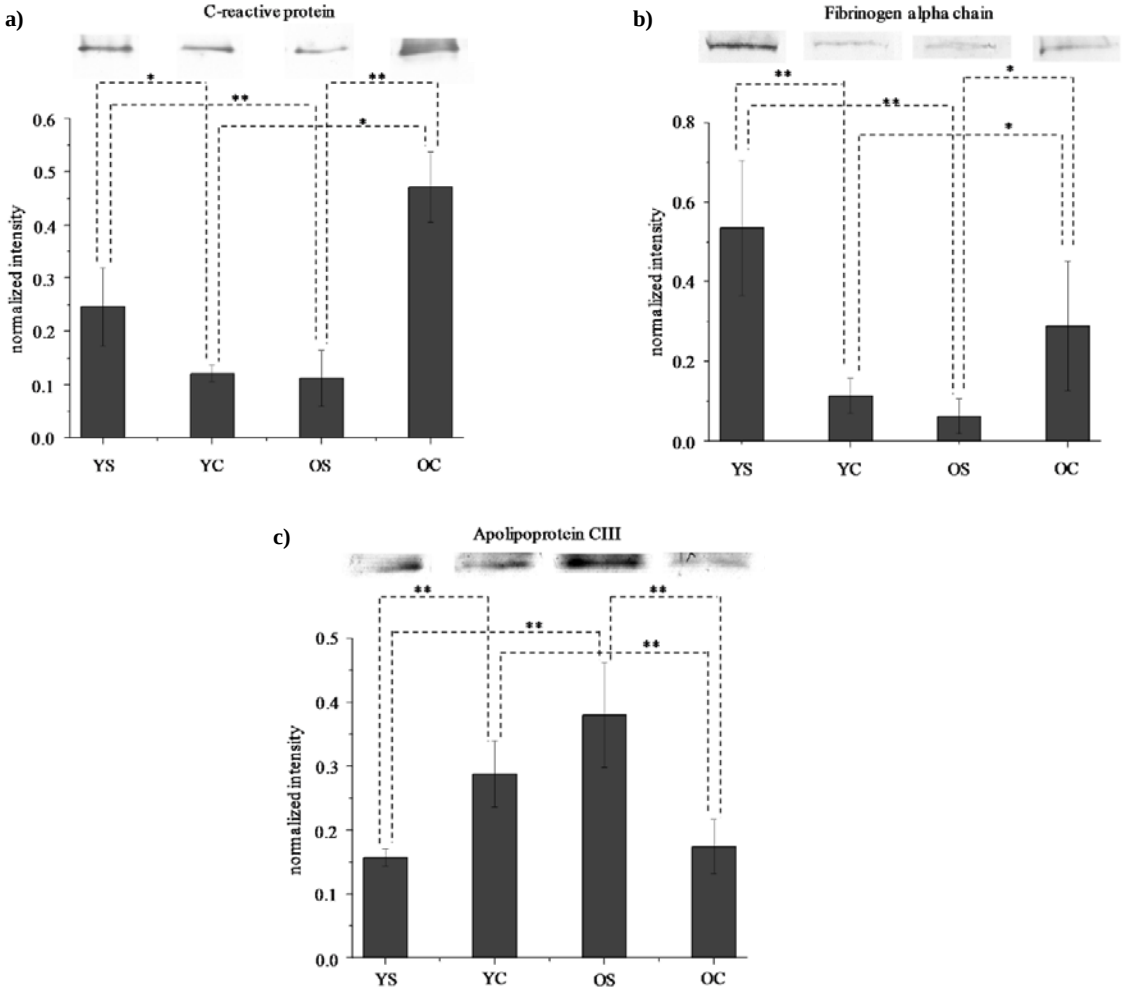

Figure 4.3. Western blotting images for **a)** C-reactive protein, **b)** fibrinogen α chain, and **c)** ApoCIII. The histogram under the images displays the normalized intensity ± standard deviation (N = 6) of the proteins across each group. The intensity for each individual band is normalized to the total intensity of the blot.

CRP, and LPS binding protein (LBP) levels were higher in younger adults with severe sepsis but lower in older adults with severe sepsis relative to age-matched controls, suggesting that lower levels of these proteins is associated with increased risk and incidence of severe sepsis in older adults. On the other hand, ApoAII, ApoCIII, and N-acetylmuranoyl-L-alanineamidase have lower and higher levels in younger and older with severe sepsis, respectively, suggesting that higher levels of these proteins may be factors for increased severe sepsis risk in older adults.

4.3.4 Pathway Analysis

Using IPA analysis, 19 biological pathways (Figure 4.5) are significantly over-represented ($p < 0.05$) for the 58 differentially-expressed proteins. The most represented pathways include LXR/RXR activation and acute phase response signaling whereby 18 proteins are associated with each of these pathways. Many differentially-expressed proteins are involved in atherosclerosis signaling, interleukin (IL)-12 signaling and production of nitric oxide (NO) and reactive oxygen species (ROS) in macrophages, and endocytosis signaling. Fewer proteins are involved in the remaining biological pathways shown in Figure 4.5 such as actin cytoskeleton and IL-6 signaling. A list of the proteins associated with specific pathways is provided in Supplemental Table S4.4.

4.4 DISCUSSION

This work investigates the effects of aging on the risk of severe sepsis in the acute plasma proteome of elderly CAP patients. While sepsis can occur as early as the neonatal stage[198,199],

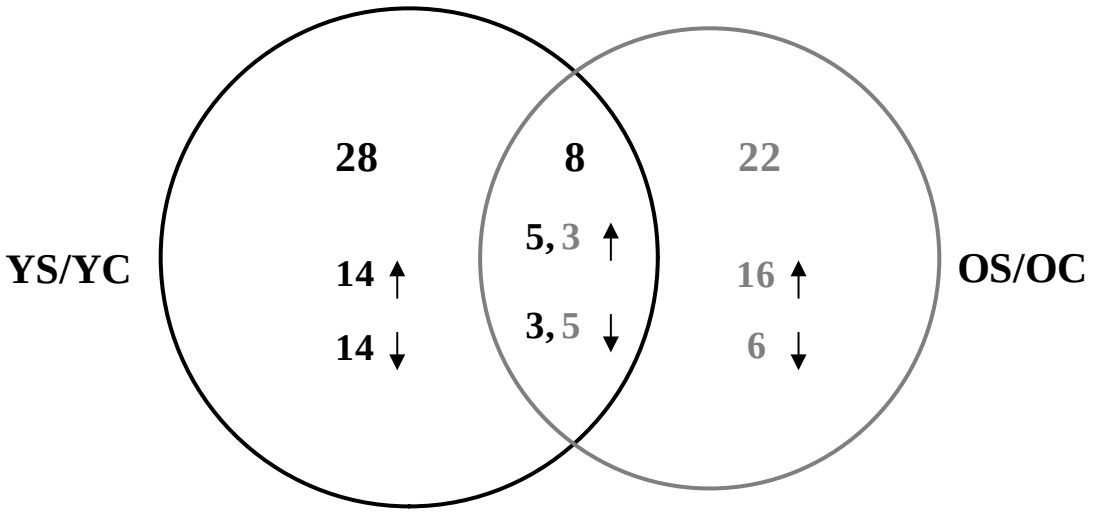

Figure 4.4. Venn diagram of differentially-expressed proteins for each age group (i.e., YS/YC 50-65 years old and OS/OC 70-85 years old). The number of proteins that have higher (↑) or lower (↓) fold-change values in each comparison are also shown.

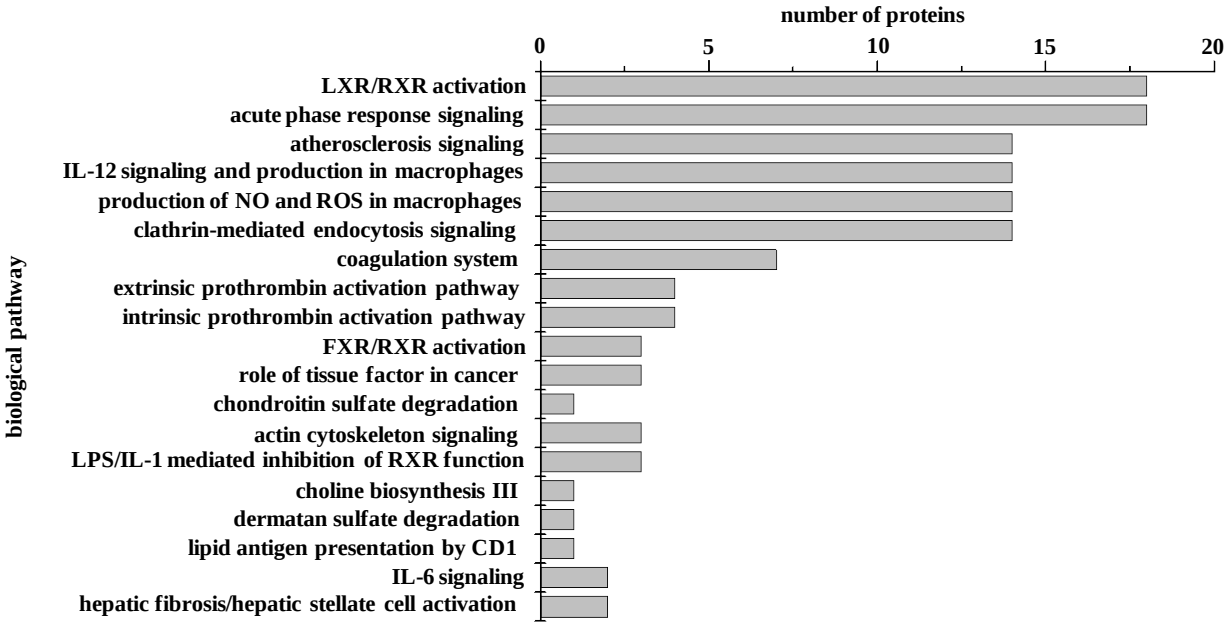

Figure 4.5. Histogram plot of biological pathways associated with differentially-expressed proteins as a function of severity of sepsis (N = 58). The *p* value cutoff for the IPA pathways is $p < 0.05$.

incidence and morbidity increases with age and rises sharply after 65 years[188,200,201] presumably due to immunosenescence[50,189,201] and high levels of inflammatory proteins[192-195,202]. However, no significant differences with age have been reported for inflammatory and coagulation proteins and cell surface markers in patients with severe sepsis[48].

Our plasma proteomics study identified 58 differentially-expressed proteins in CAP patients that subsequently developed severe sepsis relative to those who did not in groups of elderly adults (Table 4.3). We note that some of the differences observed may be due to both a mixture of pre-existing conditions and differences in the initial acute phase response, as our study groups did not include a nonseptic subset. Below is a discussion of the proteins involved in the biological pathways such as acute phase signaling, coagulation pathway, and lipid metabolism. Other pathways are briefly discussed and the implications of these changes for understanding aging and severe sepsis in the elderly are presented.

4.4.1 Acute Phase Response

Sepsis is a pro-inflammatory state which is characterized by elevated levels of pro-inflammatory cytokines, such as IL-6, IL-10 and tumor necrosis factor (TNF)-α[23]. These pro-inflammatory cytokines regulate acute phase responses and the expression of acute phase proteins (APPs)[203]. Altered expression of APPs has been demonstrated in sepsis[191,204-208]. For example, increased levels of α-1-acid glycoprotein (A1AG), A1ACT, and LBP and decreased levels of transthyretin (TTR) are observed in 65 year old sepsis patients[205,206] and cecal ligand and puncture (CLP) mouse[207] and pig models[208]. It also appears that acute phase response

Table 4.3. List of proteins that are differentially-expressed between groups.

Acc. No.[a]	Protein Name	YS/YC (mean ± SD[b])	OS/OC (mean ± SD)	n[c]
O14791	Apolipoprotein L1	/	1.39 ± 0.70	10
O95445	Apolipoprotein M	/	1.44 ± 0.48	8
P01008	Antithrombin-III	0.60 ± 0.06	/	10
P01011	Alpha-1-antichymotrypsin	1.58 ± 0.87	0.68 ± 0.18	10
P02649	Apolipoprotein E	2.11 ± 0.30	0.65 ± 0.17	10
P02652	Apolipoprotein A-II	0.50 ± 0.08	1.45 ± 0.46	10
P02654	Apolipoprotein C-I	/	2.17 ± 1.02	10
P02656	Apolipoprotein C-III	0.69 ± 0.29	1.43 ± 0.77	10
P02671	Fibrinogen alpha chain	2.44 ± 0.72	0.60 ± 0.13	10
P02675	Fibrinogen beta chain	2.10 ± 0.58	/	10
P02679	Fibrinogen gamma chain	2.08 ± 0.72	/	10
P02735	Serum amyloid A protein	3.06 ± 1.09	/	10
P02741	C-reactive protein	3.27 ± 1.07	0.52 ± 0.22	10
P02749	Beta-2-glycoprotein 1	/	1.58 ± 0.61	10
P02750	Leucine-rich alpha-2-glycoprotein	2.14 ± 0.30	/	10
P02751	Fibronectin	/	0.62 ± 0.31	10
P02753	Retinol-binding protein 4	0.53 ± 0.09	/	10
P02763	Alpha-1-acid glycoprotein 1	2.03 ± 0.43	/	10
P02766	Transthyretin	0.44 ± 0.09	/	10
P02774	Vitamin D-binding protein	0.57 ± 0.08	/	10
P02775	Platelet basic protein	/	0.76 ± 0.21	9
P04114	Apolipoprotein B-100	1.52 ± 0.25	/	7
P04259	Keratin, type II cytoskeletal 6B	0.52 ± 0.06	/	7
P04275	von Willebrand factor	2.05 ± 0.34	/	10
P04278	Sex hormone-binding globulin	0.70 ± 0.26	/	7
P05090	Apolipoprotein D	/	1.47 ± 0.32	10
P05154	Plasma serine protease inhibitor	0.73 ± 0.46	/	6
P05452	Tetranectin	0.64 ± 0.10	/	10
P05546	Heparin cofactor 2	0.71 ± 0.26	/	10
P06276	Cholinesterase	/	1.45 ± 0.47	9
P06396	Gelsolin	0.55 ± 0.10	/	10
P07996	Thrombospondin-1	/	0.65 ± 0.34	6
P10909	Clusterin	0.73 ± 0.30	/	10
P13645	Keratin, type I cytoskeletal 10	0.58 ± 0.06	/	10
P15169	Carboxypeptidase N catalytic chain	1.31 ± 0.36	/	10
P16070	CD44 antigen	1.62 ± 0.55	/	7
P18428	Lipopolysaccharide-binding protein	2.20 ± 0.50	0.76 ± 0.32	10
P19652	Alpha-1-acid glycoprotein 2	2.17 ± 0.60	/	10

Table 4.3. ***(continued)*** List of proteins that are differentially-expressed between groups.

Acc. No.	Protein Name	YS/YC (mean ± SD)	OS/OC (mean ± SD)	n
P19823	Inter-alpha-trypsin inhibitor heavy chain H2	/	1.40 ± 0.53	10
P19827	Inter-alpha-trypsin inhibitor heavy chain H1	/	1.58 ± 0.58	10
P20851	C4b-binding protein beta chain	1.39 ± 0.46	/	6
P29622	Kallistatin	/	1.69 ± 0.57	10
P35542	Serum amyloid A-4 protein	0.48 ± 0.04	/	10
P35858	Insulin-like grow th factor-binding protein complex acid labile subunit	/	1.39 ± 0.46	9
P61626	Lysozyme C	1.91 ± 0.96	/	8
P61769	Beta-2-microglobulin	1.89 ± 1.02	/	6
P80108	Phosphatidylinositol-glycan-specific phospholipase D	0.39 ± 0.06	/	9
Q03591	Complement factor H-related protein 1	1.31 ± 0.60	/	10
Q04756	Hepatocyte grow th factor activator	/	1.81 ± 0.68	10
Q15431	Synaptonemal complex protein 1	/	1.37 ± 0.62	6
Q6UXB8	Peptidase inhibitor 16	/	2.03 ± 0.78	6
Q86UD1	Out at first protein homolog	/	0.74 ± 0.19	6
Q86UV6	Tripartite motif-containing protein 74	/	1.85 ± 0.79	6
Q96KN2	Beta-Ala-His dipeptidase	/	2.06 ± 0.93	6
Q96PD5	N-acetylmuramoyl-L-alanine amidase	0.58 ± 0.06	1.35 ± 0.39	10
Q9BXR6	Complement factor H-related protein 5	/	0.72 ± 0.18	10
Q9NXD2	Myotubularin-related protein 10	/	1.78 ± 0.69	7
Q9Y6R7	IgGFc-binding protein	/	0.70 ± 0.26	9

[a] accession number provided from the uniprot human database (04/25/2010, 20295 sequences).

[b] mean and SD values are calculated based on the reporter ion ratios for proteins quantified in at least 6 experiments.

[c] the number of experiments in which the corresponding proteins are quantified.

increases with disease severity. For example, sepsis patients have higher levels of CRP and lower levels of serum amyloid A4 relative to patients with systemic inflammatory response syndrome (SIRS), another precursor to sepsis[191,204].

In our studies, 18 differentially-expressed proteins including CRP, LBP, A1ACT, and TTR are involved in acute phase response (Figure 4.5) and the levels in younger adults are consistent with other studies[191,204-208]. For example, CRP (fold-change YS/YC 3.27 ± 1.07), LBP (2.20 ± 0.50), A1ACT (1.58 ± 0.87), and A1AG (2.03 ± 0.43) have higher concentrations while TTR (0.44 ± 0.09) has lower concentrations in younger adults who developed severe sepsis compared to those did not. Acute phase response also varies depending on patient age. CRP (0.52 ± 0.22), LBP (0.76 ± 0.32), and A1ACT (0.68 ± 0.18) have lower concentrations in older adults who later developed severe sepsis suggesting that lower expression of these proteins at older age leads to severe sepsis. CRP and LBP have protective effects by neutralizing the toxicity of pathogens[205,209-212], such that decreased expression of these proteins in older patients may help explain higher risk and mortality of severe sepsis. Both aging and severe sepsis alter the immune system and response to infection[213]. Taken together, these results of acute phase response imply that a hypoinflammatory response in older adults may increase risk of severe sepsis, consistent with other literature reports[23,214,215].

4.4.2 Coagulation Pathway

Pro-inflammatory cytokines can also activate the coagulation pathway. Briefly, the activation of a series of coagulation factors cleave prothrombin to thrombin, which in turn converts soluble fibrinogen into fibrin, upon which cross-linked fibrin forms blood clots[23,216]. In

sepsis patients, pro-coagulation overwhelms fibrinolysis (or anti-coagulation) leading to the presence of more blood clots[23,216]. This has been demonstrated by decreased levels of anti-coagulant proteins [e.g., antithrombin III (ATIII), and heparin cofactor II] and increased levels of pro-coagulant proteins [e.g., fibrinogen, Von Willebrand factor (VWF)] in sepsis patients[207,217-219].

In these studies, elevated levels of FAC (2.44 ± 0.58), fibrinogen beta chain (2.10 ± 0.58), fibrinogen gamma chain (2.08 ± 0.72) and VWF (2.05 ± 0.34) were found in younger adults who developed severe sepsis. Fibrinogen has higher concentrations and ATIII has lower concentrations in sepsis[207,217]. Higher levels of VWF are associated with mortality in sepsis[218]. Higher levels of fibrinogen and VWF may indicate the presence of more blood clots in younger patients, consistent with literature reports[219-221], whom developed severe sepsis. This notion is further supported by decreased concentrations of ATIII (0.60 ± 0.06) and heparin cofactor II (0.71 ± 0.26) in these studies. Interestingly, fibrinogen (0.60 ± 0.13) had lower levels in older adults who developed severe sepsis. Our proteomics results support the notion that an acute response of reduced coagulation activity may be a contributing factor to higher incidence and mortality of severe sepsis found in older adults.

4.4.3 Lipid Metabolism

Apolipoproteins play important roles in liver X receptor/retinoid X receptor (LXR/RXR) activation and atherosclerosis signaling. For example, ApoB-100 can suppress the activation of LXR/RXR[222]. The activated LXR/RXR complex enhances the process of reverse cholesterol transport and cholesterol efflux, which transfers accumulated cholesterol from the blood vessel

walls to the liver for excretion[223,224]. Additionally, activated LXR/RXR can reduce the expression of pro-inflammatory cytokines (e.g., IL-6, IL-1β) by inhibition of the activity of transcription factor NF-κB[225]. The acute phase response which is activated during aging and severe sepsis can inhibit LXR/RXR activation[226]. Failed activation of the LXR/RXR complex may lead to atherosclerosis[227,228], which is associated with severe sepsis[229,230]. Apolipoproteins may have various biological functions by forming different lipoproteins [e.g., low density lipoproteins (LDL) and high density lipoproteins (HDL)]. For example, ApoB-100 is the protein component for LDL which is a cholesterol transporter[231], whereas HDL formed by ApoA and ApoCIII can inhibit oxidation and inflammation[35].

Altered levels of apoliproteins have been reported in sepsis. For example, elevated levels of ApoB-100[232] and lower concentrations of ApoCIII in response to inflammation[233] have been reported. Consistent with this, we observed increased expression of ApoB-100 (1.52 ± 0.25) and decreased expression of ApoCIII (0.69 ± 0.29) in younger adults who developed severe sepsis. These changes may suggest suppressed activation of the LXR/RXR pathway and subsequent higher risk of atherosclerosis in younger adults (although we do not have data to support this notion). Additionally, ApoCIII has different isoforms based on the number (i.e., 0, 1, 2, and 3) of sialic acids per protein: ApoCIII-0, ApoCIII-1, ApoCIII-2, and ApoCIII-3[234]. The ApoCIII isoform ratios have been demonstrated to be correlated with mortality in younger severe sepsis patients (~ 49 years old)[234]. For example, the ratio of ApoCIII-2/ApoCIII-1 higher than may indicate increased risk of death in younger severe sepsis patients[234]. ApoE also has different isoforms: ApoE2, ApoE3, ApoE4. It has been shown that the levels of ApoE2 correlate positively with that of factor VIII, which is necessary for blood clotting[235]. Also, higher levels of

ApoE3 may reduce the risk of severe sepsis[235]. In this study, higher levels of ApoE (2.11 ± 0.30) were found in younger adults consistent with a rat model[236], however lower levels (0.65 ± 0.17) were detected in older adults in our study. Also, higher levels of ApoCI (2.17 ± 1.02) and ApoM (1.44 ± 0.48) were detected in older adults who developed severe sepsis. Although ApoCI levels correlate with the survivorship in ~ 25 year old severe sepsis patients[237], higher concentration of ApoCI has been reported to promote atherosclerosis[238,239]. ApoM has also been reported to have lower concentrations in young adult severe sepsis patients [240,241] and contributes to the anti-inflammatory response in sepsis[241]. Higher levels of ApoM in older adults who developed severe sepsis in our studies suggest that these patients have a reduced inflammatory state during acute response. That lipid metabolism is altered in these studies points to atherosclerosis as a contributing factor of severe sepsis incidence; however further analyses are necessary to support this hypothesis.

4.4.4 Other Pathways

Other key pathways identified in these studies such as IL-12 and IL-6 signaling support a hypoinflammatory response in older adults (Table 4.3)[242]. Enhanced production of NO and ROS in macrophages has been previously reported in aging and sepsis[243,244]. We detect differentially-expressed proteins involved in the production of NO and ROS (i.e., retinol binding protein 1, lysozyme C and clusterin) which support elevated oxidative stress in the elderly[244,245] and severe sepsis patients[243,246].

The nested-case control study design employed herein has identified many potential factors that may contribute to higher incidence of severe sepsis in adults older than 65. There is a

substantial role of inflammation and coagulation processes in acute host response and our proteomics results suggest that older individuals have hypoinflammatory and reduced coagulation responses. While other factors such as lipid metabolism and production of ROS are implicated, additional experiments are necessary in order to determine better the effects of age on these processes. For example, it would be worthwhile in future studies to measure oxidative stress markers in this CAP cohort and to examine the correlation between incidence of severe sepsis and age with atherosclerosis. A limitation to these studies is the small sample populations (N = 10) used to measure a wide range of proteins that are known to vary substantially in plasma tissue[117]. Future studies include selecting key proteins to follow their expression levels in a larger cohort using an independent method, such as ELISA.

4.5 CONCLUSIONS

The incidence and mortality of severe sepsis increases with aging, especially after 65 years. This study investigated the effects of aging on initial host response to sepsis in CAP patients who eventually develop severe sepsis after hospitalization. Using a proteomics approach, several altered biological pathways were identified. Acute phase response and coagulation were highly represented in these studies, and novel pathways such as lipid metabolism, atherosclerosis, and production of NO and ROS were observed. Interestingly, differentially-expressed proteins involved in these pathways show opposite expression levels of change dependent on patient age (i.e., 50-65 and 70-85 years old). These findings provide more insight to factors that may explain higher risk, increased incidence, and mortality in older adults

with severe sepsis. Such insight will be helpful for the development of age-specific and personalized severe sepsis treatments.

5.0 PROTEOME CHARACTERIZATION OF SPLENOCYTES FROM AN APP/PS-1 ALZHEIMER'S DISEASE MODEL[247]*

(*note that information in the chapter is written based on a published paper, Cao, Z.; Robinson, R. A. S. *Proteomics* **2014**, *14*, 291)

5.1 INTRODUCTION

Currently, there are ~ 27 million Alzheimer's disease (AD) patients worldwide and it is predicted that one in 85 people globally will be diagnosed with AD by 2050[248]. AD is a neurodegenerative disorder with symptoms that include progressive memory deficits, cognitive impairment and changes in behavior and personality[248]. Pathological hallmarks of the disease in the brains of AD patients include senile plaques (SP) and neurofibrillary tangles as well as mitochondrial dysfunction, oxidative stress, and neuronal loss[248]. SP are composed of amyloid β (Aβ) peptides which are generated from the cleavage of amyloid precursor protein (APP) by β- and γ-secretases[248,249]. Mutations in the genes coding APP and presenilin-1 (PS-1), which is a sub-component of γ-secretase, are present in familial AD and are associated with increased incidence of AD[249].

Recently, studies focused on the alteration of the immune system in the AD brain and periphery have attracted considerable attention. An increased number of activated microglia has been reported in AD brain[250]. Elevated levels of interleukin (IL)-1β, IL-6, and tumor necrosis factor (TNF)-α may contribute to AD pathology[250]. The number of macrophages is reduced in AD[251] and spleen tissues from a triple transgenic (APP×PS-1×tau) AD mouse model have decreased dendritic cells[252]. The activation of natural killer (NK) cells is suppressed in AD[70]. Subpopulations of T-cells (e.g., CD4+ and CD8+) in the AD peripheral immune system also

change, although there are conflicting reports[252,253]. Furthermore, since the blood-brain barrier (BBB) is compromised in AD[250,251], changes in the peripheral immune system may also affect the function of brain[250,251].

APP/PS-1 mice have increased Aβ production and accelerated Aβ deposits[254]. By 12 months of age, numerous SPs are present in the hippocampus and caudal cortex[254] and animals exhibit decreased speed of relearning than controls[254]. Increased protein oxidation and lipid peroxidation and proteome alterations have been observed in brain and neurons from APP/PS-1 mice[79,80,255-257]. CD90+ cells and a heterogenerous mixture of CD90- cells in APP/PS-1mice have increased oxidative stress (**Chapter 6**)[255]. Additionally, the immune system in the brain and periphery is altered as evidenced by increased activation of microglia[81,258], alterations in the distribution of monocytes[259] and the cell cycle of lymphocytes[84].

Recently, it has been reported that peripheral immune cells behave differently in AD[260]. For example, the number of B-cells is lower in AD while no changes are observed in the number of T-cells. To-date there are no proteomics reports however, which focus on the analysis of the various immune cell populations in the context of AD. This work represents one of the first studies to characterize protein expression in different peripheral immune cell types in an AD mouse model. Herein, we provide the first proteome map of splenocyte populations in a human double transgenic knock-in APP/PS-1 mouse model to serve as a reference for proteome studies aimed at elucidating the role of peripheral immunity in AD.

5.2 EXPERIMENTAL AND MATERIALS

5.2.1 Animals

APP/PS-1 male mice [B6.Cg-Tg(APPswe,PSEN1dE9)85Dbo/Mmjax, stock number 005864, genetic background C57BL/6J][254] were purchased from Jackson Laboratory and housed in the Division of Laboratory Animal Resources at the University of Pittsburgh. Mice were fed standard Purina rodent laboratory chow *ad libitum* on a 12 h light/dark cycle. All animal protocols were approved by the Institutional Animal Care and Use Committee at the University of Pittsburgh.

5.2.2 Splenocyte Isolation

Spleen tissue was mashed to obtain a single cell suspension. CD90.2 magnetic microbeads (MiltenyiBiotec, Auburn, CA, USA) were employed to separate splenocytes into two subsets: CD90+ and CD90-. CD90.2 recognizes the Thy1.2 antigen in peripheral T-cells from lymphoid organs and blood in inbred mouse strains (e.g., C57BL/6J). The CD90- subset contains a heterogenerous mixture of B-cells, macrophages, and NK cells.

5.2.3 Protein Extraction and Digestion

Proteins were extracted from CD90+ or CD90- subsets with RIPA buffer[255]. Rapid freezing and thawing was repeated three times to lyse cells. The solution was centrifuged at 14,000g at 4ºC for 20 min to remove cellular debris. Supernatant was collected and protein concentration determined by a BCA assay (Thermo Scientific; Waltham, MA, USA). Sample pooling was employed in this study due to the limited amount of proteins extracted from CD90+

and CD90- cells from each individual mouse [261,262]. Additionally, it has been demonstrated that sample pooling is useful for characterization of the population rather than each individual[261,262] which was adopted for this global study. Proteins from CD90+ and CD90- subsets isolated from six AD male mice (14 months of age) were pooled and acetone precipitated. Protein pellets were suspended in 0.1% w/v RapiGest SF (Waters, Milford, MA, USA) solution in 50 mM NH_4HCO_3, reduced with dithiothreitol, alkylated with iodoacetamide, and digested with TPCK-treated trypsin (Sigma-Aldrich, St. Louis, MO, USA). Trifluoroacetic acid was added and incubated for 45 min at 37 ºC to quench digestion. Samples were centrifuged at 13,000 rpm for 10 min, the supernatant cleaned with an Oasis HLB cartridge (Waters; Milford, MA, USA), and dried with a SpeedVac.

5.2.4 Offline SCX-LC-MS/MS Analysis

Digests were fractionated into strong cation exchange (SCX) fractions and subject to triplicate LC-MS/MS analyses on a LTQ Orbitrap Velos MS instrument. Procedures are similar to those used in **Chapter 2** and **4**[97,130] whereby mobile phase A and B for these analyses were 3% (v/v) acetonitrile with 0.1% formic acid and 100% (v/v) acetonitrile with 0.1% formic acid, respectively. However, the LC gradient was modified as follows: 0-15 min, 10% mobile phase B; 15-315 min, 10-40% B; 315-410 min, 40-60% B; 410-425 min, 60-90% B; 425-439 min, 90% B; 439-440 min, 10% B; 440-480 min, 10% B. The reversed-phase analytical column was 75 μm i.d. × 26 cm. MS survey scans were performed in the Orbitrap (R = 60,000) over 300-1800 *m/z* and top 10 CID data dependent acquisition was performed in the LTQ.

5.2.5 Data Analysis

.RAW files were analyzed with Proteome Discoverer 1.3 software. MS/MS spectra were searched against the IPI mouse database (08/16/2012, 59534 sequences). SEQUEST search parameters were as follows: two maximum trypsin miscleavages; precursor and fragment mass tolerances of 10 ppm and 0.8 Da, respectively; carbamidomethyl modification on cysteine was a static modification; oxidation of methionine was a dynamic modification. Decoy database searching was employed to control the false discovery rate (FDR) and generate lists of peptides with high (FDR < 0.01) and medium (FDR < 0.05) confidence.

5.3 RESULTS AND DISCUSSION

Splenocytes were separated into CD90+ and CD90- subset, and the purity of each subset is ~ 95% as shown in the flow cytometry results (Figure 5.1). Splenocyte counts were $2.96 \pm 0.33 \times 10^7$ cells and $6.46 \pm 0.70 \times 10^7$ (mean ± standard deviation, N = 6) cells in the CD90+ and CD90- subsets, respectively. Few studies report the absolute number of T-cells isolated from mouse spleen tissues, however, the percentage of T-cells (31%) is similar to that observed in other AD mouse models[252]. Offline SCX-LC MS/MS analysis led to identification of 1092 and 1223 unique peptides in the CD90+ and CD90- subsets, respectively. Overall, 906 proteins were identified in both subsets (Figure 5.2) and with more stringent criteria [(e.g., at least two spectral counts (SCs) for each protein) this number reduces to 711 proteins. Additionally, 275 and 334 proteins are unique to CD90+ and CD90- subsets, respectively (Figure 5.2), implying no SCs

were detected for these proteins in the other subset. A list of proteins and peptides identified in this study is provided in Supplemental Table S5.1 and S5.2, respectively.

ProteinCenter software (Thermo Scientific; Waltham, MA, USA) was employed to characterize proteins identified in CD90+ and CD90- subsets, and they show similar distributions with regards to cellular components, biological processes, and molecular functions (Figure 5.2b-d). Identified proteins were distributed into 17 cellular locations (Figure 5.2b) with cytoplasmic proteins (24.9% and 23.8% for CD90+ and CD90- subset, respectively) representing a large portion of each dataset. Cytoskeletal proteins including actin-related proteins (e.g., moesin, cofilin-1, talin-1, and Roh family proteins) were also identified in both of the cell subsets (Figure 5.2b). Altered levels of cytoskeletal proteins have been reported to cause neuronal death in AD [263], however, no proteomics studies show how these proteins affect peripheral immune cell function. Within the context of the immune system, cytoskeletal proteins play vital roles in cell migration. Recently, increased recruitment of immune cells (e.g., T-cells, dendritic cells and monocytes) to the brain during neuroinflammation in AD has been reported[264-266]. Additionally, alterations in the levels of cytoskeletal proteins may affect the division, proliferation, and activation of immune cells. Individual cytoskeletal proteins, such as annexin A5 and profilin-1, have higher SCs in CD90+ cells whereas myosin and ezrin have higher SCs in CD90- cells.

Identified proteins were also characterized by biological processes (Figure 5.2c). The top three processes were metabolic, regulation of biological process, and response to stimulus. Increased stimulation of T-cells has been reported in AD, which may be caused by toxic molecules (e.g., Aβ) crossing the BBB[74,251]. Cytokines produced by activated T-cells promote the stimulation of other immune cells (e.g., macrophages and monocytes)[74]. Thus, proteins involved

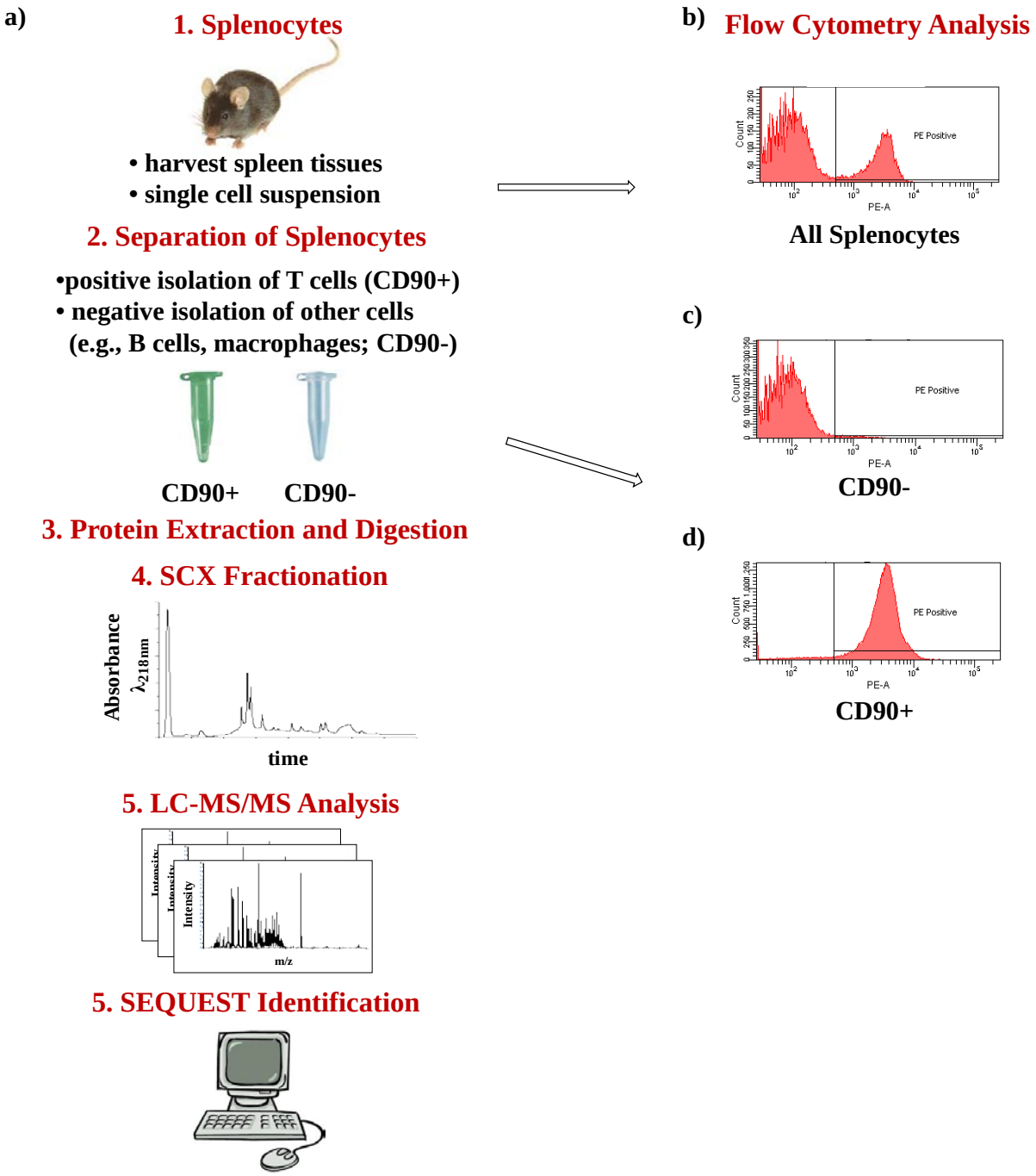

Figure 5.1. a) Proteomics workflow which includes harvesting of splenocytes, sample preparation, and LC-MS/MS analysis. An anti-CD90.2 antibody conjugated with phycoerythrin (PE) was employed to label CD90+ T-cells in the flow cytometry experiment. Plots of isolated cell populations of **b)** all cells before magnetic bead separation, **c)** CD90- subsets, and **d)** CD90+ T-cells.

in response to stimulus for example, should be detected in both subsets. As an example, we observe Thy-1 membrane glycoprotein (or CD90) and lysozyme C-2 in CD90+ and CD90- subset, respectively. Proteins involved in cell differentiation (3.5%), proliferation (2.4%), division (0.8%), and growth (0.3%) were also identified. Characterizing the proteins identified in these processes may help shed light on the behavior in AD immune cells. For example, conflicting results have been reported about the proliferative response of T-cells in AD[267,268]. Our studies have identified calponin-2 and calreticulin, for example, which are involved in proliferation, and are identified in CD90+ and CD90- subset, respectively.

The most abundant molecular functions were protein binding, catalytic activity, and nucleotide binding (Figure 5.2d). Notably, ten and 14 antioxidant proteins which are involved in oxidative stress [e.g., glutathione peroxidase-1 (GPx-1) and thioredoxin reductase 1] were identified in CD90+ and CD90-, respectively. For example, GPx-1 protects tissues and cells from oxidative damage by reduction of reactive oxygen species. Increased activity of GPx-1 may indicate elevated oxidative stress[269]. Increased oxidative stress in the brain has been implicated in the pathogenesis and progression of AD[270]. Recently, our laboratory measured that oxidative stress, as evidenced by elevated levels of 3-nitro-tyrosine and protein carbonylation, increased in CD90+ and CD90- subsets during AD progression (**Chapter 6**)[255]. GPx-1 has a higher rank in CD90- as compared to CD90+ cells. These results correlate with the higher levels of oxidative stress observed in CD90- cells[255]. Identification of these antioxidant proteins and how they are distributed in the CD90+ and CD90- subsets sheds light on the pathways that may lead to global oxidative stress in this model [255,257].

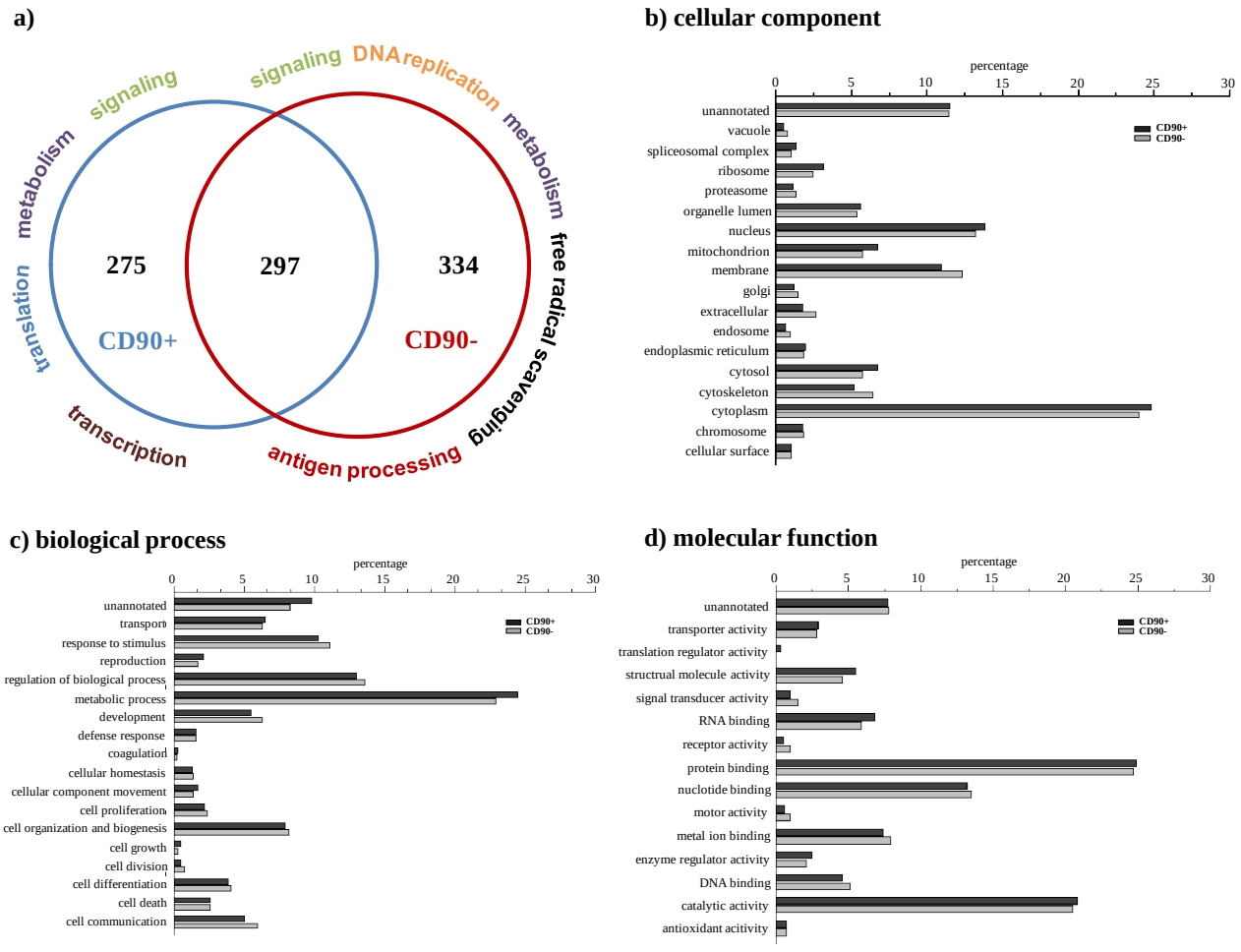

Figure 5.2. a) Venn diagram of the number of proteins identified in CD90+ and CD90- subsets with associated biological processes listed. Histogram plots of the percentage of proteins identified in CD90+ (black rectanguler) and CD90- (gray rectanguler) involved in a specific **b)** cellular component, **c)** biological function, and **d)** molecular function based on ProteinCenter analyses.

To better study the proteome of CD90+ and CD90- cells, the biological functions of proteins unique to each subset were compared. Proteins associated with transcription and protein translation were significantly overrepresented in CD90+ cells whereas DNA replication, free radical scavenging, and antigen processing were significantly overrepresented in CD90- cells (Figure 5.2a). Rank of protein abundance [271,272]-a robust measurement based on SCs [271,272]-for proteins identified in both CD90+ and CD90- subsets was also compared (Figure 5.3). One hundred and eighty-nine proteins have similar rank (*data not shown*) between CD90+ and CD90- subsets and are significantly involved in RNA post-transcriptional modification, post-translational modification, protein folding, cell death and survival, and DNA replication. The most abundant protein in CD90+ and CD90- cells are histone H2AZ and heat shock cognate 71 kDa proteins, respectively. Of the 297 proteins that overlap between cells, 47 proteins have a higher rank in CD90+ cells (Figure 5.3a) and are involved in protein translation, cellular function and maintenance, energy production, and lipid metabolism. Annexin A5, a cytoskeletal protein which maintains cellular function, was selected for Western blotting analysis. Similar to the proteomics data, annexin A5 has higher abundance in CD90+ cells (Figure 5.3a inserts). Fifty-nine proteins have higher rank in CD90- cells (Figure 5.3b) and are involved in free radical scavenging, cell signaling, and post-translational modification. Assessing the relative abundances of proteins in each subset as well as identifying proteins unique to a specific subset may help with understanding the role of each protein in AD.

Finally, proteins from CD90+ and CD90- subset were further compared by biological pathways. Eighteen and 19 pathways were identified for CD90+ and CD90- subset, respectively (Supplemental Table S5.3). Pathways related to energy metabolism are identified in both of

CD90+ and CD90- subset, such as citrate cycle, glycolysis/gluconegenesis, and oxidative phosphorylation. Notably, CD90+ proteins are involved in the pathways associated with dementia including AD. As shown in Figure 5.4a, six proteins in AD are detected in this study, which have higher rank in CD90+ cells. Out of the six proteins, four mitochondrial proteins were identified (Figure 5.4a): complex I (NADH Dehydrogenase, C-I), complex IV (or cytochrome c oxidase, C-IV), complex V (or ATP synthase, C-V), and cytochrome c (CytC), which regulate energy metabolism, oxidative stress, and apoptosis[250,273]. Deficiencies of C-I and C-IV may induce higher concentration of reactive oxygen species and inhibit production of ATP in AD[250,274] whereas C-V is related to T-cell proliferation and activation[275]. Increased oxidative stress leads to the release of CytC to the cytoplasm resulting in apoptosis[276]. The roles of peripheral mitochondrial proteins in AD has been reviewed recently[277].

However, phagosome and antigen processing and presentation are uniquely identified for CD90- proteins, which are consistent with the function of CD90- cells (e.g., macrophages, dendritic cells, and neutrophils). In this study, eight proteins detected in the CD90- cells are involved in antigen processing and presentation (Figure 5.4b). For example, calnexin (CANX), which is essential for the assembly of major histocompatibility complex[278], was observed in this study. Alterations in the levels of CANX have been reported in AD[274].

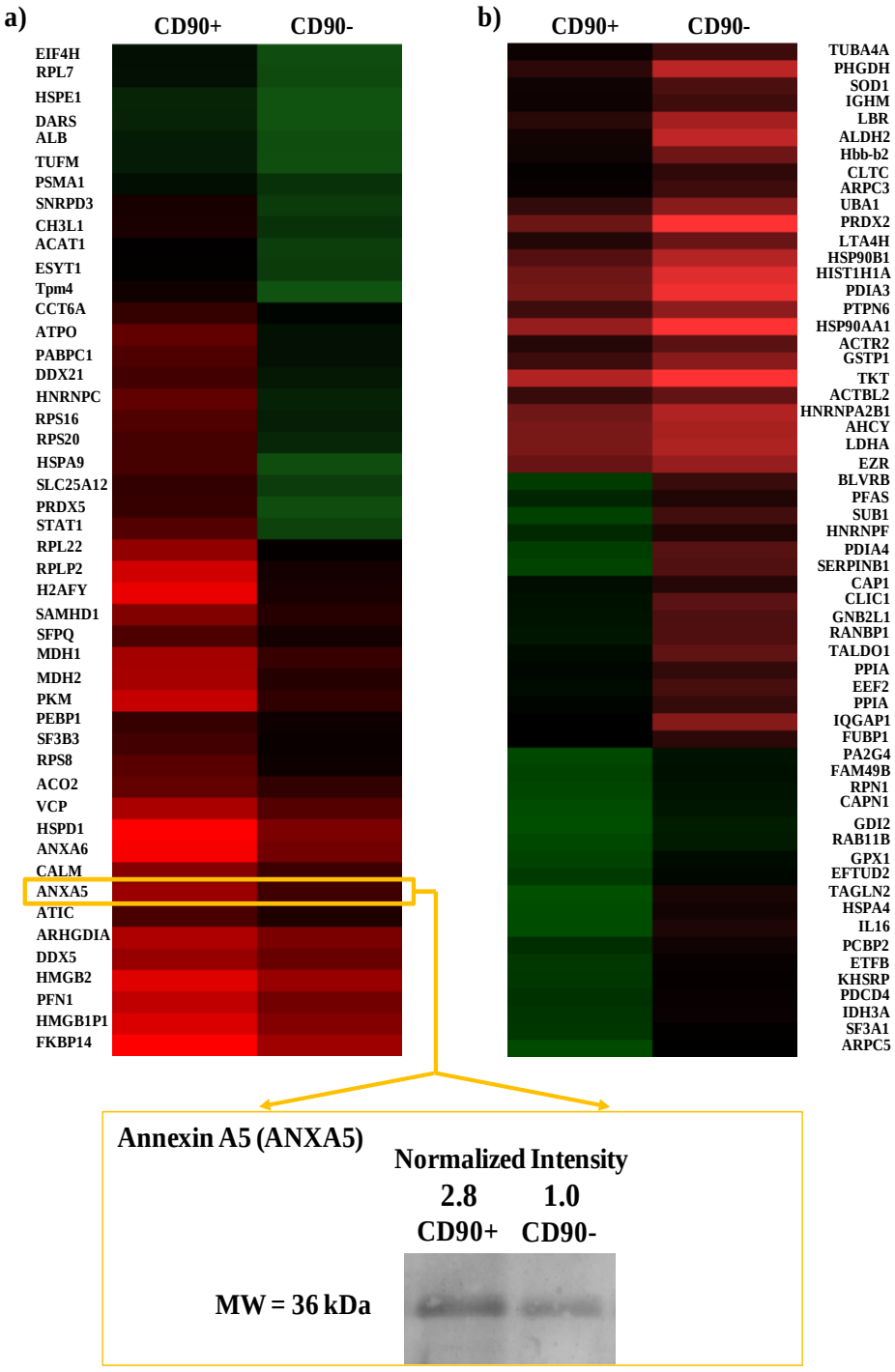

Figure 5.3. Heatmap display of protein abundance rank for proteins which have higher abundance in **a)** CD90+ (N = 47) and **b)** CD90- (N = 59) subsets, respectively. Insert in **a)** shows the Western blotting data for annexin A5.

a) Alzheimer's disease

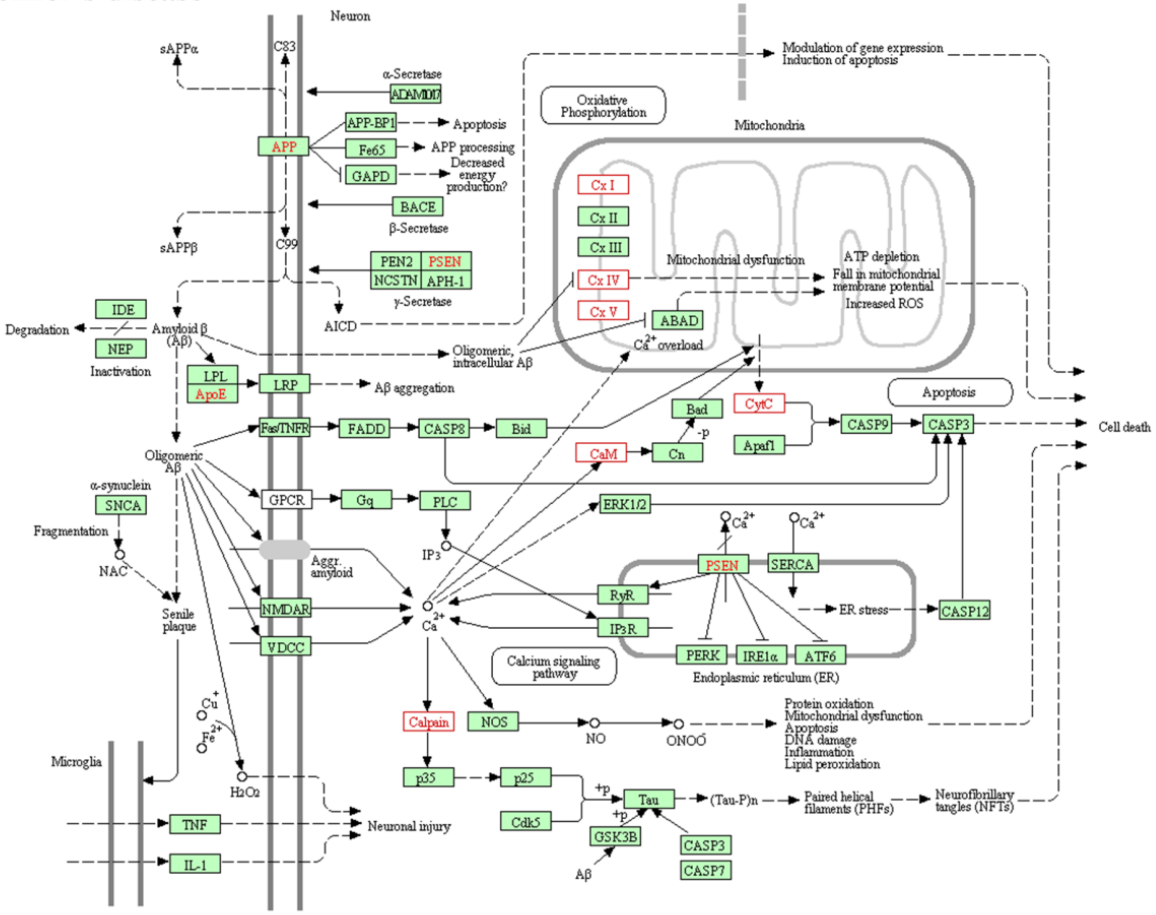

b) Antigen processing and presentation

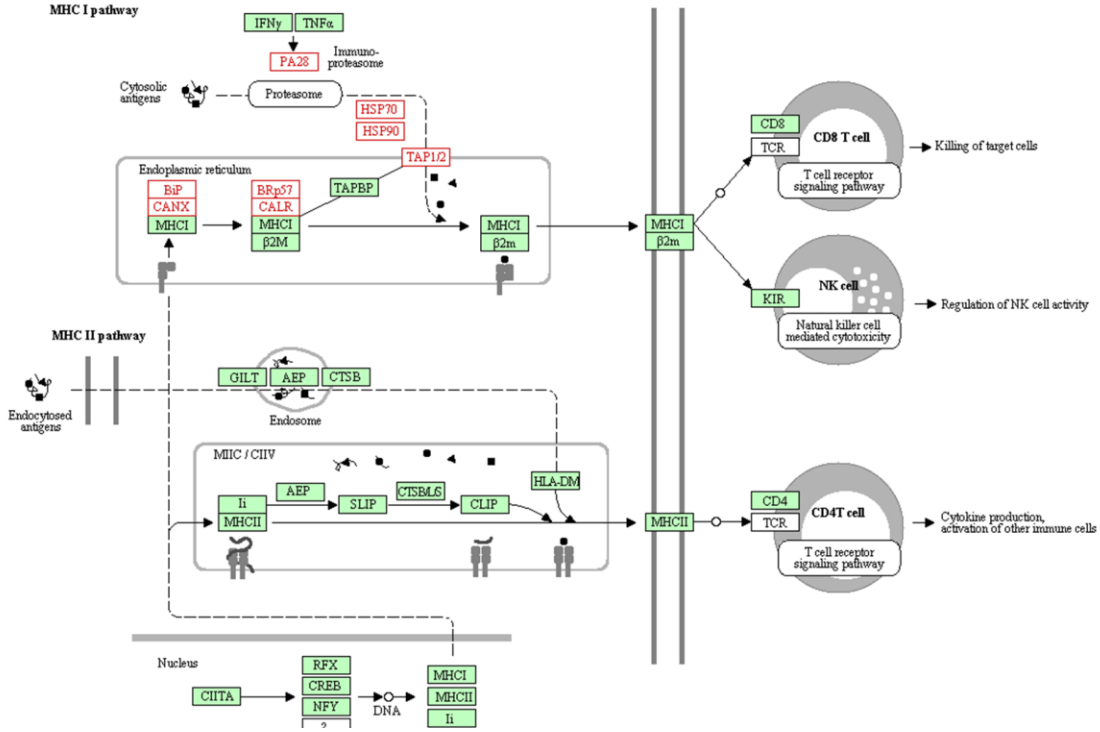

Figure 5.4. KEGG pathway analysis of the **a)** Alzheimer's disease and **b)** Antigen processing and presentation pathways for CD90+ and CD90- proteins identified in this study, respectively (denoted by red label and box).

5.4 CONCLUSIONS

This work has provided a comprehensive map of CD90+ and CD90- splenocytes in double transgenic APP/PS-1 mice. Nine hundred and six proteins were identified and are involved in various biological pathways, such as dementia, antigen processing and presentation, and energy metabolism. Proteome comparison of specific subsets of splenocytes may help provide better insight into AD pathology.

6.0 OXIDATIVE STRESS IN CD90+ T-CELLS OF APP/PS-1 TRANSGENIC MICE[255]*

(*note that information in this chapter is written based on a published paper, Robinson, R. A. S.; Cao, Z.; Williams, C. *Journal of Alzheimer's Disease* **2013**, *37*, 661)

6.1 INTRODUCTION

The immune system has been linked to the etiology of AD and may serve as an early marker of disease[74,279-284]. In AD patients, suppressor cells and helper T-cells have abnormal function[285,286], decreased proliferative activity[268,287], activation responses[288], and functionality of natural killer (NK) cells[289]. Conflicting reports exist however, with regards to the changes of specific cell types. For example, the number of T- and NK cells are reported as unchanged in AD patients[70,290], while in other studies, the levels of CD8+ and CD3+ T-cells, CD19+ B-cells, and NK cells are decreased in AD patients compared to age-matched controls[70,252,266,286,291,292]. Cytokine levels in the periphery vary[287,293-296] and AD patients have a lessened T-cell proliferative response to amyloid beta precursor protein (APP) peptides[268] and other antigenic factors[297,298]. Additional factors that may contribute to altered immunity in AD patients are telomere shortening[299], intracellular calcium response[300], and oxidative stress[301].

Consistent with findings in human patients, altered immunity has recently been reported in a triple transgenic (3xTg) AD mouse model[74]. Based on lower thymus weights, chemotaxis function, proliferation, anti-tumoral NK activity, and interleukin (IL)-2 levels in younger 3xTg-AD mice, it is apparent that the immune system can be used as an early marker of disease[74]. Older 3xTg-AD mice have higher chemotaxis function and IL-2 secretion in comparison to controls[74]. Predisposition to systemic immune challenges during late neonatal stages of

development, leads to AD-like pathology in wild-type (WT) mice that becomes more pronounced if there is additional exposure to immune challenge during adulthood[280]. Such findings imply that systemic immune challenges or peripheral dysfunction can be risk factors for developing AD.

Interestingly, oxidative stress is also implicated in the immune system of 3xTg AD mice; lower activity of antioxidants glutathione peroxidase, glutathione reductase, and total glutathione and increased xanthine oxidative activity is observed in spleen of 3xTg AD mice[74]. Because of the correlation of these changes with premature immunosenescence, oxidative stress appears to be a precursor of altered immune function and/or disease pathogenesis in AD. We sought to determine if oxidative stress is present in the peripheral immune system of a double transgenic AD mouse model that has mutations in the genes coding APP and presenilin-1 (PS-1), a sub-component of γ-secretase. Mutations in APP and PS-1 are present in familial AD and are associated with increased incidence of AD[249].

6.2 EXPERIMENTAL AND MATERIALS

6.2.1 Animals

APP/PS-1 male mice [B6.Cg-Tg(APPswe,PSEN1dE9)85Dbo/Mmjax, stock number 005864, genetic background C57BL/6J express the chimeric mouse/human (Mo/Hu) APP695swe (i.e., K595N and M596L) and a mutant human PS1-dE9[254,302] were purchased from Jackson Laboratory and housed in the Division of Laboratory Animal Resources at the University of Pittsburgh. Mice were fed standard Purina rodent laboratory chow *ad libitum* on a 12 h light/dark cycle. All animal protocols were approved by the Institutional Animal Care and Use Committee

at the University of Pittsburgh. Spleen tissues were harvested from control and AD mice at three, seven, and 12 months which correspond to time points before, during, and after the pathological and physical symptoms of AD[254,302].

6.2.2 Splenocytes Isolation

Spleen tissue was mashed to obtain single cell suspensions and CD90.2 magnetic microbeads (MiltenyiBiotec Inc. Auburn, CA, USA) were used to separate T-cells (hereafter referred to as CD90+ T-cells) from other non T-cell populations (e.g., B-cells, NK cells, macrophages; hereafter referred to as CD90- cells) according to manufacturer's instruction. Proteins were extracted with RIPA buffer and three cycles of rapid freezing and thawing was performed to lyse cells. Samples were centrifuged at 14,000 g at 4 ºC for 20 min to remove cellular debris. Supernatant was collected and protein concentration was determined by BCA assay. An aliquot of the sample was acetone precipitated and reconstituted in PBS buffer for further analyses.

6.2.3 Oxidative Stress Measurements

For PCO measurements, five µL of each sample was incubated with 12% SDS and 20 mM 2,4-Dinitrophenylhydrazine (DNPH) solution for 20 min at room temperature. For 3NT measurements, five µL of each sample was incubated with 12% SDS and Laemmli buffer for 20 min at room temperature. A neutralization solution was added to stop the reaction. Derivatized proteins (250 ng) were loaded onto a nitrocellulose membrane with a slot blot apparatus. The membranes were blocked with 3% (w/v) BSA solution overnight at 4 ºC and incubated with a 1 :

2000 dilution of anti-DNP antibody (Millipore, Billerica, MA, USA) or a 1 : 2500 dilution of anti-3-nitrotyrosine antibody produced in mouse (Sigma-Aldrich, St Louis, MO, USA) for 2 hours. After four cycles of rinsing, anti-rabbit IgG alkaline phosphatase secondary antibody (Sigma) or anti-mouse IgG alkaline phosphatase (Sigma-Aldrich, St Louis, MO, USA) was added with the dilution factor 1 : 5000 and incubated with membranes for 1 h. The membranes were washed in wash blot and developed using 5-bromo-4-chloro-3-indolyl phosphate (BCIP)/nitro blue terazolium chloride (NBT) color-imetric development. Blots were dried, scanned and quantitated with Scion Image. The data was analyzed using two-way ANOVA ($p < 0.05$) testing with Origin 8.0.

6.3 RESULTS AND DISCUSSION

Proteins extracted from CD90+ T-cells and CD90- cells were used to measure global levels of common oxidative stress parameters-PCO and 3NT (Figure 6.1). Samples from three-month old WT were set as the controls and different age groups and genotype (i.e., AD) were compared to the control levels. WT mice exhibit increased levels of PCO and 3NT in both CD90+ T-cells and CD90- cells with increasing age. The effects are more pronounced between each age group for PCO and 3NT levels measured in CD90- cells and 3NT levels measured in CD90+ T-cells. For example, in CD90+ T-cells, there is an ~ 80% increase in 3NT levels from seven to 12 months (Figure 6.1c). APP/PS-1 mice also exhibit age-dependent increases in PCO and 3NT levels in CD90+ T-cells and CD90- cells. Larger differences in oxidative levels exist between seven and 12 months, which correlates with increased Aβ deposition in the brain[254,302].

For example, in CD90+ T-cells there are ~ 80% and ~ 100% increases in PCO (Figure 6.1a) and 3NT (Figure 6.1c) levels, respectively, from seven to 12 months in APP/PS-1 mice. Finally, from the ANOVA analysis there is also a significant difference in oxidative PCO levels between WT and APP/PS-1 mice at seven and 12 months (Figure 6.1a, $p < 0.01$ and $p < 0.05$).

Oxidative stress plays a significant role in the pathogenesis of AD as has been evidenced by measurements in brain[79,303], plasma [304-306], cerebrospinal fluid[270,307], and other tissues such as heart[307-309]. Recently, there has been evidence to suggest that oxidative stress levels are elevated in the peripheral immune system of AD patients or mouse models[74,310] leading to new insight to this disorder. Our results are consistent with these findings and suggest that oxidative stress is present in the peripheral immune system of an AD mouse model and that these levels increase in an age-dependent manner that tracks disease progression. These findings are based on measures of global protein oxidation which are commonly used to assess oxidative stress in many disorders including AD[311-313].

The APP/PS-1 model used in these studies has been used extensively to study aspects of familial AD[79,254,302]. While APP/PS-1 do not have neurofibrillary tangles, they do repeatedly display symptoms such as memory loss, impairment in learning ability, and decreased cognition as a function of age[254,302]. By nine months of age, Aβ deposition occurs in the brains of these mice, resulting in SP formation by 12 months[254,302] and increases in plaque formation can be correlated with augmented levels of Aβ(1-42)[254,302]and oxidative stress[79,303,312]. Most relevant to this work is the evidence which links altered immunity to neurodegeneration in this model. It has been reported that immunization with glatiramer acetate and myelin oligodendrocyte glycoprotein-derived peptide (targets of immune cells) improve Aβ clearance, memory and

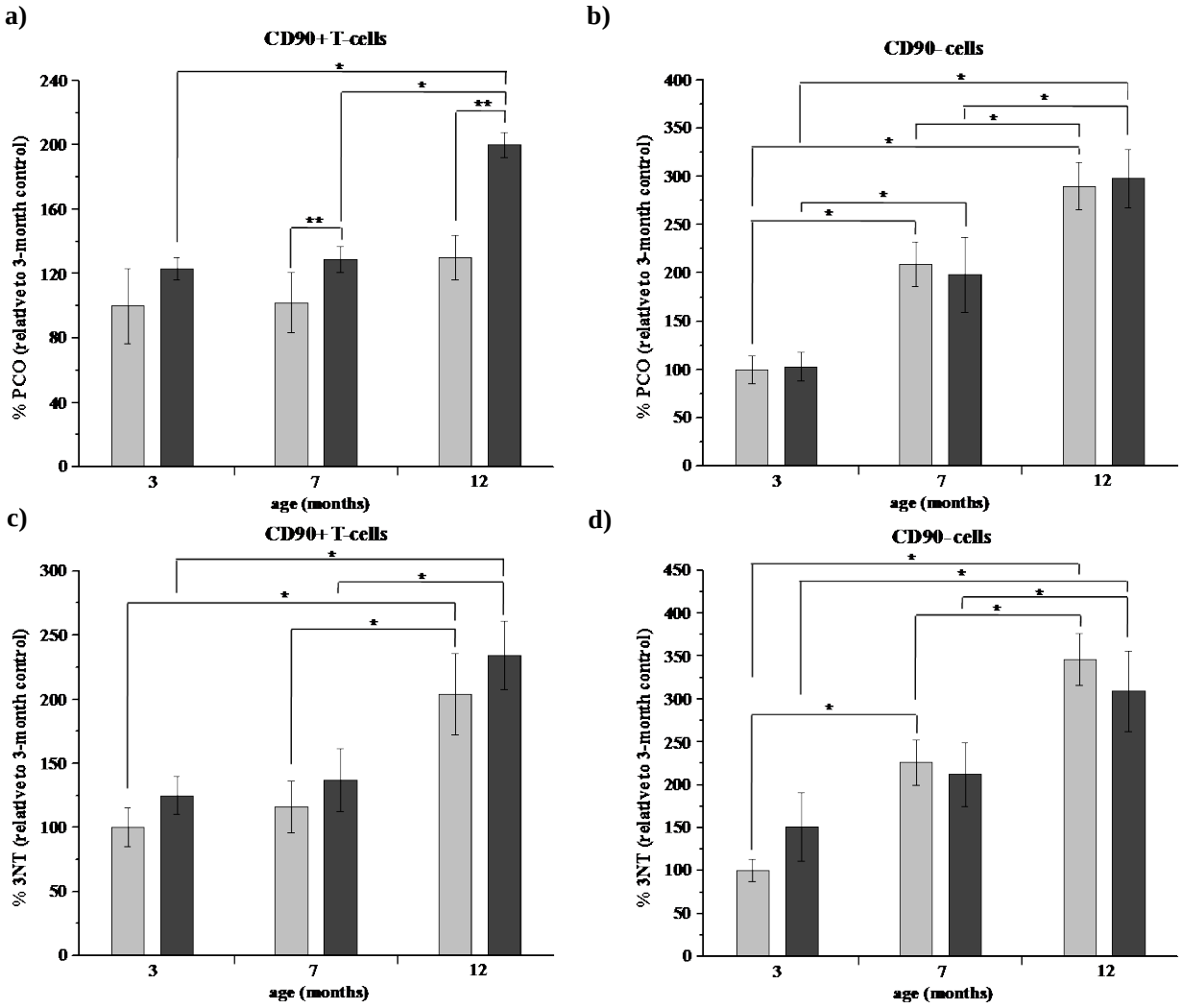

Figure 6.1. Histogram plots for levels of protein carbonylation (PCO) and 3-nitrotyrosine (3NT) in CD90+ T-cells and CD90- cells isolated from control (gray rectangular) and AD (black rectangular) mice at three, seven, and 12 months. Intensities are normalized to three-month old WT controls (N = 6). Error bar: ± SEM. * $p < 0.01$, ** $p < 0.05$.

learning, and increase anti-inflammatory cytokines and reduce pro-inflammatory cytokines in macrophages[314-316]. Additionally, the CD90+ T-cell proteome of this AD mouse model has recently been characterized by our laboratory and includes the identification of many proteins involved in free radical scavenging and transcription and translational processes (**Chapter 5**)[247].

To-date there are no reports of oxidative stress in the peripheral immune system of APP/PS-1 mice. Based on studies in the 3xTgAD model which point to oxidative stress as an early indicator of disease pathogenesis, our results reported herein are consistent with this notion. As the levels of PCO and 3NT increase with disease progression in this model, oxidative stress measurements in CD90+ T-cells could be used as an early sign of AD. It is clear that elevated oxidative stress in CD90+ T-cells and CD90- cells is also partially related to immunosenescence as both WT and APP/PS-1 mice exhibit age-dependent changes in levels. In order to better understand the relationship between oxidative stress and its effects on immune function and inflammation pathways, we have initiated a large-scale proteomics study of CD90+ T-cells with disease progression in APP/PS-1 mice (**Chapter 7**). Those studies report on many proteins involved in oxidative stress and immune pathways such as aldose reductase, granzymes A and B, and lamin1. Due to low concentrations and the necessity for enrichment, no cytokines were observed in CD90+ T-cells.

6.4 CONCLUSIONS

In conclusion, this work presents the first report of oxidative stress measurements in CD90+ T-cells and CD90- cells in APP/PS-1 mice and shows that PCO and 3NT levels may be

useful for measuring early signs of AD and tracking disease progression in peripheral immune tissue. Future studies may include understanding the effects of oxidative stress on immune function in APP/PS-1 and/or human subjects.

7.0 TRACKING THE T-CELL PROTEOME DURING THE PROGRESSION OF ALZHEIMER'S DISEASE

7.1 INTRODUCTION

Alzheimer's disease (AD) currently affects ~ 27 million people worldwide and it is predicted that this number will double every 20 years until at least 2040[248,317]. Clinically, AD patients are characterized by progressive memory deficits, cognitive impairment, and changes in behavior and personality[248,317]. It is clear that alterations in the central nervous system (CNS) play important roles in the pathology of AD. Such alterations include the accumulation of senile plaques (SP) and neurofibrillary tangles (NFTs), regionalized neuronal death, loss of synaptic connections, increased oxidative stress, mitochondrial dysfunction, and reduced energy metabolism[303,318,319]. Neuroinflammation, which is manifested by activated microglia and astrocytes and increased levels of cytokines and chemokines, is observed in AD CNS[64,320].

While AD is primarily characterized by changes in the CNS alterations in peripheral immunity may also contribute to disease etiology. Impaired peripheral immunity is associated with AD and other neurodegenerative disorders including Parkinson's disease (PD), Huntington's disease (HD), Down syndrome (DS), amyotrophic lateral sclerosis (ALS), and multiple sclerosis[321-324]. Low-grade chronic inflammation associated with aging increases the risk of AD in the elderly[321]. Inflammation caused by infectious agents may also contribute to the pathogenesis of AD[325]. Herpes simplex virus type 1 (HSV-1), a neurotropic virus, has been found in AD brain[325] and is observed in the elderly[326]. Cytomegalovirus also increases the risk of AD which is related to compromised immunity caused by infection[326].

Dysfunctional immune cells are present in AD. Macrophages and monocytes have lessened phagocytic ability [68,69]. The cytotoxic function of natural killer (NK) cells is impaired although no changes are observed in the number of NK cells[70]. The number and anti-amyloid β (Aβ) response of B-cells is lower in AD[321,327]. Conflicting reports exist regarding T-cells[69]. For example, some studies report decreased numbers of T-cells in AD patients[292,328] whereas others found no changes[321,329]. AD patients have decreased numbers of naïve T-cells but increased numbers of memory cells [321], consistent with the elderly[330]. Shortened telomeres in T-cells[331] result in increased production of pro-inflammatory cytokines [e.g., interleukin (IL)-6 and tumor necrosis factor (TNF)-α] and natural killer-like activities[331]. T-cells also have elevated calcium response[300], increased apoptosis[332], and hyper-activity[73].

Communication between the peripheral immune system and CNS affects AD brain function. Monocytes and T-cells infiltrate the AD brain[67]. Once in the brain, these cells can activate microglia and exacerbate neuroinflammation and Aβ precipitation[321]. For example, IL-2 in the brain damages neuronal integrity[333]. Interferon-γ produced by T-helper 1 cells promotes SP formation[334]. Peripheral immune cells can exert damaging effects on the brain without directly entering the CNS. For example, cytokines secreted by peripheral T-cells, monocytes and macrophages can cross the blood-brain barrier (BBB) and enhance neuroinflammation, while the cells themselves do not cross the BBB[321,335].

Mouse models represent an important means to investigate the immunopathology of AD and in fact dysfunction of the immune system in various mouse models has been reported. In triple transgenic (3xTg) AD mice, reduced weight of immune organs (e.g., thymus, spleen, and adrenal glands) indicates premature immunosenescence[74]. 3xTg mice have decreased

chemotaxis, antitumoral natural killer activity, and IL-2 secretion[74] and show signs of systemic autoimmunity[75]. Regulation of the inflammatory response by blocking IL-1 signaling attenuates cognitive defects in 3xTg mice[76]. Human double transgenic knock-in amyloid precursor protein/presenilin-1 mouse (APP/PS-1) is another important AD model[78,254]. APP/PS-1 mice have increased oxidative stress in T-cells that is exacerbated with later stages of disease (**Chapter 6**)[336]. Additionally, they have increased activation of microglia[81,82], altered monocyte subpopulations[337], and enhanced lymphocytes proliferation[84]. Aβ deposition in APP/PS-1 mouse brain is accompanied by T-cell infiltration caused by respiratory infection[338]. Such findings from AD mouse models help to better elucidate the role of immunity in AD pathogenesis. Furthermore, changes in immune cells may provide novel biomarkers for diagnosis and treatment of AD.

Recently, our laboratory compared the proteome of CD90+ T-cells and CD90- cells from APP/PS-1 mice and identified that CD90+ proteins are more involved in transcription and translation, whereas CD90- proteins are more involved in DNA replication, free radical scavenging, and antigen processing (**Chapter 5**)[247]. Based on this APP/PS-1 splenocyte reference map, we extend our proteomics investigation of immune cells in APP/PS-1 mice in this work. Specifically, the CD90+ T-cell proteome of APP/PS-1 mice is compared to age-matched wild-type (WT) controls at three, seven, and 12 months of age. At three months, APP/PS-1 mice behave similarly to WT. At seven months, Aβ plaques start to deposit in the brain and mice mimic the cognitive deficits associated with early stages of AD[78,254]. By 12 months of age, numerous SP are present in the hippocampus and caudal cortex[78,254]. Here, CD90+ T-cell proteins are digested, and tryptic peptides are tagged with isobaric tags for relative and absolute

quantitation (iTRAQ) reagents and analyzed with liquid chromatography coupled to tandem mass spectrometry (LC-MS/MS). Differentially-expressed proteins give insight into changes in T-cells that affect peripheral immune function during the progression of AD.

7.2 MATERIALS AND METHODS

7.2.1 Animals

APP/PS-1 male mice [B6.Cg-Tg(APPswe,PSEN1dE9)85Dbo/Mmjax, stock number 005864, genetic background C57BL/6J express the chimeric mouse/human (Mo/Hu) APP695swe (i.e., K595N and M596L) and a mutant human PS1-dE9] [254] and the genetically heterogeneous WT (stock number 000664, genetic background C57BL/6J) were purchased from Jackson Laboratory and housed in the Division of Laboratory Animal Resources at the University of Pittsburgh. Mice were fed standard Purina rodent laboratory chow *ad libitum* on a 12 h light/dark cycle. All animal protocols were approved by the Institutional Animal Care and Use Committee at the University of Pittsburgh. APP/PS-1 mice and WT controls were euthanized using CO_2 and sacrificed at three, seven, and 12 months of age (N = 6 for each genotype at each time point). Spleen tissues were harvested and T-cells were isolated immediately.

7.2.2 T-cell Isolation and Protein Extraction

Spleen tissue was mashed to obtain a single cell suspension. CD90.2 magnetic microbeads (Miltenyi Biotec, Auburn, CA, USA) were employed to positively isolate T cells according to the manufacturer's instruction (hereafter referred to as CD90+ T-cells). Proteins

were extracted with RIPA buffer (0.05 M Tris, 0.15 M NaCl, 3 mM SDS, 10 mM Sodium Deoxycholate, 1 mM pheylmethylsufonyl fluoride, 1% v/v Tritan X-100, 1 µg/mL leupeptin, 1 µg/mL pepstatin, 1 µg/mL aprotinin) and three cycles of rapid freezing and thawing was performed to lyse cells. Samples were centrifuged at 14,000g at 4ºC for 20 min to remove cellular debris. Supernatant was collected and protein concentration was determined by BCA assay.

7.2.3 Protein Digestion and iTRAQ Labeling

Proteins from CD90+ T-cells were acetone precipitated. Protein pellets were suspended in 0.1% w/v RapiGest SF (Waters, Milford, MA, USA) solution in 50mM NH_4HCO_3, reduced with dithiothreitol, alkylated with iodoacetamide, and digested with TPCK-treated trypsin (Sigma, St. Louis, MO, USA). Trifluoroacetic acid was added and incubated for 45 min at 37 ºC to quench digestion. Samples were centrifuged at 13,000 rpm for 10 min, the supernatant cleaned with an Oasis HLB cartridge (Waters), and dried with a SpeedVac. A pooled sample consisting of an equal molar amount of all samples (N = 36) was used. Each sample was labeled with an iTRAQ reagent following the manufacturer's protocol (Applied Biosystems; Foster City, CA) with slight modifications. Briefly, each iTRAQ reagent was solubilized with 70 µL ethanol and transferred to peptide mixtures. After 1.5 h of incubation, the reaction was quenched by adding 50 µL of water. Equal amounts of each iTRAQ-labeled sample were combined, cleaned with an Oasis HLB cartridge, and dried with a SpeedVac.

7.2.4 Strong Cation Exchange Fractionation and LC-MS/MS Analysis

Offline strong cation exchange (SCX) was used to fractionate peptide mixtures as previously described [97]. Three SCX fractions were collected and cleaned with an Oasis HLB cartridge (Waters; Milford, MA, USA), followed by online desalting and reverse phase chromatography analysis on a Nano2D- Eksigent LC system equipped with an autosampler (Eksigent; Dublin, CA, USA). The LC eluent was analyzed with positive ion mode nanoflow electrospray using a Thermo-Fisher Scientific LTQ-Orbitrap Velos mass spectrometer (Thermo Scientific; Waltham, MA, USA). Data-dependent acquisition parameters were: the MS survey scan in the Orbitrap was 60,000 resolution over 300-1800 *m/z*; the top six most intense peaks in the MS survey scan were isolated and fragmented with CID and HCD; CID was performed in the ion trap with normalized collision energy 35%; HCD was recorded in the Orbitrap with normalized collision energy 45% and 7,500 resolution; dynamic exclusion was enabled; a repeat count of two for a duration of 60 s was allowed and selected ions were placed on an exclusion list for 90 s. Each SCX fraction was subject to triplicate LC-MS/MS analysis.

7.2.5 Data Analysis

.RAW files were analyzed with Proteome Discoverer 1.3 software (Thermo Scientific; Waltham, MA, USA). Both CID and HCD spectra were used to obtain sequence information against the International Protein Index mouse database (08/16/2012, 59534 sequences). SEQUEST search parameters were as follows: two maximum trypsin miscleavages; precursor mass tolerance 10 ppm; fragment mass tolerance 0.8 Da; static modifications were iTRAQ-8plex/+304.205 Da (N-terminus, Lys), and carbamidomethyl modification/+57.021 Da (Cys);

dynamic modification of oxidation/+15.995 Da (Met). Decoy database searching was employed to generate medium ($p < 0.05$) and high ($p < 0.01$) confidence peptide lists. All the peptides with medium and high confidence were used to identify and quantify proteins. The reporter ions (i.e., *m/z* 113-119) were identified with the following parameters: centroid with smallest delta mass, 20 ppm for reporter ion mass tolerance. The isotope correction was employed according to the manufacturer's protocol (AB Sciex; Framingham, MA, USA). Additionally, protein ratios in each experiment were normalized based on the protein median ratio option in the software. Only proteins with at least two spectral counts (SCs) in a biological replicate were considered for further analysis.

7.2.6 Statistical Analysis

Reporter ion ratios were obtained by comparison against the pooled sample for statistical testing: WT_{3m}/pool, APP/PS-1_{3m}/pool, WT_{7m}/pool, APP/PS-1_{7m}/pool, WT_{12m}/pool, and APP/PS-1_{12m}/pool. To compare protein levels between APP/PS-1 and WT mice at three, seven, and 12 months, student's *t* test was performed on proteins quantified in at least four biological replicates . Bonferroni multiple testing correction was applied and proteins with adjusted *p*-value < 0.05 were considered as significantly different. Protein ratios were calculated by comparing a specific age group of APP/PS-1 mice with the respective age-matched controls as follows: (APP/PS-1 / $WT)_{3m}$, (APP/PS-1 / $WT)_{7m}$, and (APP/PS-1 / $WT)_{12m}$. Fold-change cutoff values were set to APP/PS-1 / WT ≥ 1.30 or ≤ 0.77 as previously described [97]. Finally, these proteins were grouped based on their biological functions.

7.2.7 Western Blotting Analysis

The changes in the expression of annexin A5, lamin B1, and aldose reductase were verified with Western blotting analysis. T-cell proteins (10 µg) were denatured in an appropriate sample buffer and electrophoretically separated on a Criterion precast gel (Biorad Laboratories; Hercules, CA, USA) at 140 V. Proteins from the gel were transferred onto a nitrocellulose membrane paper using a fast transfer blot system (Biorad Laboratories; Hercules, CA, USA). Blots were washed three times in wash blot. BSA blocking solution (3%) was added to the membrane and incubated on a rocker for 2 h. A 1 : 2500 dilution of rabbit polyclonal anti-annexin A5 primary antibody (Abcam; Cambridge, MA, USA), 1 : 5000 dilution of rabbit polyclonal anti-lamin B1 primary antibody (Abcam; Cambridge, MA, USA) or 1 : 2500 dilution of rabbit polyclonal anti-aldose redcutase primary antibody (Santa Cruz Biotechnology, Inc; Dallas, Texas, USA) was added and incubated at 4°C overnight. The blot was rinsed and incubated with a 1 : 7500 dilution of anti-rabbit IgG alkaline phosphatase secondary antibody (Sigma-Aldrich; St. Louis, MO, USA) for 1 h on a rocker. The blot was rinsed and colorometrically developed using 0.51 mM 5-bromo-4-chloro-3′-indolylphosphate *p*-toluidine salt (BCIP) and 0.24 mM nitrotetrazolium blue (NBT). The dried blot was scanned using a Canon scanner, saved as a TIFF file, and densitometry analyses were carried out with Scion Image Software. Within each experiment, the intensity for the sample from each group was normalized to the total blot intensity and used to generate mean and standard deviation values. Student's *t* test was performed on normalized band intensities.

7.3 RESULTS

7.3.1 Data Characterization

Quantitative proteomics was used to identify differentially-expressed proteins in T-cells during the progression of AD. Protein samples from APP/PS-1 and WT mice aged three, seven, and 12 months were assigned to various iTRAQ114-119 channels and a pooled sample was labeled with iTRAQ113 (Table 7.1). Figure 7.1 is a bar graph of the number of proteins and SCs identified in six biological replicate experiments. An average of 80448 ± 4735 [mean ± standard deviation (SD)] SCs and 411 ± 21 (mean ± SD) proteins were identified. The cumulative number of unique proteins identified is 927 (SC ≥ 2).

7.3.2 Differentially-Expressed Proteins

Protein ratios were obtained by comparing intensities of iTRAQ reporter ions corresponding to samples from APP/PS-1 mice with respective age-matched WT control mice as follows: $(APP/PS\text{-}1 / WT)_{3m}$, $(APP/PS\text{-}1 / WT)_{7m}$, $(APP/PS\text{-}1 / WT)_{12m}$. Thirty-three proteins have significantly different levels ($p < 0.05$) in APP/PS-1 mice: five, 22, and 31 proteins are altered at three, seven, and 12 months, respectively (Table 7.2). The number of altered T-cell proteins increases with progression of pathological AD hallmarks. Our study design allows us to assess how each individual protein varies with disease progression. For example, no significant difference for protein frizzled-6 (1.01 ± 0.10, $p = 1.52$) was observed between APP/PS-1 and WT mice at three months. At seven months, APP/PS-1 mice had increased levels of frizzled-6 (1.48 ± 0.17, $p = 0.02$), that continued to increase at 12 months (1.85 ± 0.35, $p = 2E\text{-}3$).

Table 7.1. iTRAQ quantitation channel assignment for each biological replicate.

experiment	iTRAQ reporter ions						
	113	**114**	**115**	**116**	**117**	**118**	**119**
1	pool	WT_{3mon}	AD_{3mon}	WT_{7mon}	AD_{7mon}	WT_{12mon}	AD_{12mon}
2	pool	WT_{3mon}	AD_{3mon}	WT_{7mon}	AD_{7mon}	WT_{12mon}	AD_{12mon}
3	pool	WT_{7mon}	AD_{7mon}	WT_{3mon}	AD_{3mon}	WT_{12mon}	AD_{12mon}
4	pool	WT_{7mon}	AD_{7mon}	WT_{3mon}	AD_{3mon}	WT_{12mon}	AD_{12mon}
5	pool	WT_{12mon}	AD_{12mon}	WT_{7mon}	AD_{7mon}	WT_{3mon}	AD_{3mon}
6	pool	WT_{12mon}	AD_{12mon}	WT_{7mon}	AD_{7mon}	WT_{3mon}	AD_{3mon}

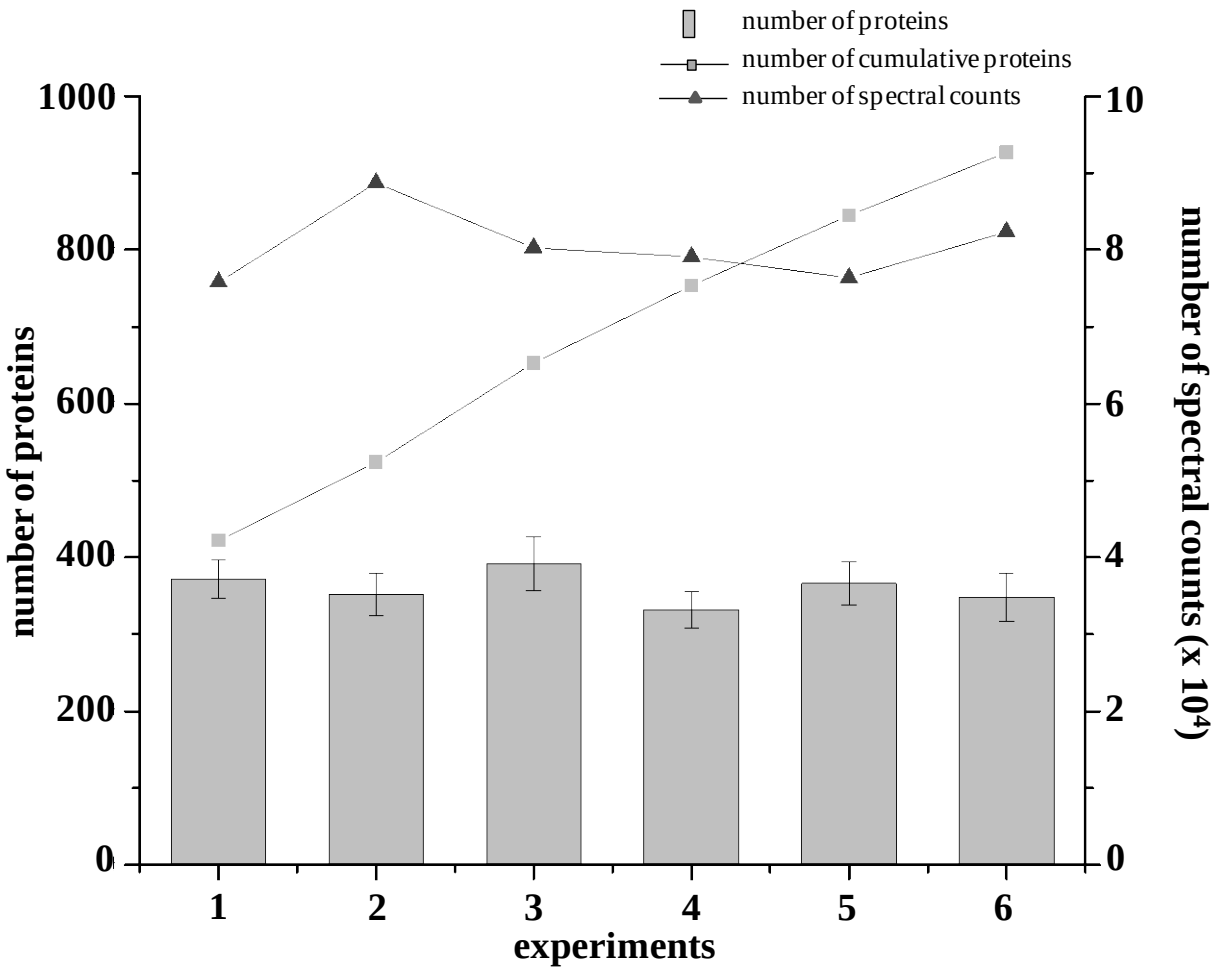

Figure 7.1. Histogram of the average number (mean ± standard deviation) of proteins (gray rectangular) identified in each experiment. The number of spectral counts (black triangle) identified in each experiment and cumulative number of proteins (gray squre) identified across the six experiments are also shown.

In addition to an individual assessment of how protein expression varies, it is also worthwhile to understand how proteins with similar functions change with disease progression. There are five major pathways that differentially-expressed T-cell proteins are involved in: cytoskeletal structure, energy metabolism, oxidative stress, molecular chaperone activity, and apoptosis. Upon grouping individual proteins into these pathways (Figure 7.2), we observe on average an increase in cytoskeletal structure, energy metabolism, oxidative stress, and molecular chaperone proteins with disease progression in APP/PS-1 mice. Apoptosis-related proteins are constant on average, although it is clear (Figure 7.2 and Table 7.2) that individual proteins may increase or decrease with disease progression in APP/PS-1 mice.

7.3.3 Western Blotting Analysis

Three proteins, annexin A5, aldose reductase, and lamin B, were selected for Western blotting analysis (Figure 7.3). The relative abundances of annexin A5 obtained from iTRAQ and Western analysis are 1.0 : 1.0 : 1.7 : 2.8 : 2.9 : 4.6 and 1.0 : 1.2 : 1.4 : 2.6 : 2.3 : 4.0 (WT_{3m} : APP/PS-1_{3m} : WT_{7m} : APP/PS-1_{7m} : WT_{12m} : APP/PS-1_{12m}; N = 6 and 4 for iTRAQ experiments and Western analysis, respectively) (Figure 7.3a). Based on good agreement across all channels for annexin A5 in iTRAQ experiments and Western analysis ($p < 0.05$), we only focused on 12-month samples for lamin B1 and aldose reductase. The relative abundances of lamin B1 obtained from iTRAQ and Western analysis were 2.3 : 1.0 (N = 6, $p < 0.05$) and 2.1 : 1.0 (N = 6, $p < 0.01$), respectively (Figure 7.3b); the relative abundances of aldose reductase obtained from iTRAQ and Western analysis were 1.0 : 3.5 (N = 6, $p < 0.05$) and 1.0 : 2.2 (N = 6, $p < 0.05$), respectively (Figure 7.3c). Similar quantitative results were obtained between Western blotting

analysis and iTRAQ experiments for these proteins. Slight differences in aldose reductase ratios between Western and iTRAQ experiments may be caused by the suppression of iTRAQ protein ratios at the MS/MS level[144]. Both experiments indicate that annexin A5 and aldose reductase levels are higher in APP/PS-1 mice at 12 months whereas lamin B1 is lower relative to WT.

7.4 DISCUSSION

This is the first proteomics study to monitor the T-cell proteome during the progression of AD. While AD is a neurodegenerative disease, it is also a systemic inflammatory disease with elevated levels of pro-inflammatory cytokines, such as IL-6, IL-1β, and TNF-α[321]. Peripheral T-cells are major contributors to this inflammation. T-cells are activated in AD and have increased cytokine production[73,321]. Alterations in the population and function of T-cells may affect a patient's ability to fight against toxic Aβ products[73,321]. However, the molecular mechanisms for these alterations are not well understood. In this study, we have identified 33 differentially-expressed proteins in CD90+ T-cells of APP/PS-1 mice at different disease stages. These proteins are involved in cytoskeletal structure, energy metabolism, oxidative stress, apoptosis, and molecular chaperone activity (Table 7.2).

7.4.1 Cytoskeletal Proteins

Cytoskeletal proteins are important for T-cell migration and activation[335,339] and are altered in AD brain[340]. Upon stimulation, cytoskeleton changes T-cells from a round shape into a migrating morphology. Once T-cells bind to antigen presenting cells, they change shape into a

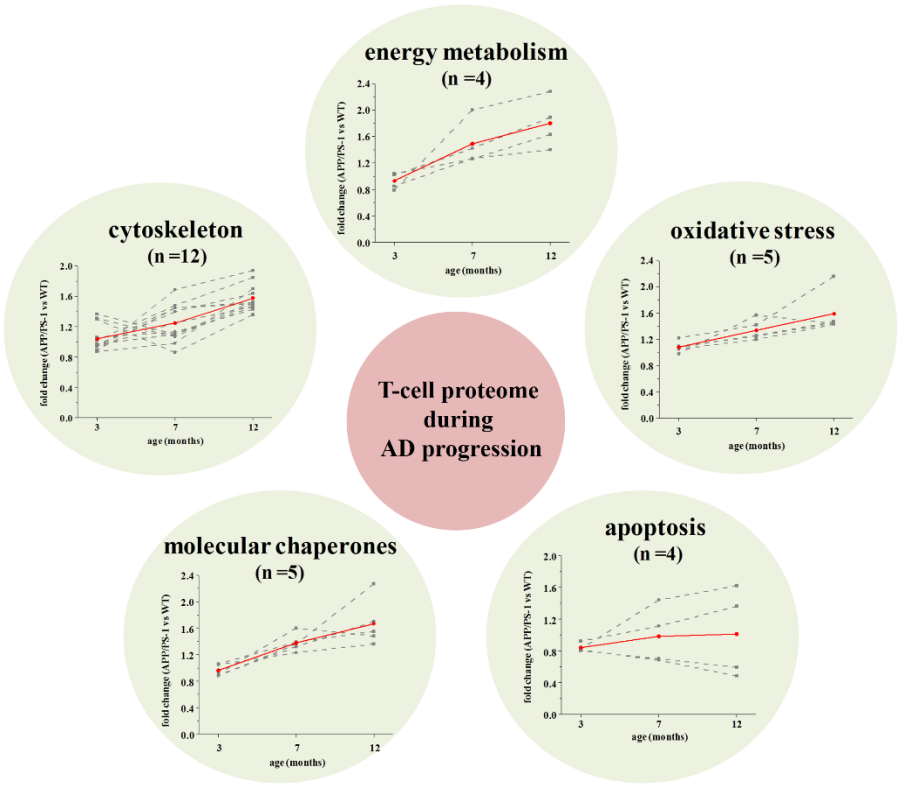

Figure 7.2. Illustrative depiction of biological pathways in which differentially-expressed T-cell proteins during AD progression are invovled. Dotted lines corresponse the fold-change for individual protein in each biological pathway. Red lines are the average fold-change for all proteins involved in each biological pathway.

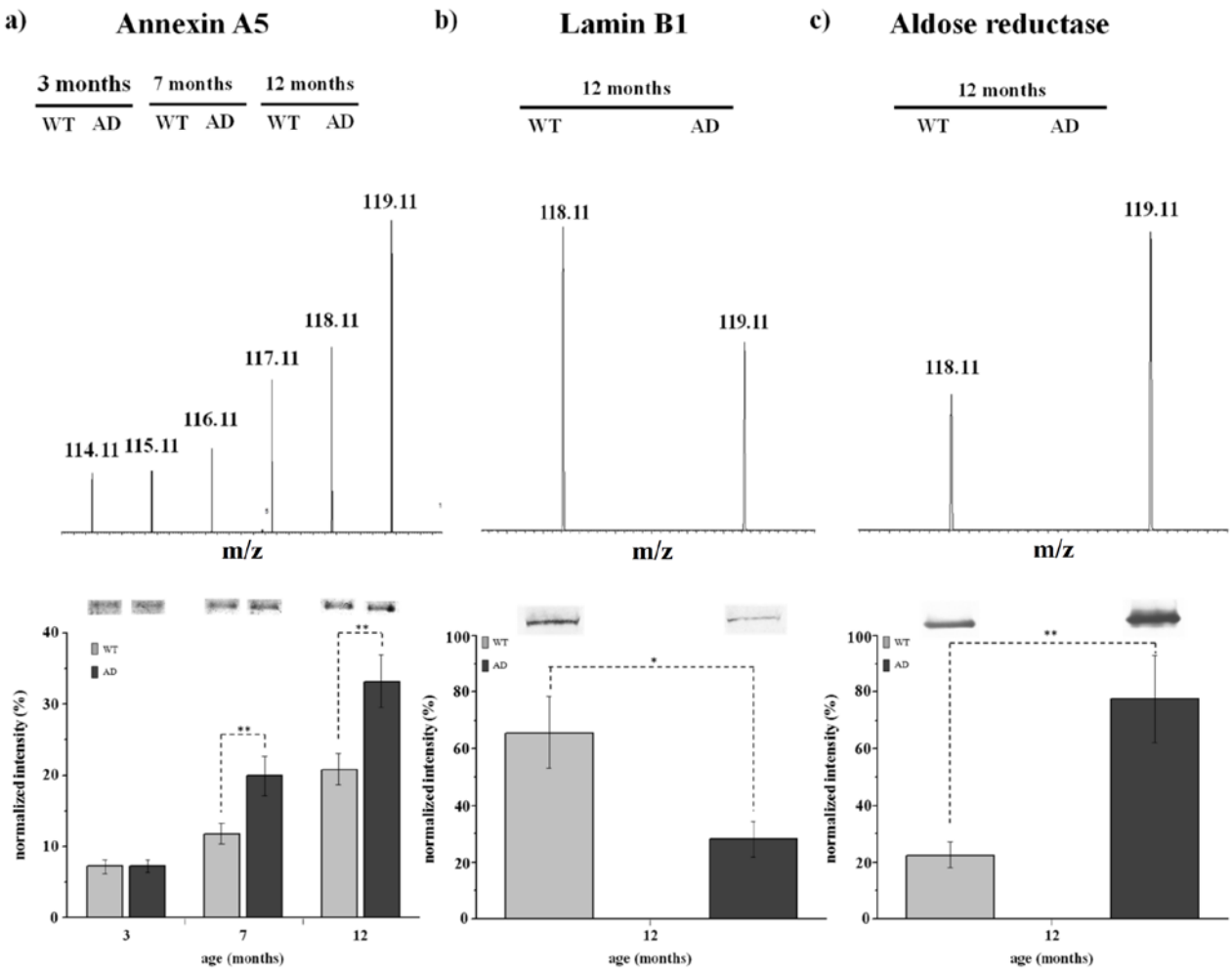

Figure 7.3. Examples of reporter ion intensities (top panel) and Western blotting images (bottom panel) for **a)** annexin A5, **b)** lamin B1, and **c)** aldose reductase. The histogram under the Western blotting images displays the normalized intensity ± standard deviation (N = 4, 6, 6 for annexin A5, lamin B1 and aldose reductase, respectively) across each group. The intensity for each individual band is normalized to the total intensity of the blot. * $p < 0.01$ and ** $p < 0.05$.

Table 7.2. List of differentially-expressed T-cell proteins in APP/PS-1 mice.

IPI[a]	Protein Description	Fold change (APP/PS-1 / WT)[b]			Function[c]
		3 months	7 months	12 months	
IPI00109044.8	myosin light chain, regulatory B-like	**1.31 ± 0.12 (*p* = 2E-3)**	1.07 ± 0.08 (*p* = 2.15)	**1.51 ± 0.22 (*p* = 0.02)**	cytoskeletal structure
IPI00110588.4	moesin	0.97 ± 0.10 (*p* = 10.58)	1.10 ± 0.13 (*p* = 9.50)	**1.53 ± 0.43 (*p* = 3E-5)**	cytoskeletal structure
IPI00117095.1	frizzled-6	1.02 ± 0.10 (*p* = 1.52)	**1.48 ± 0.17 (*p* = 0.02)**	**1.85 ± 0.35 (*p* = 2E-3)**	cytoskeletal structure
IPI00117352.1	tubulin beta-5 chain	1.06 ± 0.10 (*p* = 10.2)	1.13 ± 0.28 (*p* = 13.20)	**1.43 ± 0.11 (*p* = 0.04)**	cytoskeletal structure
IPI00123181.4	myosin-9	**1.37 ± 0.34 (*p* = 0.03)**	1.10 ± 0.22 (*p* = 32.83)	**1.46 ± 0.29 (*p* = 0.02)**	cytoskeletal structure
IPI00136110.4	phosphatidylinositol-4,5-bisphosphate 3-kinase	0.94 ± 0.17 (*p* = 18.48)	1.25 ± 0.26 (*p* = 0.02)	**1.47 ± 0.36 (*p* = 8E-4)**	cytoskeletal structure
IPI00138691.6	actin-related protein 2/3 complex subunit 4	0.87 ± 0.12 (*p* = 13.53)	0.98 ± 0.33 (*p* = 7.92)	**1.70 ± 0.45 (*p* = 9E-3)**	cytoskeletal structure
IPI00177038.1	actin-related protein 2	0.89 ± 0.16 (*p* = 20.46)	**1.45 ±0.17 (*p* = 6E-3)**	**1.52 ± 0.32 (*p* = 0.04)**	cytoskeletal structure
IPI00230395.5	annexin A1	0.95 ± 0.13 (*p* = 21.78)	**1.40 ± 0.16 (*p* = 0.03)**	**1.64 ± 0.14 (*p* = 1E-3)**	cytoskeletal structure
IPI00317309.5	annexin A5	0.96 ±0.29 (*p* = 19.80)	**1.45 ± 0.32 (*p* = 0.02)**	**1.50 ± 0.46 (*p* = 0.02)**	cytoskeletal structure
IPI00380895.7	myosin-3	**1.30 ± 0.19 (*p* = 9E-4)**	0.86 ±0.14 (*p* = 19.85)	**1.36 ± 0.11 (*p* = 1E-3)**	cytoskeletal structure
IPI00399943.3	actin-related protein 2/3 complex subunit 5	0.88 ±0.17 (*p* = 22.44)	**1.69 ±0.24 (*p* = 0.03)**	**1.94 ± 0.43 (*p* = 3E-6)**	cytoskeletal structure
IPI00323592.2	malate dehydrogenase 2	1.02 ± 0.19 (*p* = 25.74)	**1.42 ± 0.58 (*p* = 0.04)**	**1.89 ± 0.59 (*p* = 4E-4)**	energy metabolism
IPI0033632.11	malate dehydrogenase 1	0.85 ± 0.20 (*p* = 14.85)	1.27 ±0.33 (*p* = 10.56)	**1.40 ± 0.32 (*p* = 0.03)**	energy metabolism
IPI00407130.4	pyruvate kinase	0.79 ±0.16 (*p* = 18.81)	**2.00 ± 0.34 (*p* = 0.02)**	**2.28 ± 0.46 (*p* = 6E-5)**	energy metabolism
IPI00555069.3	phosphoglycerate kinase 1	1.04 ± 0.27 (*p* = 17.49)	1.26 ± 0.48 (*p* = 0.02)	**1.63 ± 0.50 (*p* = 0.02)**	energy metabolism

Table 7.2. (***continued***) List of differentially-expressed T-cell proteins in APP/PS-1 mice.

IPI	Protein Description	Fold change (APP/PS-1 / WT)			Function
		3 months	7 months	12 months	
IPI00113996.7	flavin reductase	1.08 ±0.33 (*p* = 3.75)	1.26 ± 0.27 (*p* = 0.03)	**1.47 ± 0.53 (*p* = 0.02)**	oxidative stress
IPI00117910.3	peroxiredoxin-2	1.22 ± 0.13 (*p* = 9.25)	**1.42 ± 0.25 (*p* = 4E-3)**	**2.16 ± 0.48 (*p* = 0.02)**	oxidative stress
IPI00130589.8	superoxide dismutase [Cu-Zn]	1.05 ± 0.14 (*p* = 4.15)	1.20 ± 0.26 (*p* = 10.28)	**1.43 ± 0.35 (*p* = 0.03)**	oxidative stress
IPI00223757.4	aldose reductase	1.09 ±0.11 (*p* = 8.58)	1.25 ±0.41 (*p* = 11.55)	**1.45 ± 0.32 (*p* = 0.02)**	oxidative stress
IPI00759999.1	isoform cytoplasmic+peroxisomal of	0.98 ± 0.26 (*p* = 20.46)	**1.57 ± 0.32 (*p* = 2E-3)**	**1.44 ± 0.65 (*p* = 0.03)**	oxidative stress
IPI00123886.2	isoform 1 of DNA-dependent protein kinase	0.92 ±0.28 (*p* = 10.56)	1.11 ±0.55 (*p* = 19.14)	**1.36 ± 0.63 (*p* = 0.02)**	apoptosis
IPI00223713.5	histone H1.2	0.82 ±0.29 (*p* = 13.53)	**1.44 ± 0.34 (*p* = 0.04)**	**1.62 ± 0.58 (*p* = 0.02)**	apoptosis
IPI00230394.5	lamin-B1	0.81 ± 0.41 (*p* = 7.59)	**0.68 ± 0.27 (*p* = 0.03)**	**0.48 ± 0.20 (*p* = 0.02)**	apoptosis
IPI00466069.3	elongation factor 2	0.80 ± 0.32 (*p* = 2.64)	**0.70 ± 0.27 (*p* = 0.02)**	**0.59 ± 0.20 (*p* = 0.02)**	apoptosis
IPI00308885.6	isoform 1 of 60 kDa heat shock protein,	1.06 ± 0.49 (*p* = 4.95)	**1.39 ± 0.48 (*p* = 0.04)**	**1.55 ± 0.62 (*p* = 3E-4)**	molecular chaperone
IPI00319992.1	78 kDa glucose-regulated protein	1.05 ± 0.25 (*p* = 5.94)	1.23 ± 0.36 (*p* = 9.57)	**1.36 ± 0.16 (*p* = 0.03)**	molecular chaperone
IPI00323357.3	heat shock cognate 71 kDa protein	0.88 ± 0.26 (*p* = 11.88)	**1.36 ±0.47 (*p* = 0.03)**	**2.27 ±0.89 (*p* = 0.05)**	molecular chaperone
IPI00330804.4	heat shock protein HSP 90-alpha	0.91 ± 0.22 (*p* = 28.05)	**1.60 ± 0.82 (*p* = 0.03)**	**1.48 ± 0.49 (*p* = 0.04)**	molecular chaperone
IPI00554929.3	heat shock protein HSP 90-beta	0.89 ± 0.27 (*p* = 8.58)	**1.32 ± 0.56 (*p* = 0.04)**	**1.70 ± 0.61 (*p* = 4E-3)**	molecular chaperone
IPI00462291.5	high mobility group box1	0.89 ± 0.31 (*p* = 19.80)	**1.54 ±0.49 (*p* = 0.03)**	**0.70 ± 0.24 (*p* = 0.02)**	granzyme A signaling
IPI00648105.1	uncharacterized protein	**0.48±0.27 (*p* = 0.04)**	**0.58±0.32 (*p* = 0.03)**	**0.63 ± 0.39 (*p* = 0.03)**	/
IPI00123570.3	putative uncharacterized protein	**0.47±0.17 (*p* = 0.02)**	**0.71±0.23 (*p* = 0.04)**	0.80 ± 0.17 (*p* = 1.52)	/

[a] protein ID provided by international protein index (IPI) database (08/16/2012, 59534 sequences).

[b] protein fold-change values are shown as average ± standard deviation (n=6); p-value was obtained

[c] protein functions are obtained from literature and uniprot

stopped morphology and are activated[335]. Alterations in T-cell cytoskeletal proteins may affect migration. For example, moesin is a member of ezrin-radirin-moesin protein family, which is an important component of actin-based cytoskeleton. T-cells which are moesin-deficient or have low levels of moesin have reduced migration[341,342]. On the other hand, CD4+ T-cells isolated from the elderly have increased migration that may be explained by elevated levels of myosin IIA[330].

In this study, 12 cytoskeletal proteins are differentially-expressed during the progression of AD (Table 7.2). Five proteins have significantly increased concentrations in APP/PS-1 mice at seven and 12 months. Annexin A5 had higher concentrations in seven (1.45 ± 0.32, $p = 0.02$) and 12 (1.50 ± 0.46, $p = 0.02$) month-old APP/PS-1 mice compared to WT. Elevated levels of four proteins (i.e., moesin, tubulin beta-5 chain, actin-related protein 2/3 complex subunit 4) are only observed in 12 month-old APP/PS-1 mice. Increased levels of cytoskeletal proteins (e.g., cofilin-1 and actin) are observed in lymphocytes from PD patients[343]. These results correlate with increased migration of T-cells toward the brain in AD[73]. Although the mechanism for this migration is still unclear, neuroinflammation in AD may signal T-cell trafficking toward the brain[73,321]. Over-expression of C-X-C motif chemokine receptor 2[344] and macrophage inflammatory protein-1α[345] mediate the transendothelial migration of T-cells. Systemic inflammation associated with AD may also increase the migration of T-cells. In this case, T-cells would travel throughout the body to scan for antigens[346]. In addition, cytoskeletal proteins are involved in immune cell activation[347]. Increased levels of cytoskeletal proteins in our proteomics studies are consistent with elevated activation makers on T-cells during AD progression[266].

7.4.2 Energy Metabolism

Altered energy metabolism is a widely accepted phenomenon in AD[348-352]. Differential expression of energy-related genes (e.g., genes coding NADH dehydrogenase and succinate dehydrogenase) and proteins (e.g., ATP synthase, α-enolase, malate dehydrogenase) is associated with neuronal and synaptic loss in AD[349-352]. Aging influences energy metabolism in lymphocytes[339,353]. We observe higher levels of energy metabolism-related proteins in APP/PS-1 mice at later disease stages: phosphoglycerate kinase 1 (PGK-1) [$(APP/PS\text{-}1 / WT)_{7m}$: 1.26 ± 0.48, p = 0.02; $(APP/PS\text{-}1 / WT)_{12m}$: 1.63 ± 0.50, p = 0.02], pyruvate kinase (PK) [$(APP/PS\text{-}1 / WT)_{7m}$: 2.00 ± 0.34, p = 0.02; $(APP/PS\text{-}1 / WT)_{12m}$: 2.28 ± 0.46, p = 6E-5], malate dehydrogenease 1 (MDG-1) [$(APP/PS\text{-}1 / WT)_{12m}$: 1.40 ± 0.32, p = 0.03], and malate dehydrogenease 2 (MDG-2) [$(APP/PS\text{-}1 / WT)_{7m}$: 1.42 ± 0.58, p =0.04; $(APP/PS\text{-}1 / WT)_{12m}$: 1.89 ± 0.59, p = 4E-4].

PGK-1 and PK catalyze the formation of ATP in glycolysis [354]. MDG-1 and MDG-2 reduce NAD^+ to NADH, another form of energy. Elevated levels of PK and MDG-2 occur in APP/PS-1 mice compared to WT at seven and 12 months, and PGK-1 and MDG-1 have relatively higher concentrations at 12 months. These findings suggest elevated energy metabolism in AD T-cells, which is likely necessary for the production of cytokines and increased migration during AD progression. Similarly, microglia and astrocytes have increased activity of metabolic enzymes (e.g., pyruvate kinase) in AD[355]. This phenomenon also exists in lymphocytes from PD patients[343].

7.4.3 Oxidative Stress and Apoptosis

Oxidative stress plays a key role in the pathogenesis of AD, PD, HD, ALS, DS, and multiple sclerosis[356]. AD brain is characterized by protein oxidation, lipid peroxidation, DNA and RNA oxidation, and higher levels of reactive oxygen species[303,319]. Recently, we observed that oxidative stress in AD extends to the periphery[336]. Elevated oxidative stress as measured by protein carbonyls and 3-nitrotyrosine occurs in CD90+ T-cells from APP/PS-1 mice with disease progression[336]. Herein, five proteins involved in the redox process have altered levels (Table 7.2). Flavin reductase and peroxiredoxin-2 have increased levels in APP/PS-1 mice beginning at seven months and at 12 months (flavin reductase: 1.47 ± 0.53, p = 0.02; peroxiredoxin-2: 2.16 ± 0.48, p = 0.02) (Table 1). Increased levels of superoxide dismutase [Cu-Zn] (SOD) (1.43 ± 0.32, p = 0.03) and aldose reductase (1.45 ± 0.32, p = 0.02) are observed at 12 months in APP/PS-1 mice. Both SOD and aldose reductase are a part of the cellular antioxidant defense system. Increased levels of SOD and aldose reductase have been reported in AD brain[303,319]. Consistent findings in T-cells have been reported. T-cells from AD patients have increased levels of 8-hydroxy-2'-deoxyguanosine[301], oxidized purines[357], and decreased levels of glutathione[358]. T-cells have diminished ability to repair oxidative damage[357]. Our proteomics results of changes in redox proteins provide further evidence for oxidative stress in CD90+ T-cells with AD progression.

Oxidative stress can induce apoptosis[359]. Increased apoptosis of lymphocytes occurs in AD patients[360-362]. Four proteins involved in apoptosis are differentially-expressed herein: isoform 1 of DNA-dependent protein kinase catalytic subunit [DPKC; $(APP/PS\text{-}1 / WT)_{12m}$: 1.36 ± 0.63, p = 0.02], elongation factor-2 [EF-2; $(APP/PS\text{-}1 / WT)_{7m}$: 0.70 ± 0.27, p = 0.02;

(APP/PS-1 / WT)$_{12m}$: 0.59 ± 0.20, p = 0.02], lamin B1 [LMNB1; (APP/PS-1 / WT)$_{7m}$: 0.68 ± 0.27, p = 0.03; (APP/PS-1 / WT)$_{12m}$: 0.48 ± 0.20, p = 0.02], and histone H1.2 [HH1.2; (APP/PS-1 / WT)$_{7m}$: 1.44 ± 0.34, p = 0.04; [(APP/PS-1 / WT)$_{12m}$: 1.62 ± 0.58, p = 0.02]. Elevated DPKC levels in AD brain correlate with oxidative stress[363]. Decreased levels of EF-2, which has anti-apoptotic properties, are associated with CD4+ T-cells in HIV patients[364]. EF-2 is inactive in cortex and hippocampus of AD patients and may cause neuronal death[365]. Lower concentrations of LMNB1 induce apoptosis[366,367] and translocation of HH1.2 from nucleus into the cytoplasm [368]. Reduced levels of HH1.2 increase resistance to apoptosis[369]. In AD brain, neurons and astrocytes have elevated levels of HH1.2 which could contribute to neuronal death[370-372]. Our results suggest that T-cells from APP/PS-1 mice have increased apoptosis consistent with other findings in this model [373] and in PD, HD, and DS[374-376]. Increased apoptosis may induce immunosuppression in patients with neurodegenerative disorders[377], however, further experiments are necessary to support this notion.

7.4.4 Molecular Chaperones

Heat shock proteins (HSPs) are molecular chaperones which are responsible for the folding, degradation and translocation of proteins, and protection of cells in stressed conditions (e.g., heat and oxidative stress)[377]. Age-related expression of HSPs occurs [378]. HSPs accumulate in brains of patients with AD, PD, and ALS as a result of oxidative stress and higher levels of misfolded proteins[379,380]. Elevated levels of stress-related proteins in lymphocytes are correlated with risk of AD[381]. In this study, five HSPs have higher levels in APP/PS-1 mice after disease onset: isoform 1 of 60 kDa heat shock protein [(APP/PS-1 / WT)$_{7m}$: 1.39 ± 0.48, p = 0.04;

(APP/PS-1 / WT)$_{12m}$: 1.55 ± 0.62, p = 3E-4], 78 kDa glucose-regulated protein [(APP/PS-1 / WT)$_{12m}$: 1.36 ± 0.16, p = 0.03], heat shock cognate 71 kDa protein [(APP/PS-1 / WT)$_{7m}$: 1.36 ± 0.47, p =0.03; (APP/PS-1 / WT)$_{12m}$: 2.27 ± 0.89, p = 0.05], heat shock protein HSP 90α [(APP/PS-1 / WT)$_{7m}$: 1.60 ± 0.82, p =0.03; (APP/PS-1 / WT)$_{12m}$: 1.48 ± 0.49, p = 0.04], and heat shock protein HSP 90β [(APP/PS-1 / WT)$_{7m}$: 1.32 ± 0.56, p =0.04; (APP/PS-1 / WT)$_{12m}$: 1.70 ± 0.61, p = 4E-3]. HSP expression in T-cells could be elevated in response to oxidative stress and/or apoptosis[75,382]. HSPs play important roles in regulating the immune system and are crucial in T-cell activation, proliferation, and cytokine production[383]. It is possible that T-cells are activated and that there is higher cytokine production in APP/PS-1 mice. Further studies are necessary to understand how HSPs regulate T-cell function in AD.

7.5 CONCLUSIONS

In summary, we have monitored the CD90+ T-cell proteome in APP/PS-1 mice with disease progression. Cytoskeletal, energy metabolism, oxidative stress, apoptosis, and molecular chaperone proteins are generally higher in expression in APP/PS-1 mice relative to age-matched controls. Proteome changes suggest T-cell activation, oxidative stress and response to stress with chaperones, higher energy metabolism necessary for cell migration, and apoptosis are prevalent in peripheral cells with disease progression. This study gives insight to the fact that AD is characterized by global changes outside of the CNS which may explain premature immunosenescence and increased susceptibility to infection in AD patients. One limitation for this study is that male mice are employed to investigate the peripheral immune system in AD.

Further studies are necessary to determine how the proteome alterations and gender influence T-cell function in the APP/PS-1 mouse model.

(*It should be noted that at the time of dissertation submission data related to the work in this chapter are unrecoverable)*

8.0 FUTURE DIRECTIONS

8.1 SUMMARY

Previous chapters have described the development of novel proteomics methods and the application of proteomics tools to understand roles of immunosenescence in aging-related diseases, sepsis and AD. In **Chapter 2**, a quantitative proteomics workflow for human plasma including TMD, protein digestion, iTRAQ labeling, SCX fractionation, and RPLC-MS/MS analysis was developed. This workflow allows for the detection of novel plasma proteins which have not been reported previously. In addition, a statistical model was established which provides information for the determination of differentially-expressed proteins and further experimental design (e.g., number of biological replicates required). **Chapter 3** shows a novel PQD-MS^3-based data acquisition method for isobaric tag quantitation. This method increases the number of identified and quantified proteins and peptides with high quantitative accuracy. PQD-MS^3 also offers a mean to quantify proteins on low resolution mass spectrometry instruments (e.g., LTQ).

In **Chapter 4**, the quantitative proteomics workflow for human plasma developed in **Chapter 2** was applied to understand the molecular mechanisms associated with aging-related risk of severe sepsis among CAP patients. In this study, biological pathways which have been well studied in sepsis are identified. This confirms the value of proteomics tools in studies about pathological conditions. More importantly, novel pathways were also found in this study, for example, lipid metabolism and atherosclerosis signaling. Differentially-regulated biological pathways between younger (i.e., 55-65 years old) and older (i.e., 75-85 years old) adults may

explain the aging-related risk of severe sepsis. For example, compared to the corresponding CAP patients, the younger severe sepsis patients have hyper-inflammation and -coagulation whereas, the older severe sepsis patients have hypo-inflammation and -coagulation.

In AD studies, proteome of splenocytes from APP/PS-1 mice at advanced stage of AD is first characterized. This study provides a protein reference map for further investigation of peripheral immune system in AD. Using immunoblotting analysis techniques, increased oxidative stress in splenocytes during AD progression are found. Proteomics studies about alterations in T-cell proteins provide molecular basis for this increased oxidative stress. In addition, other biological pathways, such as cytoskeleton, energy metabolism, apoptosis, and molecular chaperones, are identified in AD progression.

Overall, proteomics methods developed in this dissertation increase the number of identified and quantified proteins, which is helpful for the discovery of novel disease biomarkers. Application of proteomics tools to the studies of sepsis and AD reveals additional information about the roles of immune system in sepsis and AD. Furthermore, these results are helpful to initiate follow-up projects, which will provide more complete and accurate picture of aging-related diseases.

8.2 FUTURE DIRECTIONS

8.2.1 Understanding the Effects of Proteome Alterations on Immune System Functions

Chapter 4 provides a list of proteins that have altered concentrations due to the severity of septic infection (i.e., severe sepsis *vs.* CAP). Out of these proteins, eight differentially-expressed proteins are identified in both younger and older patient groups. Interestingly, all of

these proteins show different regulation directions between these two age groups. For example, positive acute phase proteins (i.e., C-reactive protein, LPS-binding protein, and alpha-1-antichymotrypsin) have increased levels in the younger severe sepsis patients but decreased levels in the older severe sepsis patients. Changes in these acute phase proteins show that hyper- and hypo-inflammation are associated with the younger and older severe sepsis patients, respectively. However, no direct results regarding the alterations of immune cell functions are provided in this study. I hypothesize that the hyper- and hypo-inflammation in the younger and older severe sepsis patients may be related to their over-reactivity of immune system and immunosuppression, respectively. Due to the difficulty to access human samples, a sepsis mouse model, cecal ligation puncture (CLP) mouse, can be used. Twelve and 24 hours after CLP surgery correspond to the early and late phase of sepsis, respectively. Four groups of CLP mouse can be generated: six-month old mice (mimicking the younger adult patients) at 12 and 24 hours after CLP surgery and 14-month old mice (mimicking older adult patients) at 12 and 24 hours after CLP surgery. The intracellular levels of IL-2 and IFN-γ (two activation markers of immune cells) in T-cells and other immune cells (e.g., B-cells and macrophages) can be compared across these four groups.

Chapter 7 presents the changes in T-cell proteome during AD progression and increased levels of proteins involved in cytoskeleton, energy metabolism, oxidative stress, apoptosis, and chaperones are found. Further studies are necessary to gain better insight into how these alterations affect the function of T-cells. For example, increased levels of cytoskeletal proteins may be related to the increased migration of T-cells found in AD patients[73]. However, the migration of T-cells in APP/PS-1 mice has not been investigated yet. Another follow-up project

is the investigation of how apoptosis affects the function of T-cells in AD. Apoptosis of immune cells has been suggested to induce immunosuppression[384]. Therefore, it is worthwhile to measure the relation between the levels of apoptosis markers (e.g., Bax, B-cell lymphoma 2, and caspase-3) and activity markers (e.g., IL-2 and IFN-γ) in T-cells from APP/PS-1 mice. In addition, increased plasma levels of anti-inflammatory cytokines in APP/PS-1 mice can be used as additional evidence for immunosuppression.

8.2.2 Development of Novel Treatments to Decrease the Mortality of Sepsis or to Slow the Progression of AD

Different biological pathways have been identified to be associated with the age-related risk of severe sepsis among CAP patients in **Chapter 4**. Among these, four pathways related to retinoid X receptor (RXR) are identified: liver X receptor (LXR)/RXR activation, farnesoid X receptor (FXR)/RXR activation, LPS/IL-1 mediated inhibition of RXR function, and peroxisome proliferator-activated receptor alpha (PPARα)/RXRα activation. RXR plays a central role in the nuclear receptor superfamily because it forms heterodimers with many other nuclear receptors and therefore are involved in a variety of physiological processes including immune response[385]. For example, in the innate immune system, activation of RXR prevents the apoptosis and inflammatory response of macrophages[386]. In the adaptive immune system, RXR regulates the differentiation of T-cells into regulatory or helper T-cells[387]. Knockout of RXR gene results in diminished proliferation and increased apoptosis in T-cells[388]. In addition, RXR protects human endothelial cells from oxidative stress induced by high-dose glucose[389]. In sepsis, infection-induced damage to liver is reduced by the activation of RXR[390]. However, the effects of RXR on

T-cells in septic infection have not been examined yet. I hypothesize that activation of RXR may protect T-cells from oxidative stress induced by infection (e.g., LPS stimulation). To test this hypothesis, CD4+ T-cells were isolated from the spleen of 6-month wild type mice. These cells were cultured in medium with or without LPS-stimulation for 24 hours. As shown in Figure 8.1a, LPS-stimulated CD4+ T-cells have increased levels of oxidative stress compared to controls. Increased levels of RXR are also observed in LPS-stimulated CD4+ T-cells (Figure 8.1b). Increased levels of RXR might be responsible for the increased protein expression induced by LPS in CD4+ T-cells. For example, Apo E is a gene target for RXR[389]. Increased plasma concentrations of ApoE were observed in severe sepsis patients at 55-65 years old (**Chapter 4**). This process may require higher levels of RXR. However, further experiments are necessary to test the correlation between ApoE and RXR levels in response to infection. Additionally, the effects of aging on the roles of RXR in T-cells can be tested.

In **Chapter 7**, multiple biological pathways are altered in T-cells during the progression of AD. Combination of different therapies may provide a more effective means to treat AD. Antioxidant (e.g., vitamin C and N-acetylcysteine) and anti-apoptotic (e.g., humanins and statins) drugs have been reported separately to reduce the accumulation of Aβ plaques and slow the progression of AD[391,392]. The combination of antioxidant and anti-apoptotic drugs can be tested. The effects of this combined treatment on AD should be compared with each individual treatment.

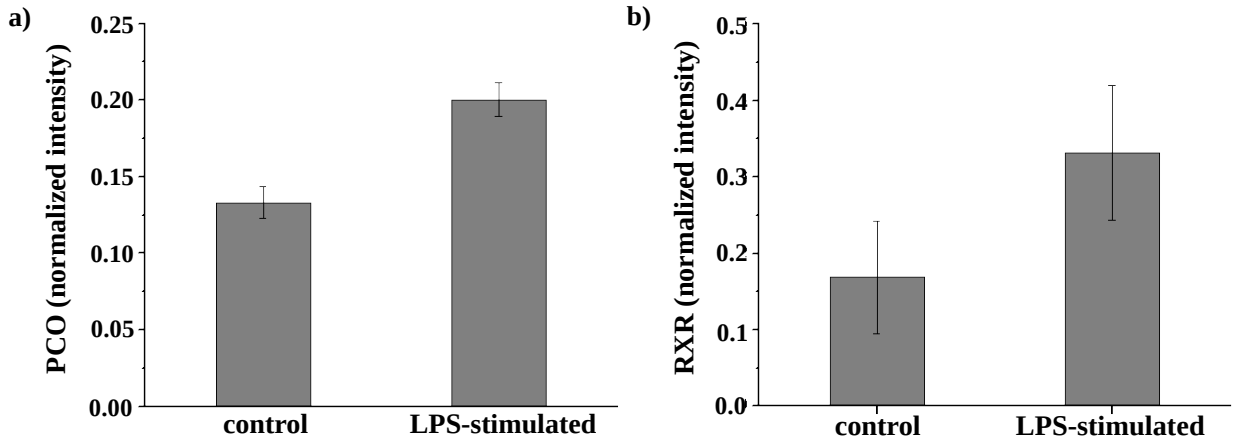

Figure 8.1. Increased levels of **a**) oxidative stress and **b**) RXR in CD4+ T-cells stimulated with LPS.

8.3 CONCLUDING REMARKS

The role of immunosenescence in aging-related diseases is one of the most popular but challenging scientific topics. Herein, works presented in this dissertation investigated alterations associated with the immune system in sepsis and AD using proteomics technologies. Findings from these works provide insight into the molecular mechanisms associated with sepsis and AD from the prospective of immune system.

Firstly, results from sepsis studies imply that age is an important factor affecting host response to sepsis. Hyper- and hypo-inflammatory response is found in the younger and older severe sepsis patients, respectively. These findings suggest that doctors need to be cautious when interpreting clinical data from sepsis patients at different ages. For example, high plasma concentrations of CRP may lead to the development of severe sepsis in younger CAP patients but low CRP concentrations may indicate poor outcome in older CAP patients. These observations also suggest that different treatments need to be performed based on the ages of sepsis patients.

Secondly, in APP/PS-1 mouse, splenocytes have increased oxidative stress during the progression of AD. Altered levels of T-cell proteins involved in oxidative stress provide molecular mechanisms for this phenomenon. Increased apoptosis, migration and energy metabolism in T-cells are also found in the progression of AD. These results confirm that alterations of the peripheral immune system do occur during the progression of AD. Findings from these studies also warrant further investigation of the changes of T-cell functions in AD.

Overall, this dissertation confirms that alterations in the immune system may contribute to the pathogenesis of aging-related diseases-sepsis and AD. Additionally, novel insight to

molecular changes associated with septic infection and AD has been gained. Besides the proteomics technologies, tools in genomics, transcriptomics, and metabolomics should be employed to further systematically investigate immunosenescence in sepsis and AD. Insight obtained from these studies should be helpful for the development of novel methods for the prevention and treatment of sepsis and AD.

BIBLIOGRAPHY

(1) López-Otín, C.; Blasco, M. A.; Partridge, L.; Serrano, M.; Kroemer, G. *Cell* **2013**, *153*, 1194.

(2) Harman, D. *Mutation Research/DNAging* **1992**, *275*, 257.

(3) Ukraintseva, S.; Yashin, A. *Demographic Research* **2003**, *9*, 163.

(4) Troen, B. R. *Mount Sinai Journal of Medicine* **2003**, *70*, 3.

(5) Koedam, E. L. G. E.; Lauffer, V.; van der Vlies, A. E.; van der Flier, W. M.; Scheltens, P.; Pijnenburg, Y. A. L. *Journal of Alzheimer's Disease* **2010**, *19*, 1401.

(6) Wieland, G. D. *Science of Aging Knowledge Environment* **2005**, *2005*, DOI: 10.1126/sageke.2005.39.pe29.

(7) Wiener, J. M.; Tilly, J. *International Journal of Epidemiology* **2002**, *31*, 776.

(8) Pawelec, G.; Adibzadeh, M.; Pohla, H.; Schaudt, K. *Trends in Immunology* **1995**, *16*, 420.

(9) Caruso, C.; Buffa, S.; Candore, G.; Colonna-Romano, G. *Immunity and Aging* **2009**, *6*, DOI:10.1186/1742.

(10) Gruver, A. L.; Hudson, L. L.; Sempowski, G. D. *Journal of Pathology* **2007**, *211*, 144.

(11) Goronzy, J. J.; Weyand, C. M. *Nature Immunology* **2013**, *14*, 428.

(12) Martorana, A.; Bulati, M.; Buffa, S.; Pellicanò, M.; Caruso, C.; Candore, G.; Colonna-Romano, G. *Longevity and Healthspan* **2012**, *1*, DOI:10.1186/2046.

(13) Akbaraly, T. N.; Hamer, M.; Ferrie, J. E.; Lowe, G.; Batty, G. D.; Hagger-Johnson, G.; Singh-Manoux, A.; Shipley, M. J.; Kivimäki, M. *Canadian Medical Association Journal* **2013**, *185*, E763.

(14) Cao, Z.; Robinson, R. A. S. *Proteomics – Clinical Applications* **2014**, *8*, 35.

(15) Lever, A.; Mackenzie, I. *British Medical Journal* **2007**, *335*, 879.

(16) Angus, D. C.; Linde-Zwirble, W. T.; Lidicker, J.; Clermont, G.; Carcillo, J.; Pinsky, M. R. *Critical Care Medicine* **2001**, *29*, 1303.

(17) Carrigan, S. D.; Scott, G.; Tabrizian, M. *Clinical Chemistry* **2004**, *50*, 1301.

(18) Rangel-Frausto, M.; Pittet, D.; Costigan, M.; Hwang, T.; Davis, C. S.; Wenzel, R. P. *The Journal of the American Medical Association* **1995**, *273*, 117.

(19) Kumar, G.; Kumar, N.; Taneja, A.; Kaleekal, T.; Tarima, S.; McGinley, E.; Jimenez, E.; Mohan, A.; Khan, R. A.; Whittle, J.; Jacobs, E.; Nanchal, R. *CHEST Journal* **2011**, *140*, 1223.

(20) Thomas, M.; Peter, J. V.; Williams, A.; Job, V.; George, R. *Postgraduate Medical Journal* **2010**, *86*, 83.

(21) Acharya, V. N. *Journal of Postgraduate Medicine* **1992**, *38*, 52.

(22) Dremsizov, T.; Clermont, G.; Kellum, J. A.; Kalassian, K. G.; Fine, M. J.; Angus, D. C. *CHEST Journal* **2006**, *129*, 968.

(23) Cohen, J. *Nature* **2002**, *420*, 885.

(24) Carvalho, P. R. A.; Trotta, E. D. A. *Journal of Pediatrics* **2003**, *79*, S195.

(25) Hotchkiss, R. S.; Karl, I. E. *New England Journal of Medicine* **2003**, *348*, 138.

(26) Rivers, E.; Nguyen, B.; Havstad, S.; Ressler, J.; Muzzin, A.; Knoblich, B.; Peterson, E.; Tomlanovich, M. *New England Journal of Medicine* **2001**, *345*, 1368.

(27) Annane, D.; Bellissant, E.; Bollaert, P. E.; Briegel, J.; Keh, D.; Kupfer, Y. *British Medical Journal* **2004**, *329*, 480.

(28) Casserly, B.; Gerlach, H.; Phillips, G. S.; Marshall, J. C.; Lemeshow, S.; Levy, M. M. *Critical Care Medicine* **2012**, *40*, 1417.

(29) Patel, G. P.; Balk, R. A. *American Journal of Respiratory and Critical Care Medicine* **2012**, *185*, 133.

(30) Turgeon, A. F.; Hutton, B.; Fergusson, D. A.; McIntyre, L.; Tinmouth, A. A.; Cameron, D. W.; Hébert, P. C. *Annals of Internal Medicine* **2007**, *146*, 193.

(31) Joannidis, M. *Seminars in Dialysis* **2009**, *22*, 160.

(32) Berger, M. M.; Chioléro, R. L. *Critical Care Medicine* **2007**, *35*, S584.

(33) Ward, P. A.; Guo, R. F.; Riedemann, N. C. *Critical Care Research and Practice* **2012**, *2012*, 8.

(34) Hotchkiss, R. S.; Monneret, G.; Payen, D. *The Lancet Infectious Diseases* **2013**, *13*, 260.

(35) Wu, A.; Hinds, C. J.; Thiemermann, C. *Shock* **2004**, *21*, 210.

(36) An, G.; Namas, R. A.; Vodovotz, Y. *Critical Reviews in Biomedical Engineering* **2012**, *40*, 341.

(37) Rivers, E. P.; Jaehne, A. K.; Nguyen, H. B.; Papamatheakis, D. G.; Singer, D.; Yang, J. J.; Brown, S.; Klausner, H. *Shock* **2013**, *39*, 127.

(38) Skibsted, S.; Bhasin, M. K.; Aird, W. C.; Shapiro, N. I. *Critical Care* **2013**, *17*, DOI: 10.1186/cc12693.

(39) Stearns-Kurosawa, D. J.; Osuchowski, M. F.; Valentine, C.; Kurosawa, S.; Remick, D. G. *Annual Review of Pathology: Mechanisms of Disease* **2011**, *6*, 19.

(40) Nguyen, A.; Yaffe, M. B. *Critical Care Medicine* **2003**, *31*, S1.

(41) Karvunidis, T.; Mares, J.; Thongboonkerd, V.; Matejovic, M. *Shock* **2009**, *31*, 545.

(42) Ward, P. A. *EMBO Molecular Medicine* **2012**, *4*, 1234.

(43) Hotchkiss, R. S.; Monneret, G.; Payen, D. *Nature Reviews Immunology* **2013**, *13*, 862.

(44) Schouten, M.; Wiersinga, W. J.; Levi, M.; van der Poll, T. *Journal of Leukocyte Biology* **2008**, *83*, 536.

(45) Victor, V. M.; Rocha, M.; De la Fuente, M. *International Immunophamacology* **2004**, *4*, 327.

(46) Melo, E. S.; Barbeiro, H. V.; Ariga, S.; Goloubkova, T.; Curi, R.; Velasco, I. T.; Vasconcelos, D.; Soriano, F. G. *Brazilian Journal of Medical and Biological Research* **2010**, *43*, 57.

(47) Girard, T. D.; Opal, S. M.; Ely, E. W. *Clinical Infectious Diseases* **2005**, *40*, 719.

(48) Kale, S. S.; Yende, S.; Kong, L.; Perkins, A.; Kellum, J. A.; Newman, A. B.; Vallejo, A. N.; Angus, D. C. *PLoS ONE* **2010**, *5*, e13852.

(49) Martin, G. S.; Mannino, D. M.; Moss, M. *Critical Care Medicine* **2006**, *34*, 15.

(50) Fulop, T.; Castle, S.; Larbi, A.; Fortin, C.; Lesur, O.; Pawelec, G. In *Handbook on Immunosenescence*; Fulop, T., Franceschi, C., Hirokawa, K., Pawelec, G., Eds.; Springer Netherlands: **2009**, p 965.

(51) Kale, S. S.; Yende, S. *Aging Diseases* **2011**, *2*, 501.

(52) Tateda, K.; Matsumoto, T.; Miyazaki, S.; Yamaguchi, K. *Infection and Immunity* **1996**, *64*, 769.

(53) Turnbull, I. R.; Wizorek, J. J.; Osborne, D.; Hotchkiss, R. S.; Coopersmith, C. M.; Buchman, T. G. *Shock* **2003**, *19*, 310.

(54) Saito, H.; Sherwood, E. R.; Varma, T. K.; Evers, B. M. *Mechanisms of Ageing and Development* **2003**, *124*, 1047.

(55) Kelly, E.; MacRedmond, R. E.; Cullen, G.; Greene, C. M.; McElvaney, N. G.; O'Neill, S. J. *Respirology* **2009**, *14*, 210.

(56) Bruunsgaard, H.; Pedersen, M.; Pedersen, B. K. *Current Opinion in Hematology* **2001**, *8*, 131.

(57) Qiu, C.; Kivipelto, M.; von Strauss, E. *Dialogues in Clinical Neuroscience* **2009**, *11*, 111.

(58) Mohr, E.; Mendis, T.; Rusk, I. N.; Grimes, J. D. *Journal of Psychiatry & Neuroscience* **1994**, *19*, 17.

(59) Connolly, C.; Bullock, R. *Psychiatric Bulletin* **2003**, *27*, 11.

(60) Serrano-Pozo, A.; Frosch, M. P.; Masliah, E.; Hyman, B. T. *Cold Spring Harbor Perspectives in Medicine* **2011**, *1*, DOI: 10.1101/cshperspect.a006189.

(61) Butterfield, D. A. *Brain Research* **2004**, *1000*, 1.

(62) Butterfield, D. A.; Perluigi, M.; Sultana, R. *European Journal of Pharmacology* **2006**, *545*, 39.

(63) Ferreira, I. L.; Resende, R.; Ferreiro, A. C. R.; Pereira, C. F. *Current Drug Targets* **2010**, *11*, 1193.

(64) Hensley, K. *Journal of Alzheimer's Disease* **2010**, *21*, 1.

(65) Honjo, K.; van Reekum, R.; Verhoeff, N. P. *Alzheimer's & Dementia* **2009**, *5*, 348.

(66) Cohen, R. M. *Focus* **2009**, *7*, 28.

(67) Rezai-Zadeh, K.; Gate, D.; Town, T. *Journal of Neuroimmune Pharmacology* **2009**, *4*, 462.

(68) Fiala, M.; Lin, J.; Ringman, J.; Kermani-Arab, V.; Tsao, G.; Patel, A.; Lossinsky, A. S.; Graves, M. C.; Gustavson, A.; Sayre, J.; Sofroni, E.; Suarez, T.; Chiappelli, F.; Bernard, G. *Journal of Alzheimer's Disease* **2005**, *7*, 221.

(69) Feng, Y.; Li, L.; Sun, X. H. *Neuroscience Bulletin* **2011**, *27*, 115.

(70) Jadidi-Niaragh, F.; Shegarfi, H.; Naddafi, F.; Mirshafiey, A. *Scandinavian Journal of Immunology* **2012**, *76*, 451.

(71) Lombardi, V. R.; García, M.; Rey, L.; Cacabelos, R. *Journal of Neuroimmunology* **1999**, *97*, 163.

(72) Sulger, J.; Dumais-Huber, C.; Zerfass, R.; Henn, F. A.; Aldenhoff, J. B. *Biological Psychiatry* **1999**, *45*, 737.

(73) Town, T.; Tan, J.; Flavell, R.; Mullan, M. *Neuromolecular Medicine* **2005**, *7*, 255.

(74) Giménez-Llort, L.; Maté, I.; Manassra, R.; Vida, C.; De la Fuente, M. *Annals of the New York Academy of Sciences* **2012**, *1262*, 74.

(75) Marchese, M.; Cowan, D.; Head, E.; Ma, D.; Karimi, K.; Ashthorpe, V.; Kapadia, M.; Zhao, H.; Davis, P.; Sakic, B. *Journal of Alzheimer's Disease* **2014**, *39*, 191.

(76) Kitazawa, M.; Cheng, D.; Tsukamoto, M. R.; Koike, M. A.; Wes, P. D.; Vasilevko, V.; Cribbs, D. H.; LaFerla, F. M. *The Journal of Immunology* **2011**, *187*, 6539.

(77) Borchelt, D. R.; Ratovitski, T.; Lare, J. V.; Lee, M. K.; Gonzales, V.; Jenkins, N. A.; Copeland, N. G.; Price, D. L.; Sisodia, S. S. *Cell Press* **1997**, *19*, 939.

(78) Phillips, M.; Boman, E.; Österman, H.; Willhite, D.; Laska, M. *PLoS ONE* **2011**, *6*, e19567.

(79) Abdul, H. M.; Sultana, R.; St. Clair, D. K.; Markesbery, W. R.; Butterfield, D. A. *Free Radical Biology and Medicine* **2008**, *45*, 1420.

(80) Mohmmad Abdul, H.; Sultana, R.; Keller, J. N.; St. Clair, D. K.; Markesbery, W. R.; Butterfield, D. A. *Journal of Neurochemistry* **2006**, *96*, 1322.

(81) Lucin, K. M.; Wyss-Coray, T. *Neuron* **2009**, *64*, 110.

(82) Heneka, M. T.; Kummer, M. P.; Stutz, A.; Delekate, A.; Schwartz, S.; Vieira-Saecker, A.; Griep, A.; Axt, D.; Remus, A.; Tzeng, T. C.; Gelpi, E.; Halle, A.; Korte, M.; Latz, E.; Golenbock, D. T. *Nature* **2012**, *493*, 674.

(83) Naert, G.; Rivest, S. *Frontiers in Cellular Neuroscience* **2012**, *6*, DOI: 10.3389/fncel.2012.00051.

(84) Esteras, N.; Bartolomé, F.; Alquézar, C.; Antequera, D.; Muñoz, Ú.; Carro, E.; Martín-Requero, Á. *European Journal of Neuroscience* **2012**, *36*, 2609.

(85) Schenk, D.; Barbour, R.; Dunn, W.; Gordon, G.; Grajeda, H.; Guido, T.; Hu, K.; Huang, J.; Johnson-Wood, K.; Khan, K.; Kholodenko, D.; Lee, M.; Liao, Z.; Lieberburg, I.; Motter, R.; Mutter, L.; Soriano, F.; Shopp, G.; Vasquez, N.; Vandevert, C.; Walker, S.; Wogulis, M.; Yednock, T.; Games, D.; Seubert, P. *Nature* **1999**, *400*, 173.

(86) Morgan, D.; Diamond, D. M.; Gottschall, P. E.; Ugen, K. E.; Dickey, C.; Hardy, J.; Duff, K.; Jantzen, P.; DiCarlo, G.; Wilcock, D.; Connor, K.; Hatcher, J.; Hope, C.; Gordon, M.; Arendash, G. W. *Nature* **2000**, *408*, 982.

(87) Weksler, M. E.; Gouras, G.; Relkin, N. R.; Szabo, P. *Immunological Review* **2005**, *205*, 244.

(88) Cannizzo, E. S.; Clement, C. C.; Sahu, R.; Follo, C.; Santambrogio, L. *Journal of Proteomics* **2011**, *74*, 2313.

(89) Oveland, E.; Karlsen, T. V.; Haslene-Hox, H.; Semaeva, E.; Janaczyk, B.; Tenstad, O.; Wiig, H. *Journal of Proteome Research* **2012**, *11*, 5338.

(90) Dear, J. W.; Leelahavanichkul, A.; Aponte, A.; Hu, X.; Constant, S. L.; Hewitt, S. M.; Yuen, P. S. T.; Star, R. A. *Critical Care Medicine* **2007**, *35*, 2319.

(91) Musunuri, S.; Wetterhall, M.; Ingelsson, M.; Lannfelt, L.; Artemenko, K.; Bergquist, J.; Kultima, K.; Shevchenko, G. *Journal of Proteome Research* **2014**, *13*, 2056.

(92) Lovestone, S.; Güntert, A.; Hye, A.; Lynham, S.; Thambisetty, M.; Ward, M. *Experter Review of Proteomics* **2007**, *4*, 227.

(93) D'Ascenzo, M.; Relkin, N. R.; Lee, K. H. *Current Opinion in Molecular Therapeutics* **2005**, *7*, 557.

(94) Maarouf, C. L.; Andacht, T. M.; Kokjohn, T. A.; Castaño, E. M.; Sue, L. I.; Beach, T. G.; Rocher, A. E. *Current Alzheimer Research* **2009**, *6*, 399.

(95) Choi, Y. S.; Choe, L. H.; Lee, K. H. *Expert Review of Proteomics* **2010**, *7*, 919.

(96) Kiddle, S. J.; Sattlecker, M.; Proitsi, P.; Simmons, A.; Westman, E.; Bazenet, C.; Nelson, S. K.; Williams, S.; Hodges, A.; Johnston, C.; Soininen, H.; Kłoszewska, I.; Mecocci, P.; Tsolaki, M.; Vellas, B.; Newhouse, S.; Lovestone, S.; Dobson, R. J. B. *Journal of Alzheimer's Disease* **2014**, *38*, 515.

(97) Cao, Z.; Yende, S.; Kellum, J. A.; Angus, D. C.; Robinson, R. A. S. *Journal of Proteome Research* **2013**, *13*, 422.

(98) Wilkins, M. R.; Pasquali, C.; Appel, R. D.; Ou, K.; Golaz, O.; Sanchez, J. C.; Yan, J. X.; Gooley, A. A.; Hughes, G.; Humphery-Smith, I.; Williams, K. L.; Hochstrasser, D. F. *Biotechnology (NY)* **1996**, *14*, 61.

(99) Zhang, Y.; Fonslow, B. R.; Shan, B.; Baek, M. C.; Yates III, J. R. *Chemical Reviews* **2013**, *113*, 2343.

(100) Eng, J.; McCormack, A.; Yates III, J. R. I. *Journal of American Society of Mass Spectrometry* **1994**, *5*, 976.

(101) Bantscheff, M.; Lemeer, S.; Savitski, M.; Kuster, B. *Analytical and Bioanalytical Chemistry* **2012**, *404*, 939.

(102) Ross, P. L.; Huang, Y. N.; Marchese, J. N.; Williamson, B.; Parker, K.; Hattan, S.; Khainovski, N.; Pillai, S.; Dey, S.; Daniels, S.; Purkayastha, S.; Juhasz, P.; Martin, S.; Bartlet-Jones, M.; He, F.; Jacobson, A.; Pappin, D. J. *Molecular & Cellular Proteomics* **2004**, *3*, 1154.

(103) Olsen, J. V.; Schwartz, J. C.; Griep-Raming, J.; Nielsen, M. L.; Damoc, E.; Denisov, E.; Lange, O.; Remes, P.; Taylor, D.; Splendore, M.; Wouters, E. R.; Senko, M.; Makarov, A.; Mann, M.; Horning, S. *Molecular & Cellular Proteomics* **2009**, *8*, 2759.

(104) McAlister, G. C.; Huttlin, E. L.; Haas, W.; Ting, L.; Jedrychowski, M. P.; Rogers, J. C.; Kuhn, K.; Pike, I.; Grothe, R. A.; Blethrow, J. D.; Gygi, S. P. *Analytical Chemistry* **2012**, *84*, 7469.

(105) Hebert, A. S.; Merrill, A. E.; Bailey, D. J.; Still, A. J.; Westphall, M. S.; Strieter, E. R.; Pagliarini, D. J.; Coon, J. J. *Nature Method* **2013**, *10*, 332.

(106) Hebert, A. S.; Merrill, A. E.; Stefely, J. A.; Bailey, D. J.; Wenger, C. D.; Westphall, M. S.; Pagliarini, D. J.; Coon, J. J. *Molecular & Cellular Proteomics* **2013**, *12*, 3360.

(107) Thompson, A.; Schäfer, J.; Kuhn, K.; Kienle, S.; Schwarz, J.; Schmidt, G.; Neumann, T.; Hamon, C. *Analytical Chemistry* **2003**, *75*, 1895.

(108) Washburn, M. P.; Wolters, D.; Yates III, J. R. *Nature Biotechnology* **2001**, *19*, 242.

(109) Nägele, E.; Vollmer, M.; Hörth, P.; Vad, C. *Expert Review of Proteomics* **2004**, *1*, 37.

(110) Pelzing, M.; Neusüss, C. *Electrophoresis* **2005**, *26*, 2717.

(111) Issaq, H. J. *Electrophoresis* **2001**, *22*, 3629.

(112) Gedela, S.; Medicherla, N. *Chromatographia* **2007**, *65*, 511.

(113) Fonslow, B. R.; Yates III, J. R. *Journal of Separation Science* **2009**, *32*, 1175.

(114) Yamashita, M.; Fenn, J. B. *The Journal of Physical Chemistry* **1984**, *88*, 4451.

(115) Köcher, T.; Pichler, P.; Schutzbier, M.; Stingl, C.; Kaul, A.; Teucher, N.; Hasenfuss, G.; Penninger, J. M.; Mechtler, K. *Journal of Proteome Research* **2009**, *8*, 4743.

(116) The Reference Genome Group of the Gene Ontology, C. *PLoS Computational Biology* **2009**, *5*, e1000431.

(117) Anderson, N. L.; Anderson, N. G. *Molecular & Cellular Proteomics* **2002**, *1*, 845.

(118) Gil-Dones, F.; Darde, V.; Vivanco, F.; Barderas, M. In *Heart Proteomics*; Vivanco, F., Ed.; Humana Press: **2013**; vol. 1005, p 245.

(119) Fonslow, B. R.; Stein, B. D.; Webb, K. J.; Xu, T.; Choi, J.; Park, S. K.; Yates III, J. R. *Nature Method* **2013**, *10*, 54.

(120) Cui, H.; Kong, Y.; Zhang, H. *Journal of Signal Transduction* **2012**, *2012*, 13.

(121) Berlett, B. S.; Stadtman, E. R. *Journal of Biological Chemistry* **1997**, *272*, 20313.

(122) Uttara, B.; Singh, A. V.; Zamboni, P.; Mahajan, R. T. *Current Neuropharmacology* **2009**, *7*, 65.

(123) Kolls, J. K. *Journal of Clinical Investigation* **2006**, *116*, 860.

(124) Palmieri, B.; Sblendorio, V. In *Advanced Protocols in Oxidative Stress II*; Armstrong, D., Ed.; Humana Press: **2010**; vol. 594, p 3.

(125) Barriuso, B.; Astiasarán, I.; Ansorena, D. *European Food Research Technology* **2013**, *236*, 1.

(126) Collins, A. R. *The American Journal of Clinical Nutrition* **2005**, *81*, 261S.

(127) Dalle-Donne, I.; Rossi, R.; Giustarini, D.; Milzani, A.; Colombo, R. *Clinica Chimica Acta* **2003**, *329*, 23.

(128) Nachtigall, I.; Tafelski, S.; Rothbart, A.; Kaufner, L.; Schmidt, M.; Tamarkin, A.; Kartachov, M.; Zebedies, D.; Trefzer, T.; Wernecke, K. D.; Spies, C. *Critical Care* **2011**, *15*, R151.

(129) Viña, J.; Lloret, A. *Journal of Alzheimers Disease* **2010**, *20*, S527.

(130) Cao, Z.; Yende, S.; Kellum, J. A.; Robinson, R. A. S. *International Journal of Proteomics* **2013**, *2013*, Article ID 654356.

(131) Gong, Y.; Li, X.; Yang, B.; Ying, W.; Li, D.; Zhang, Y.; Dai, S.; Cai, Y.; Wang, J.; He, F.; Qian, X. *Journal of Proteome Research* **2006**, *5*, 1379.

(132) Issaq, H. J.; Xiao, Z.; Veenstra, T. D. *Chemical Reviews* **2007**, *107*, 3601.

(133) Tu, C.; Rudnick, P. A.; Martinez, M. Y.; Cheek, K. L.; Stein, S. E.; Slebos, R. J. C.; Liebler, D. C. *Journal of Proteome Research* **2010**, *9*, 4982.

(134) Juhasz, P.; Lynch, M.; Sethuraman, M.; Campbell, J.; Hines, W.; Paniagua, M.; Song, L.; Kulkarni, M.; Adourian, A.; Guo, Y.; Li, X.; Martin, S.; Gordon, N. *Journal of Proteome Research* **2010**, *10*, 34.

(135) Mortezai, N.; Harder, S. n.; Schnabel, C.; Moors, E.; Gauly, M.; Schlüter, H.; Wagener, C.; Buck, F. *Journal of Proteome Research* **2010**, *9*, 6126.

(136) Qian, W.-J.; Kaleta, D. T.; Petritis, B. O.; Jiang, H.; Liu, T.; Zhang, X.; Mottaz, H. M.; Varnum, S. M.; Camp, D. G.; Huang, L.; Fang, X.; Zhang, W. W.; Smith, R. D. *Molecular & Cellular Proteomics* **2008**, *7*, 1963.

(137) Shuford, C. M.; Hawkridge, A. M.; Burnett, J. C.; Muddiman, D. C. *Analytical Chemistry* **2010**, *82*, 10179.

(138) Farrah, T.; Deutsch, E. W.; Omenn, G. S.; Campbell, D. S.; Sun, Z.; Bletz, J. A.; Mallick, P.; Katz, J. E.; Malmström, J.; Ossola, R.; Watts, J. D.; Lin, B.; Zhang, H.; Moritz, R. L.; Aebersold, R. *Molecular & Cellular Proteomics* **2011**, *10*, 1.

(139) Jacobs, J. M.; Adkins, J. N.; Qian, W. J.; Liu, T.; Shen, Y.; Camp, D. G.; Smith, R. D. *Journal of Proteome Research* **2005**, *4*, 1073.

(140) Aluise, C. D.; Sowell, R. A.; Butterfield, D. A. *Biochimica et Biophysica Acta (BBA) - Molecular Basis of Disease* **2008**, *1782*, 549.

(141) Boja, E.; Hiltke, T.; Rivers, R.; Kinsinger, C.; Rahbar, A.; Mesri, M.; Rodriguez, H. *Journal of Proteome Research* **2010**, *10*, 66.

(142) Han, D.; Moon, S.; Kim, H.; Choi, S. E.; Lee, S. J.; Park, K. S.; Jun, H.; Kang, Y.; Kim, Y. *Journal of Proteome Research* **2010**, *10*, 564.

(143) Latterich, M.; Abramovitz, M.; Leyland-Jones, B. *European Journal of Cancer* **2008**, *44*, 2737.

(144) Karp, N. A.; Huber, W.; Sadowski, P. G.; Charles, P. D.; Hester, S. V.; Lilley, K. S. *Molecular & Cellular Proteomics* **2010**, *9*, 1885.

(145) Gan, C. S.; Chong, P. K.; Pham, T. K.; Wright, P. C. *Journal of Proteome Research* **2007**, *6*, 821.

(146) Song, X.; Bandow, J.; Sherman, J.; Baker, J. D.; Brown, P. W.; McDowell, M. T.; Molloy, M. P. *Journal of Proteome Research* **2008**, *7*, 2952.

(147) Chong, P. K.; Gan, C. S.; Pham, T. K.; Wright, P. C. *Journal of Proteome Research* **2006**, *5*, 1232.

(148) Zhou, C.; Simpson, K. L.; Lancashire, L. J.; Walker, M. J.; Dawson, M. J.; Unwin, R. D.; Rembielak, A.; Price, P.; West, C.; Dive, C.; Whetton, A. D. *Journal of Proteome Research* **2012**, *11*, 2103.

(149) Mahoney, D. W.; Therneau, T. M.; Heppelmann, C. J.; Higgins, L.; Benson, L. M.; Zenka, R. M.; Jagtap, P.; Nelsestuen, G. L.; Bergen, H. R.; Oberg, A. L. *Journal of Proteome Research* **2011**, *10*, 4325.

(150) Kellum, J. A.; Kong, L.; Fink, M. P.; Weissfeld, L. A.; Yealy, D. M.; Pinsky, M. R.; Fine, J.; Krichevsky, A.; Delude, R. L.; Angus, D. C.; GenIMS Investigators *Archives of Internal Medicine* **2007**, *167*, 1655.

(151) Horgan, G. W. *Journal of Proteome Research* **2007**, *6*, 2884.

(152) Ye, H.; Sun, L.; Huang, X.; Zhang, P.; Zhao, X. *Molecular and Cellular Biochemistry* **2010**, *343*, 91.

(153) Cairns, D. A. *Proteomics* **2011**, *11*, 1037.

(154) Karp, N. A.; Lilley, K. S. *Proteomics* **2007**, *7*, 42.

(155) Levin, Y. *Proteomics* **2011**, *11*, 2565.

(156) Oberg, A. L.; Vitek, O. *Journal of Proteome Research* **2009**, *8*, 2144.

(157) Hughes, C.; Krijgsveld, J. *Trends in Biotechnology* **2012**, *30*, 668.

(158) Becker, G. W. *Briefings in Functional Genomics & Proteomics* **2008**, *7*, 371.

(159) Ong, S. E.; Blagoev, B.; Kratchmarova, I.; Kristensen, D. B.; Steen, H.; Pandey, A.; Mann, M. *Molecular & Cellular Proteomics* **2002**, *1*, 376.

(160) Chakraborty, A.; Regnier, F. E. *Journal of Chromatography A* **2002**, *949*, 173.

(161) Boersema, P. J.; Raijmakers, R.; Lemeer, S.; Mohammed, S.; Heck, A. J. R. *Nature Protocols* **2009**, *4*, 484.

(162) Colangelo, C.; Williams, K. In *New and Emerging Proteomic Techniques*; Humana Press: **2006**; vol. 328, p 151.

(163) Miyagi, M.; Rao, K. C. S. *Mass Spectrometry Reviews* **2007**, *26*, 121.

(164) Kellermann, J.; Lottspeich, F. In *Quantitative Methods in Proteomics*; Marcus, K., Ed.; Humana Press: **2012**; vol. 893, p 143.

(165) Rose, C. M.; Merrill, A. E.; Bailey, D. J.; Hebert, A. S.; Westphall, M. S.; Coon, J. J. *Analytical Chemistry* **2013**, *85*, 5129.

(166) Zhang, J.; Wang, Y.; Li, S. *Analytical Chemistry* **2010**, *82*, 7588.

(167) Xiang, F.; Ye, H.; Chen, R.; Fu, Q.; Li, L. *Analytical Chemistry* **2010**, *82*, 2817.

(168) Evans, A. R.; Robinson, R. A. S. *Proteomics* **2013**, *13*, 3267.

(169) Kunz, R. C.; McAllister, F. E.; Rush, J.; Gygi, S. P. *Analytical Chemistry* **2012**, *84*, 6233.

(170) Dephoure, N.; Gygi, S. P. *Science Signaling* **2012**, *5*, DOI: 10.1126/scisignal.2002548.

(171) Robinson, R. A. S.; Evans, A. R. *Analytical Chemistry* **2012**, *84*, 4677.

(172) Wenger, C. D.; Lee, M. V.; Hebert, A. S.; McAlister, G. C.; Phanstiel, D. H.; Westphall, M. S.; Coon, J. J. *Nature Method* **2011**, *8*, 933.

(173) Wühr, M.; Haas, W.; McAlister, G. C.; Peshkin, L.; Rad, R.; Kirschner, M. W.; Gygi, S. P. *Analytical Chemistry* **2012**, *84*, 9214.

(174) Ting, L.; Rad, R.; Gygi, S. P.; Haas, W. *Nature Method* **2011**, *8*, 937.

(175) Dayon, L.; Sonderegger, B.; Kussmann, M. *Journal of Proteome Research* **2012**, *11*, 5081.

(176) Griffin, T. J.; Xie, H.; Bandhakavi, S.; Popko, J.; Mohan, A.; Carlis, J. V.; Higgins, L. *Journal of Proteome Research* **2007**, *6*, 4200.

(177) Wu, W. W.; Wang, G.; Insel, P. A.; Hsiao, C. T.; Zou, S.; Martin, B.; Maudsley, S.; Shen, R. F. *Journal of Proteomics* **2012**, *75*, 2480.

(178) Bantscheff, M.; Boesche, M.; Eberhard, D.; Matthieson, T.; Sweetman, G.; Kuster, B. *Molecular & Cellular Proteomics* **2008**, *7*, 1702.

(179) Douglas, D. J.; Frank, A. J.; Mao, D. *Mass Spectrometry Reviews* **2005**, *24*, 1.

(180) Pekar Second, T.; Blethrow, J. D.; Schwartz, J. C.; Merrihew, G. E.; MacCoss, M. J.; Swaney, D. L.; Russell, J. D.; Coon, J. J.; Zabrouskov, V. *Analytical Chemistry* **2009**, *81*, 7757.

(181) Dellinger, R. P.; Levy, M. M.; Rhodes, A.; Annane, D.; Gerlach, H.; Opal, S. M.; Sevransky, J. E.; Sprung, C. L.; Douglas, I. S.; Jaeschke, R.; Osborn, T. M.; Nunnally, M. E.; Townsend, S. R.; Reinhart, K.; Kleinpell, R. M.; Angus, D. C.; Deutschman, C. S.; Machado, F. R.; Rubenfeld, G. D.; Webb, S. A.; Beale, R. J.; Vincent, J. L.; Moreno, R. *Critical Care Medicine* **2013**, *41*, 580.

(182) Beutz, M. A.; Abraham, E. *Clinics in Chest Medicine* **2005**, *26*, 19.

(183) Vincent, J. L.; Sakr, Y. *Resuscitation* **2012**, *83*, 537.

(184) Davis, B. H. *Expert Review of Molecular Diagnostics* **2005**, *5*, 193.

(185) Levy, M. M.; Fink, M. P.; Marshall, J. C.; Abraham, E.; Angus, D.; Cook, D.; Cohen, J.; Opal, S. M.; Vincent, J. L.; Ramsay, G. *Critical Care Medicine* **2003**, *31*, 1250.

(186) Balk, R. A. *Critical Care Clinics* **2000**, *16*, 179.

(187) Martin, G. S.; Mannino, D. M.; Eaton, S.; Moss, M. *New England Journal of Medicine* **2003**, *348*, 1546.

(188) Martin, G. S.; Mannino, D. M.; Moss, M. *Critical Care Medicine* **2006**, *34*, 15.

(189) Opal, S. M.; Girard, T. D.; Ely, E. W. *Clinical Infectious Diseases* **2005**, *41*, S504.

(190) Wick, G.; Grubeck-Loebenstein, B. *Experimental Gerontology* **1997**, *32*, 401.

(191) Póvoa, P. *Intensive Care Medicine* **2002**, *28*, 235.

(192) McDonald, A. P.; Meier, T. R.; Hawley, A. E.; Thibert, J. N.; Farris, D. M.; Wrobleski, S. K.; Henke, P. K.; Wakefield, T. W.; Myers Jr, D. D. *Thrombosis Research* **2010**, *125*, 72.

(193) Turnbull, I. R.; Clark, A. T.; Stromberg, P. E.; Dixon, D. J.; Woolsey, C. A.; Davis, C. G.; Hotchkiss, R. S.; Buchman, T. G.; Coopersmith, C. M. *Critical Care Medicine* **2009**, *37*, 1018.

(194) Yamamoto, K.; Shimokawa, T.; Yi, H.; Isobe, K. I.; Kojima, T.; Loskutoff, D. J.; Saito, H. *The American Journal of Pathology* **2002**, *161*, 1805.

(195) Cohen, H. J.; Harris, T.; Pieper, C. F. *The American Journal of Medicine* **2003**, *114*, 180.

(196) Cao, Z.; Yende, S.; Kellum, J. A.; Robinson, R. A. S. *International Journal of Proteomics* **2013**, *2013*, 8.

(197) Cao, Z.; Evans, A. R.; Robinson, R. A. S. *Manuscript in Preparation* **2014**.

(198) Downie, L.; Armiento, R.; Subhi, R.; Kelly, J.; Clifford, V.; Duke, T. *Archives of Disease in Childhood* **2013**, *98*, 146.

(199) Karumbi, J.; Mulaku, M.; Aluvaala, J.; English, M.; Opiyo, N. *Pediatric Infectious Disease Journal* **2013**, *32*, 78.

(200) Kaplan, V.; Angus, D. C.; Griffin, M. F.; Clermont, G.; Scott, W. R.; Linde-Zwirble, W. T. *American Journal of Respiratory and Critical Care Medicine* **2002**, *165*, 766.

(201) Girard, T. D.; Ely, E. W. *Clinics in Geriatric Medicine* **2007**, *23*, 633.

(202) Bruunsgaard, H.; Pedersen, A. N.; Schroll, M.; Skinhoj, P.; Pedersen, B. K. *Clinical and Experimental Immunology* **1999**, *118*, 235.

(203) Pierrakos, C.; Vincent, J. L. *Critical Care* **2010**, *14*, R15.

(204) Shen, Z.; Want, E. J.; Chen, W.; Keating, W.; Nussbaumer, W.; Moore, R.; Gentle, T. M.; Siuzdak, G. *Journal of Proteome Research* **2006**, *5*, 3154.

(205) Zweigner, J.; Gramm, H. J.; Singer, O. C.; Wegscheider, K.; Schumann, R. R. *Blood* **2001**, *98*, 3800.

(206) Kalenka, A.; Feldmann, R. E.; Otero, K.; Maurer, M. H.; Waschke, K. F.; Fiedler, F. *Anesthesia & Analgesia* **2006**, *103*, 1522.

(207) Ren, Y.; Wang, J.; Xia, J.; Jiang, C.; Zhao, K.; Li, R.; Xu, N.; Xu, Y.; Liu, S. *Journal of Proteome Research* **2007**, *6*, 2812.

(208) Thongboonkerd, V.; Chiangjong, W.; Mares, J.; Moravec, J.; Tuma, Z.; Karvunidis, T.; Sinchaikul, S.; Chen, S. T.; Opatrný, K.; Matejovic, M. *Clinical Science* **2009**, *116*, 721.

(209) Póvoa, P.; Coelho, L.; Almeida, E.; Fernandes, A.; Mealha, R.; Moreira, P.; Sabino, H. *Clinical Microbiology and Infection* **2005**, *11*, 101.

(210) Masiá, M.; Gutiérrez, F.; Llorca, B.; Navarro, J. C.; Mirete, C.; Padilla, S.; Hernández, I.; Flores, E. *Clinical Chemistry* **2004**, *50*, 1661.

(211) Tschaikowsky, K.; Hedwig-Geissing, M.; Schmidt, J.; Braun, G. G. *PLoS ONE* **2011**, *6*, e23615.

(212) Villar, J.; Pérez-Méndez, L.; Espinosa, E.; Flores, C.; Blanco, J.; Muriel, A.; Basaldúa, S.; Muros, M.; Blanch, L.; Artigas, A.; Kacmarek, R. M. *PLoS ONE* **2009**, *4*, e6818.

(213) Sadeghi, H. M.; Schnelle, J. F.; Thomas, J. K.; Nishanian, P.; Fahey, J. L. *Experimental Gerontology* **1999**, *34*, 959.

(214) Welty-Wolf, K. E.; Carraway, M. S.; Ghio, A.; Kantrow, S. P.; Huang, Y. C. T.; Piantadosi, C. A. *Shock* **2000**, *13*, 404.

(215) Gustot, T. *Current Opinion in Critical Care* **2011**, *17*, 153.

(216) Amaral, A.; Opal, S.; Vincent, J. L. *Intensive Care Medicine* **2004**, *30*, 1032.

(217) Soares, A. J. C.; Santos, M. F.; Trugilho, M. R. O.; Neves-Ferreira, A. G. C.; Perales, J.; Domont, G. B. *Journal of Proteomics* **2009**, *73*, 267.

(218) Ware, L. B.; Eisner, M. D.; Thompson, B. T.; Parsons, P. E.; Matthay, M. A. *American Journal of Respiratory and Critical Care Medicine* **2004**, *170*, 766.

(219) Kaspereit, F.; Doerr, B.; Dickneite, G. *Blood Coagulation & Fibrinolysis* **2004**, *15*, 39.

(220) van 't Veer, C.; van der Poll, T. *Nature Method* **2008**, *14*, 606.

(221) Sunder-Plassmann, G.; Speiser, W.; Korninger, C.; Stain, M.; Bettelheim, P.; Pabinger-Fasching, I.; Lechner, K. *Annals of Hematology* **1991**, *62*, 169.

(222) Chan, D. C.; Hoang, A.; Barrett, P. H. R.; Wong, A. T. Y.; Nestel, P. J.; Sviridov, D.; Watts, G. F. *Journal of Clinical Endocrinology & Metabolism* **2012**, *97*, E1658.

(223) Larrede, S.; Quinn, C. M.; Jessup, W.; Frisdal, E.; Olivier, M.; Hsieh, V.; Kim, M.-J.; Van Eck, M.; Couvert, P.; Carrie, A.; Giral, P.; Chapman, M. J.; Guerin, M.; Le Goff, W. *Arteriosclerosis, Thrombosis, and Vascular Biology* **2009**, *29*, 1930.

(224) Zhao, C.; Dahlman-Wright, K. *Journal of Endocrinology* **2010**, *204*, 233.

(225) Myhre, A. E.; Ågren, J.; Dahle, M. K.; Tamburstuen, M. V.; Lyngstadaas, S. P.; Collins, J. L.; Foster, S. J.; Thiemermann, C.; Aasen, A. O.; Wang, J. E. *Shock* **2008**, *29*, 468.

(226) Khovidhunkit, W.; Kim, M.-S.; Memon, R. A.; Shigenaga, J. K.; Moser, A. H.; Feingold, K. R.; Grunfeld, C. *Journal of Lipid Research* **2004**, *45*, 1169.

(227) Brazil, M. *Nature Reviews Drug Discovery* **2002**, *1*, 840.

(228) Joseph, S. B.; McKilligin, E.; Pei, L.; Watson, M. A.; Collins, A. R.; Laffitte, B. A.; Chen, M.; Noh, G.; Goodman, J.; Hagger, G. N.; Tran, J.; Tippin, T. K.; Wang, X.; Lusis, A. J.; Hsueh, W. A.; Law, R. E.; Collins, J. L.; Willson, T. M.; Tontonoz, P. *Proceedings of the National Academy of Sciences* **2002**, *99*, 7604.

(229) Hackam, D. G.; Mamdani, M.; Li, P.; Redelmeier, D. A. *Lancet* **2006**, *367*, 413.

(230) Podnos, Y. D.; Jimenez, J. C.; Wilson, S. E. *Clinical Infectious Diseases* **2002**, *35*, 62.

(231) Segrest, J. P.; Jones, M. K.; De Loof, H.; Dashti, N. *Journal of Lipid Research* **2001**, *42*, 1346.

(232) Phetteplace, H. W.; Sedkova, N.; Hirano, K. I.; Davidson, N. O.; Lanza-Jacoby, S. P. *Lipids* **2000**, *35*, 1079.

(233) Lacorte, J.-M.; Beigneux, A.; Parant, M.; Chambaz, J. *FEBS Letters* **1997**, *415*, 217.

(234) Harvey, S. B.; Zhang, Y.; Wilson-Grady, J.; Monkkonen, T.; Nelsestuen, G. L.; Kasthuri, R. S.; Verneris, M. R.; Lund, T. C.; Ely, E. W.; Bernard, G. R.; Zeisler, H.; Homoncik, M.; Jilma, B.; Swan, T.; Kellogg, T. A. *Journal of Proteome Research* **2008**, *8*, 603.

(235) Conlan, M. G.; Folsom, A. R.; Finch, A.; Davis, C. E.; Sorlie, P.; Marcucci, G.; Wu, K. K. *Thrombosis and Haemostasis* **1993**, *70*, 380.

(236) Kattan, O.; Kasravi, F.; Elford, E.; Schell, M.; Harris, H. *J Immunol* **2008**, *181*, 1399

(237) Berbée, J. P.; Hoogt, C.; Haas, C. C.; Kessel, K. M.; Dallinga-Thie, G.; Romijn, J.; Havekes, L.; Leeuwen, H.; Rensen, P. N. *Intensive Care Medicine* **2008**, *34*, 907.

(238) Westerterp, M.; Van Eck, M.; de Haan, W.; Offerman, E. H.; Van Berkel, T. J. C.; Havekes, L. M.; Rensen, P. C. N. *Atherosclerosis* **2007**, *195*, e9.

(239) Westerterp, M.; Berbée, J. F.; Pires, N. M.; van Mierlo, G. J.; Kleemann, R.; Romijn, J. A.; Havekes, L. M.; Rensen, P. C. *Circulation* **2007**, *116*, 2173.

(240) Christoffersen, C.; Nielsen, L. *Critical Care* **2012**, *16*, 126.

(241) Kumaraswamy, S.; Linder, A.; Akesson, P.; Dahlback, B. *Critical Care* **2012**, *16*, R60.

(242) Diefenbach, A.; Schindler, H.; Röllinghoff, M.; Yokoyama, W. M.; Bogdan, C. *Science* **1999**, *284*, 951.

(243) Kolls, J. K. *The Journal of Clinical Investigation* **2006**, *116*, 860.

(244) Berr, C. *BioFactors* **2000**, *13*, 205.

(245) Karolkiewicz, J.; Szczêsniak, L.; Deskur-Smielecka, E.; Nowak, A.; Stemplewski, R.; Szeklicki, R. *The Aging Male* **2003**, *6*, 100.

(246) Macdonald, J.; Galley, H. F.; Webster, N. R. *British Journal of Anaesthesia* **2003**, *90*, 221.

(247) Cao, Z.; Robinson, R. A. S. *Proteomics* **2014**, *14*, 291.

(248) Brookmeyer, R.; Johnson, E.; Ziegler-Graham, K.; Arrighi, H. M. *Alzheimer's & Dementia* **2007**, *3*, 186.

(249) Russo, C.; Schettini, G.; Saido, T. C.; Hulette, C.; Lippa, C.; Lannfelt, L.; Ghetti, B.; Gambetti, P.; Tabaton, M.; Teller, J. K. *Nature* **2000**, *405*, 531.

(250) Cohen, R. M. *Focus the Journal of Lifelong Learning in Psychiatry* **2009**, *7*, 28.

(251) Britschgi, M.; Wyss‐Coray, T. In *International Review of Neurobiology*; Giacinto Bagetta, M. T. C., Stuart, A. L., Eds.; Academic Press: **2007**; vol 82, p 205.

(252) Subramanian, S.; Ayala, P.; Wadsworth, T. L.; Harris, C. J.; Vandenbark, A. A.; Quinn, J. F.; Offner, H. *Journal of Alzheimer's Disease* **2010**, *22*, 619.

(253) Zhang, R.; Miller, R. G.; Madison, C.; Jin, X.; Honrada, R.; Harris, W.; Katz, J.; Forshew, D. A.; McGrath, M. S. *Journal of Neuroimmunology* **2013**.

(254) Borchelt, D. R.; Ratovitski, T.; van Lare, J.; Lee, M. K.; Gonzales, V.; Jenkins, N. A.; Copeland, N. G.; Price, D. L.; Sisodia, S. S. *Neuron* **1997**, *19*, 939.

(255) Robinson, R. A. S.; Cao, Z.; Williams, C. *Journal of Alzheimer's Disease* **2013**, *37*, 661.

(256) Sultana, R.; Robinson, R. A. S.; Lange, M. B.; Fiorini, A.; Galvan, V.; Fombonne, J.; Baker, A.; Gorostiza, O.; Zhang, J.; Cai, J.; Pierce, W. M.; Bredesen, D. E.; Butterfield, D. A. *Antioxidants & Redox Signaling* **2012**, *17*, 1507.

(257) Robinson, R. A. S.; Lange, M. B.; Sultana, R.; Galvan, V.; Fombonne, J.; Gorostiza, O.; Zhang, J.; Warrier, G.; Cai, J.; Pierce, W. M.; Bredesen, D. E.; Butterfield, D. A. *Neuroscience* **2011**, *177*, 207.

(258) Heneka, M. T.; Kummer, M. P.; Stutz, A.; Delekate, A.; Schwartz, S.; Vieira-Saecker, A.; Griep, A.; Axt, D.; Remus, A.; Tzeng, T.-C.; Gelpi, E.; Halle, A.; Korte, M.; Latz, E.; Golenbock, D. T. *Nature* **2013**, *493*, 674.

(259) Naert, G.; Rivest, S. *Frontiers in Cellular Neuroscience* **2012**, *6*, DOI: 10.3389/fncel.2012.00051.

(260) Pellicanò, M.; Bulati, M.; Buffa, S.; Barbagallo, M.; Di Prima, A.; Misiano, G.; Picone, P.; Di Carlo, M.; Nuzzo, D.; Candore, G.; Vasto, S.; Lio, D.; Caruso, C.; Colonna-Romano, G. *Journal of Alzheimer's Disease* **2010**, *21*, 181.

(261) Diz, A. P.; Truebano, M.; Skibinski, D. O. F. *Electrophoresis* **2009**, *30*, 2967.

(262) Karp, N. A.; Lilley, K. S. *Proteomics* **2009**, *9*, 388.

(263) Penzes, P.; VanLeeuwen, J. E. *Brain Research Reviews* **2011**, *67*, 184.

(264) Sagar, D.; Lamontagne, A.; Foss, C. A.; Khan, Z. K.; Pomper, M. G.; Jain, P. *Journal of Neuroinflammation* **2012**, *9*, DOI:10.1186/1742.

(265) Fiala, M.; Zhang, L.; Gan, X.; Sherry, B.; Taub, D.; Graves, M. C.; Hama, S.; Way, D.; Weinand, M.; Witte, M.; Lorton, D.; Kuo, Y. M.; Roher, A. E. *Molecular Medicine* **1998**, *4*, 480.

(266) Shalit, F.; Sredni, B.; Brodie, C.; Kott, E.; Huberman, M. *Clinical Immunology and Immunopathology* **1995**, *75*, 246.

(267) Jóźwik, A.; Landowski, J.; Bidzan, L.; Fülop, T.; Bryl, E.; Witkowski, J. M. *PLoS ONE* **2012**, *7*, e33276.

(268) Trieb, K.; Ransmayr, G.; Sgonc, R.; Lassmann, H.; Grubeck-Loebenstein, B. *Neurobiology of Aging* **1996**, *17*, 541.

(269) Annerén, G.; Gardner, A.; Lundin, T. *Acta Neurologica Scandinavica* **1986**, *73*, 586.

(270) Christen, Y. *The American Journal of Clinical Nutrition* **2000**, *71*, 621s.

(271) Ishihama, Y.; Oda, Y.; Tabata, T.; Sato, T.; Nagasu, T.; Rappsilber, J.; Mann, M. *Molecular & Cellular Proteomics* **2005**, *4*, 1265.

(272) Petyuk, V. A.; Qian, W.-J.; Hinault, C.; Gritsenko, M. A.; Singhal, M.; Monroe, M. E.; Camp, D. G.; Kulkarni, R. N.; Smith, R. D. *Journal of Proteome Research* **2008**, *7*, 3114.

(273) Marx, F.; Blasko, I.; Pavelka, M.; Grubeck-Loebenstein, B. *Experimental Gerontology* **1998**, *33*, 871.

(274) Paulsson, K.; Wang, P. *Biochimica et Biophysica Acta (BBA) - Molecular Cell Research* **2003**, *1641*, 1.

(275) Leach, M.; Williams, D. In *Calreticulin*; Eggleton, P., Michalak, M., Eds.; Springer US: **2003**, p49.

(276) Jiang, X.; Wang, X. *Annual Review of Biochemistry* **2004**, *73*, 87.

(277) Leuner, K.; Schulz, K.; Schütt, T.; Pantel, J.; Prvulovic, D.; Rhein, V.; Savaskan, E.; Czech, C.; Eckert, A.; Müller, W. *Molecular Neurobiology* **2012**, *46*, 194.

(278) Solheim, J. C. *Immunolog Review* **1999**, *172*, 11.

(279) Blasko, I.; Grubeck-Loebenstein, B. *Drugs & Aging* **2003**, *20*, 101.

(280) Krstic, D.; Madhusudan, A.; Doehner, J.; Vogel, P.; Notter, T.; Imhof, C.; Manalastas, A.; Hifiker, M.; Pfister, S.; Schwerdel, C.; Riether, C.; Meyer, U.; Knuesel, I. *Journal of Neuroinflammation* **2012**, *9*, DOI:10.1186/1742.

(281) Engelhart, M. J.; Geerlings, M. I.; Meijer,. J.; Kiliaan, A.; Ruitenberg, A.; van Swieten, J. C.; Stijnen, T.; Hofman, A.; Witteman, J. C.; Breteler, M. M. *Archives of Neurology* **2004**, *61*, 668.

(282) Lambert, J. C.; Heath, S.; Even, G.; Campion, D.; Sleegers, K.; Hiltunen, M.; Combarros, O.; Zelenika, D.; Bullido, M. J.; Tavernier, B.; Letenneur, L.; Bettens, K.; Berr, C.; Pasquier, F.; Fievet, N.; Barberger-Gateau, P.; Engelborghs, S.; De Deyn, P.; Mateo, I.;

Franck, A.; Helisalmi, S.; Porcellini, E.; Hanon, O.; de Pancorbo, M. M.; Lendon, C.; Dufouil, C.; Jaillard, C.; Leveillard, T.; Alvarez, V.; Bosco, P.; Mancuso, M.; Panza, F.; Nacmias, B.; Bossu, P.; Piccardi, P.; Annoni, G.; Seripa, D.; Galimberti, D.; Hannequin, D.; Licastro, F.; Soininen, H.; Ritchie, K.; Blanche, H.; Dartigues, J. F.; Tzourio, C.; Gut, I.; Van Broeckhoven, C.; Alperovitch, A.; Lathrop, M.; Amouyel, P. *Nature Genetics* **2009**, *41*, 1094.

(283) McGeer, P. L.; Akiyama, H.; Itagaki, S.; McGeer, E. G. *The Canadian Journal of Neurological Sciences* **1989**, *16*, 516.

(284) Schmidt, R.; Schmidt, H.; Curb, J. D.; Masaki, K.; White, L. R.; Launer, L. J. *Annals of Neurology* **2002**, *52*, 168.

(285) Singh, V. K.; Fudenberg, H. H.; Brown Iii, F. R. *Mechanisms of Ageing and Development* **1986**, *37*, 257.

(286) Skias, D.; Bani, M.; Reder, A. T.; Luchines D.; Antel, J. P. *Neurology* **1985**, *35*, 1635.

(287) Singh, V. *Molecular Neurobiology* **1994**, *9*, 73.

(288) Nijhuis, E.; Hinloopen, B.; Nagelkerken, L. *Journal of Neuroimmunology* **1994**, *54*, 185.

(289) Araga, S.; Kagimoto, H.; Funamoto, K.; Takahashi, K. *Acta Neurologica Scandinavica* **1991**, *84*, 259.

(290) Leffell MS, L. L., and Steiger WA *Journal of American Geriatrics Society* **1985**, *33*, 4.

(291) Zhang, R.; Miller, R. G.; Madison, C.; Jin, X.; Honrada, R.; Harris, W.; Katz, J.; Forshew, D. A.; McGrath, M. S. *Journal of Neuroimmunology* **2013**, *256*, 38.

(292) Richartz-Salzburger, E.; Batra, A.; Stransky, E.; Laske, C.; Köhler, N.; Bartels, M.; Buchkremer, G.; Schott, K. *Journal of Psychiatric Research* **2007**, *41*, 174.

(293) Bagli, M.; Papassotiropoulos, A.; Hampel, H.; Becker, K.; Jessen, F.; Bürger, K.; Ptok, U.; Rao, M. L.; Möller, H. J.; Maier, W.; Heun, R. *European Archives of Psychiatry and Clinical Neurosciences* **2003**, *253*, 44.

(294) De Luigi, A.; Fragiacomo, C.; Lucca, U.; Quadri, P.; Tettamanti, M.; Grazia De Simoni, M. *Mechanisms of Ageing and Development* **2001**, *122*, 1985.

(295) Lanzrein, A. S.; Johnston, C. M.; Perry, V. H.; Jobst, K. A.; King, E. M.; Smith, A. D. *Alzheimer Disease & Associated Disorders* **1998**, *12*, 215.

(296) Licastro, F.; Pedrini, S.; Caputo, L.; Annoni, G.; Davis, L. J.; Ferri, C.; Casadei, V.; Grimaldi, L. M. E. *Journal of Neuroimmunology* **2000**, *103*, 97.

(297) Streit, W. J. *Glia* **2002**, *40*, 133.

(298) Giubilei F., A. G., Montesperelli C., Sepe-Monti M., Cannoni S., Pichi A., Tisei P., Casini A.R., Buttinelli C., Prencipe M., Salvetti M., and Ristori G. *Dementia and Geriatirc Cognitive Disorders* **2003**, *16*, 35.

(299) Zhang, J.; Kong, Q.; Zhang, Z.; Ge, P.; Ba, D.; He, W. *Cognitive and Behavioral Neurology* **2003**, *16*, 170.

(300) Sulger, J.; Dumais-Huber, C.; Zerfass, R.; Henn, F. A.; Aldenhoff, J. B. *Biological Psychiatry* **1999**, *45*, 737.

(301) Mecocci, P.; Polidori, M. C.; Ingegni, T.; Cherubini, A.; Chionne, F.; Cecchetti, R.; Senin, U. *Neurology* **1998**, *51*, 1014.

(302) Borchelt, D. R.; Thinakaran, G.; Eckman, C. B.; Lee, M. K.; Davenport, F.; Ratovitsky, T.; Prada, C. M.; Kim, G.; Seekins, S.; Yager, D.; Slunt, H. H.; Wang, R.; Seeger, M.; Levey,

A. I.; Gandy, S. E.; Copeland, N. G.; Jenkins, N. A.; Price, D. L.; Younkin, S. G.; Sisodia, S. S. *Neuron* **1996**, *17*, 1005.

(303) Butterfield, D. A.; Perluigi, M.; Sultana, R. *European Journal of Pharmacology* **2006**, *545*, 39.

(304) Sinclair, A. J.; Bayer, A. J.; Johnston, J.; Warner, C.; Maxwell, S. R. J. *International Journal of Geriatric Psychiatry* **1998**, *13*, 840.

(305) Bourdel‐Marchasson, I.; Delmas‐Beauvieux, M. C.; Peuchant, E.; Richard‐Harston, S.; Decamps, A.; Reignier, B.; Emeriau, J. P.; Rainfray, M. *Age and Ageing* **2001**, *30*, 235.

(306) Puertas, M. C.; Martínez-Martos, J. M.; Cobo, M. P.; Carrera, M. P.; Mayas, M. D.; Ramírez-Expósito, M. J. *Experimental Gerontology* **2012**, *47*, 625.

(307) Smith, M. A.; Rottkamp, C. A.; Nunomura, A.; Raina, A. K.; Perry, G. *Biochimica et Biophysica Acta (BBA) - Molecular Basis of Disease* **2000**, *1502*, 139.

(308) Huang, X.; Moir, R. D.; Tanzi, R. E.; Bush, A. I.; Rogers, J. T. *Annals of the New York Academy of Sciences* **2004**, *1012*, 153.

(309) Mariani, E.; Polidori, M. C.; Cherubini, A.; Mecocci, P. *Journal of Chromatography B* **2005**, *827*, 65.

(310) Torres, L. L.; Quaglio, N. B.; de Souza, G. T.; Garcia, R. T.; Dati, L. M. M.; Moreira, W. L.; de Melo Loureiro, A. P.; de souza-Talarico, J. N.; Smid, J.; Porto, C. S.; de Campos Bottino, C. M.; Nitrini, R.; de Moraes Barros, S. B.; Camarini, R.; Marcourakis, T. *Journal of Alzheimer's Disease* **2011**, *26*, 59.

(311) Aluise, C. D.; Robinson, R. A. S.; Cai, J.; Pierce, W. M.; Markesbery, W. R.; Butterfield, D. A. *Journal of Alzheimer's Disease* **2011**, *23*, 257.

(312) Robinson, R. A. S.; Lange, M. B.; Sultana, R.; Galvan, V.; Fombonne, J.; Gorostiza, O.; Zhang, J.; Warrier, G.; Cai, J.; Pierce, W. M.; Bredesen, D. E.; Butterfield, D. A. *Neuroscience* **2011**, *177*, 207.

(313) Sultana, R.; Robinson, R. A. S.; Di Domenico, F.; Abdul, H. M.; Clair, D. K. S.; Markesbery, W. R.; Cai, J.; Pierce, W. M.; Butterfield, D. A. *Journal of Proteomics* **2011**, *74*, 2430.

(314) Frenkel, D.; Maron, R.; Burt, D. S.; Weiner, H. L. *The Journal of Clinical Investigation* **2005**, *115*, 2423.

(315) Maetzler, W.; Berg, D.; Synofzik, M.; Brockmann, K.; Godau, J.; Melms, A.; Gasser, T.; Hörnig, S.; Langkamp, M. *Journal of Alzheimer's Disease* **2011**, *26*, 171.

(316) Butovsky, O.; Koronyo-Hamaoui, M.; Kunis, G.; Ophir, E.; Landa, G.; Cohen, H.; Schwartz, M. *Proceedings of the National Academy of Sciences* **2006**, *103*, 11784.

(317) Reitz, C.; Brayne, C.; Mayeux, R. *Nature Reviews Neurology* **2011**, *7*, 137.

(318) Serrano-Pozo, A.; Frosch, M. P.; Masliah, E.; Hyman, B. T. *Cold Spring Harbor Perspetives in Medicine* **2011**, *1*, DOI: 10.1101/cshperspect.a006189.

(319) Butterfield, D. A. *Brain Research* **2004**, *1000*, 1.

(320) McGeer, E. G.; McGeer, P. L. *Journal of Alzheimer's Disease* **2010**, *19*, 355.

(321) Martorana, A.; Bulati, M.; Buffa, S.; Pellicanò, M.; Caruso, C.; Candore, G.; Colonna-Romano, G. *Longevity and Healthspan* **2012**, *1*, DOI:10.1186/2046.

(322) Cunningham, C. *Glia* **2013**, *61*, 71.

(323) Cappellano, G.; Carecchio, M.; Fleetwood, T.; Magistrelli, L.; Cantello, R.; Dianzani, U.; Comi, C. *American Journal of Neurodegenerative Disease* **2013**, *2*, 89.

(324) Ellrichmann, G.; Reick, C.; Saft, C.; Linker, R. A. *Clinical and Developmental Immunology* **2013**, *2013*, 11.

(325) Honjo, K.; van Reekum, R.; Verhoeff, N. P. L. G. *Alzheimer's & dementia : the journal of the Alzheimer's Association* **2009**, *5*, 348.

(326) Lurain, N. S.; Hanson, B. A.; Martinson, J.; Leurgans, S. E.; Landay, A. L.; Bennett, D. A.; Schneider, J. A. *Journal of Infectious Diseases* **2013**, *208*, 564.

(327) Weksler, M. E.; Gouras, G.; Relkin, N. R.; Szabo, P. *Immunological Reviews* **2005**, *205*, 244.

(328) Xue, S. R.; Xu, D. H.; Yang, X. X.; Dong, W. L. *Chinese Medical Journal* **2009**, *122*, 1469.

(329) Pellicano, M.; Bulati, M.; Buffa, S.; Barbagallo, M.; Di Prima, A.; Misiano, G.; Picone, P.; Di Carlo, M.; Nuzzo, D.; Candore, G.; Vasto, S.; Lio, D.; Caruso, C.; Colonna-Romano, G. *Journal of Alzheimers Disease* **2010**, *21*, 181.

(330) Chou, J. P.; Effros, R. B. *Current Pharmaceutical Design* **2013**, *19*, 1680.

(331) Panossian, L. A.; Porter, V. R.; Valenzuela, H. F.; Zhu, X.; Reback, E.; Masterman, D.; Cummings, J. L.; Effros, R. B. *Neurobiology of Aging* **2003**, *24*, 77.

(332) Lombardi, V. R. M.; García, M.; Rey, L.; Cacabelos, R. *Journal of Neuroimmunology* **1999**, *97*, 163.

(333) Meola, D.; Huang, Z.; Ha, G. K.; Petitto, J. M. *Journal of Alzheimer's Disease & Parkinsonism* **2013**, *Suppl 10*, PubMed ID: 24058743.

(334) Browne, T. C.; McQuillan, K.; McManus, R. M.; O'Reilly, J. A.; Mills, K. H. G.; Lynch, M. A. *The Journal of Immunology* **2013**, *190*, 2241.

(335) Samstag, Y.; Eibert, S. M.; Klemke, M.; Wabnitz, G. H. *Journal of Leukocyte Biology* **2003**, *73*, 30.

(336) Robinson, R. A. S.; Cao, Z.; Williams, C. *Journal of Alzheimers Disease* **2013**, *37*, 661.

(337) Naert, G.; Rivest, S. *Frontiers in Cellular Neuroscience* **2012**, *6*, DOI:10.3389/fncel.2012.00051.

(338) McManus, R. M.; Higgins, S. C.; Mills, K. H. G.; Lynch, M. A. *Neurobiology of Aging* **2014**, *35*, 109.

(339) Tollefsbol, T. O.; Cohen, H. J. *Journal of Cellular Physiology* **1985**, *123*, 417.

(340) Bamburg, J. R.; Bloom, G. S. *Cell. Motil. Cytoskeleton* **2009**, *66*, 635.

(341) Hirata, T.; Nomachi, A.; Tohya, K.; Miyasaka, M.; Tsukita, S.; Watanabe, T.; Narumiya, S. *International Immunology* **2012**, *24*, 705.

(342) Flint, M. S.; Budiu, R. A.; Teng, P.-n.; Sun, M.; Stolz, D. B.; Lang, M.; Hood, B. L.; Vlad, A. M.; Conrads, T. P. *Brain, Behavior, and Immunity* **2011**, *25*, 1187.

(343) Mila, S.; Giuliano Albo, A.; Corpillo, D.; Giraudo, S.; Zibetti, M.; Bucci, E. M.; Lopiano, L.; Fasano, M. *Biomarkers in Medicine* **2009**, *3*, 117.

(344) Liu, Y. J.; Guo, D.-W.; Tian, L.; Shang, D. S.; Zhao, W. D.; Li, B.; Fang, W. G.; Zhu, L.; Chen, Y. H. *Neurobiology of Aging* **2010**, *31*, 175.

(345) Man, S. M.; Ma, Y. R.; Shang, D. S.; Zhao, W. D.; Li, B.; Guo, D. W.; Fang, W. G.; Zhu, L.; Chen, Y. H. *Neurobiology of Aging* **2007**, *28*, 485.

(346) Holmes, C. *Neuropathology and Applied Neurobiology* **2013**, *39*, 51.

(347) Burkhardt, J. K.; Carrizosa, E.; Shaffer, M. H. *Annual Review of Immunology* **2008**, *26*, 233.

(348) Ferreira, I. L.; Resende, R.; Ferreiro, E.; Rego, A. C.; Pereira, C. F. *Current Drug Targets* **2010**, *11*, 1193.

(349) Liang, W. S.; Reiman, E. M.; Valla, J.; Dunckley, T.; Beach, T. G.; Grover, A.; Niedzielko, T. L.; Schneider, L. E.; Mastroeni, D.; Caselli, R.; Kukull, W.; Morris, J. C.; Hulette, C. M.; Schmechel, D.; Rogers, J.; Stephan, D. A. *Proceedings of the National Academy of Sciences* **2008**, *105*, 4441.

(350) Beal, M. F. *Annals of Neurology* **1992**, *31*, 119.

(351) Musunuri, S.; Wetterhall, M.; Ingelsson, M.; Lannfelt, L.; Artemenko, K.; Bergquist, J.; Kultima, K.; Shevchenko, G. *Journal of Proteome Research* **2014**, *13*, 2056.

(352) Bubber, P.; Haroutunian, V.; Fisch, G.; Blass, J. P.; Gibson, G. E. *Annals of Neurology* **2005**, *57*, 695.

(353) Rosa, L. F.; De Almeida, A. F.; Safi, D. A.; Curi, R. *Physiology and Behavior* **1993**, *53*, 651.

(354) Romano, A. H.; Conway, T. *Research in Microbiology* **1996**, *147*, 448.

(355) Bigl, M.; Bruckner, M. K.; Arendt, T.; Bigl, V.; Eschrich, K. *Journal of Neural Transmission* **1999**, *106*, 499.

(356) Lin, M. T.; Beal, M. F. *Nature* **2006**, *443*, 787.

(357) Mórocz, M.; Kálmán, J.; Juhász, A.; Sinkó, I.; McGlynn, A. P.; Downes, C. S.; Janka, Z.; Raskó, I. *Neurobiology of Aging* **2002**, *23*, 47.

(358) Cecchi, C.; Latorraca, S.; Sorbi, S.; Iantomasi, T.; Favilli, F.; Vincenzini, M. T.; Liguri, G. *Neuroscience Letters* **1999**, *275*, 152.

(359) Sinha, K.; Das, J.; Pal, P.; Sil, P. *Arch Toxicol* **2013**, *87*, 1157.

(360) Schindowski, K.; Leutner, S.; Gorriz, C.; Kratsch, T.; Peters, J.; Schramm, U.; Frohlich, L.; Maurer, K.; Eckert, A.; Muller, W. E. *Society for Neuroscience Abstracts* **2001**, *27*, 250.

(361) Schindowski, K.; Peters, J.; Gorriz, C.; Schramm, U.; Weinandl, T.; Leutner, S.; Maurer, K.; Froelich, L.; Mueller, W. E.; Eckert, A. *Pharmacopsychiatry* **2006**, *39*, 220.

(362) Leuner, K.; Pantel, J.; Frey, C.; Schindowski, K.; Schulz, K.; Wegat, T.; Maurer, K.; Eckert, A.; Mueller, W. E. *Journal of Neural Transmission-Supplement* **2007**, *72*, 207.

(363) Kanungo, J. *Alzheimer's Research and Therapy* **2013**, *5*, 13.

(364) Zelivianski, S.; Liang, D.; Chen, M.; Mirkin, B. L.; Zhao, R. Y. *Apoptosis* **2006**, *11*, 377.

(365) Johnson, G.; Gotlib, J.; Haroutunian, V.; Bierer, L.; Nairn, A. C.; Merril, C.; Wallace, W. *Molecular Brain Research* **1992**, *15*, 319.

(366) Burke, B. *Journal of Cell Biology* **2001**, *153*, F5.

(367) Rao, L.; Perez, D.; White, E. *Journal of Cell Biology* **1996**, *135*, 1441.

(368) Van, N.; Shi, Y. *Nature Structural Biology* **2003**, *10*, 983.

(369) Konishi, A.; Shimizu, S.; Hirota, J.; Takao, T.; Fan, Y.; Matsuoka, Y.; Zhang, L.; Yoneda, Y.; Fujii, Y.; Skoultchi, A. I.; Tsujimoto, Y. *Cell* **2003**, *114*, 673.

(370) Duce, J. A.; Smith, D. P.; Blake, R. E.; Crouch, P. J.; Li, Q. X.; Masters, C. L.; Trounce, I. A. *Journal of Molecular Biology* **2006**, *361*, 493.

(371) Gilthorpe, J. D.; Oozeer, F.; Nash, J.; Calvo, M.; Bennett, D. L. H.; Lumsden, A.; Pini, A. *F1000Rearch* **2013**, *2*, 148.

(372) Bolton, S. J.; Russelakis-Carneiro, M.; Betmouni, S.; Perry, V. H. *Neuropathology and Applied Neurobiology* **1999**, *25*, 425.

(373) Bamberger, M. E.; Landreth, G. E. *The Neuroscientist* **2002**, *8*, 276.

(374) Gemen, E. F. A.; Verstegen, R. H. J.; Leuvenink, J.; de Vries, E. *Pediatric Blood & Cancer* **2012**, *59*, 1310.

(375) Almeida, S.; Sarmento-Ribeiro, A. B.; Januário, C.; Rego, A. C.; Oliveira, C. R. *Biomedical and Biophysical Research Communications* **2008**, *374*, 599.

(376) Calopa, M.; Bas, J.; Callén, A.; Mestre, M. *Neurobiology of Disease* **2010**, *38*, 1.

(377) Voll, R. E.; Herrmann, M.; Roth, E. A.; Stach, C.; Kalden, J. R.; Girkontaite, I. *Nature* **1997**, *390*, 350.

(378) Kuznik, B. I.; Lin'kova, N. S.; Khavinson, V. K. *Advances in Gerontology* **2012**, *2*, 175.

(379) Hamos, J. E.; Oblas, B.; Pulaski-Salo, D.; Welch, W. J.; Bole, D. G.; Drachman, D. A. *Neurology* **1991**, *41*, 345.

(380) Di Domenico, F.; Sultana, R.; Tiu, G. F.; Scheff, N. N.; Perluigi, M.; Cini, C.; Butterfield, D. A. *Brain Research* **2010**, *1333*, 72.

(381) Badia, M. C.; Lloret, A.; Giraldo, E.; Dasí, F.; Olaso, G.; Alonso, M. D.; Viña, J. *Journal of Alzheimer's Disease* **2013**, *33*, 77.

(382) Mattson, M. *Journal of NeuroVirology* **2002**, *8*, 539.

(383) Tsan, M.-F.; Gao, B. *Journal of Leukocyte Biology* **2009**, *85*, 905.

(384) Zhang, W.; Zheng, S. *Journal of Zhejiang University Science B* **2005**, *6*, 919.

(385) Mangelsdorf, D. J.; Evans, R. M. *Cell* **1995**, *83*, 841.

(386) Núñez, V.; Alameda, D.; Rico, D.; Mota, R.; Gonzalo, P.; Cedenilla, M.; Fischer, T.; Boscá, L.; Glass, C. K.; Arroyo, A. G.; Ricote, M. *Proceedings of the National Academy of Sciences* **2010**.

(387) Takeuchi, H.; Yokota-Nakatsuma, A.; Ohoka, Y.; Kagechika, H.; Kato, C.; Song, S. Y.; Iwata, M. *The Journal of Immunology* **2013**, *191*, 3725.

(388) Stephensen, C. B.; Borowsky, A. D.; Lloyd, K. C. K. *Immunology* **2007**, *121*, 484.

(389) Chai, D.; Wang, B.; Shen, L.; Pu, J.; Zhang, X. K.; He, B. *Free Radical Biology and Medicine* **2008**, *44*, 1334.

(390) Chen, Y. H.; Hong, I. C.; Kuo, K.-K.; Hsu, H.-K.; Hsu, C. *Shock* **2007**, *28*, 65.

(391) Sureda, F. X.; Junyent, F.; Verdaguer, E.; Auladell, C.; Pelegri, C.; Vilaplana, J.; Folch, J.; Canudas, A. M.; Zarate, C. B.; Pallès, M.; Camins, A. *Current Pharmceutical Design* **2011**, *17*, 230.

(392) Gilgun-Sherki, Y.; Melamed, E.; Offen, D. *Journal of Molecular Neuroscience* **2003**, *21*, 1.